

Appendix 1

Brejchova K, **Trosan P**, Studeny P, Skalicka P, Utheim TP, Bednar J, Jirsova K: Characterization and comparison of human limbal explant cultures grown under defined and xeno-free conditions. Exp Eye Res. 2018 Jun 18. Doi: 10.1016/j.exer.2018.06.019. PMID: 29928900.



Characterization and comparison of human limbal explant cultures grown under defined and xeno-free conditions

Kristyna Brejchova^{a,b,*}, Peter Trosan^b, Pavel Studeny^c, Pavlina Skalicka^{a,d}, Tor Paaske Utheim^{e,f}, Jan Bednar^b, Katerina Jirsova^{b,c}

^a Research Unit for Rare Diseases, Clinic of Paediatrics and Adolescent Medicine, 1st Faculty of Medicine, Charles University, Ke Karlovu 2, 128 08 Prague 2, Czech Republic

^b Laboratory of the Biology and Pathology of the Eye, Institute of Biology and Medical Genetics, 1st Faculty of Medicine, Charles University and General University Hospital in Prague, Albertov 4, 128 00 Prague 2, Czech Republic

^c Ophthalmology Department of 3rd Medical Faculty and University Hospital Kralovske Vinohrady, Šrobárova 1150/50, 100 34 Prague 10, Czech Republic

^d Department of Ophthalmology, 1st Faculty of Medicine, Charles University and General University Hospital in Prague, U nemocnice 499/2, 128 08 Prague 2, Czech Republic

^e Department of Medical Biochemistry, Oslo University Hospital, Kirkeveien 166, 0407 Oslo, Norway

^f Department of Plastic and Reconstructive Surgery, Oslo University Hospital, Kirkeveien 166, 0407 Oslo, Norway

ARTICLE INFO

Keywords:

Limbal epithelial stem cells
Human serum
Human platelet lysate
Explant cultures
Limbal stem cell deficiency
Fibrin

ABSTRACT

Human limbal epithelial cells (LECs) intended for treatment of limbal stem cell deficiency are commonly cultivated on a 3T3 feeder layer with complex culture medium supplemented with fetal bovine serum (FBS). However, FBS is a xenogeneic component containing poorly characterised constituents and exhibits quantitative and qualitative lot-to-lot variations. Human limbal explants were plated on untreated or fibrin coated plastic plates and cultured in two non-xenogeneic media (supplemented with either human serum or platelet lysate only). Our aim was to find out whether the characteristics of harvested LEC cultures are comparable to those of LEC cultivated in the gold standard - FBS-supplemented complex medium. The growth kinetics, cell proliferation, differentiation, stemness maintenance, apoptosis and contamination by other cell types were evaluated and compared among these conditions. In all of them LECs were successfully cultivated. Stemness was preserved in both xeno-free media. However, cells cultured with human serum on the fibrin-coated plates had the highest growth rate and cell proliferation and very low fibroblast-like cell contamination. These data suggest that xeno-free cell culture conditions can replace the traditional FBS-supplemented medium and thereby provide a safer protocol for *ex vivo* cultured limbal stem cell transplants.

1. Introduction

The stratified squamous epithelial cell layer covering the corneal surface is essential for maintaining the clarity and regular refractive surface of the cornea. The corneal epithelium constantly undergoes regeneration by poorly differentiated limbal epithelial stem cells (LESCs) located in the limbus, the narrow transitional zone segregating the corneal and conjunctival epithelium (Davanger and Evensen, 1971; Schermer et al., 1986; Tseng, 1989). LESCs undergo asymmetric cell division whereby one daughter cell is retained in the stem cell pool, while the other detaches from its basal membrane and gives rise to

highly proliferative progenitor cells. These cells, called transient amplifying cells, migrate upwards and across towards the central cornea, and differentiate and replace senescent cells, which are sloughed away from the corneal surface (Castro-Munozledo and Gomez-Flores, 2011; Lehrer et al., 1998; Sharma and Coles, 1989).

The significance of limbal stem cells for maintaining normal corneal surface homeostasis is evident in patients with limbal stem cell deficiency (LSCD), which results in pain, persistent or recurrent epithelial defects vascularization and conjunctivalization of the cornea. The well-defined causes of LSCD are chemical/thermal injuries, Stevens-Johnson syndrome, ocular cicatricial pemphigoid and aniridia, where stem cells

Abbreviations: LESCs, limbal epithelial stem cells; LECs, limbal epithelial cells; LSCD, limbal stem cell deficiency; FBS, fetal bovine serum; hPL, human platelet lysate; COM, complex medium; hSM, human serum medium; hPLM, human platelet lysate medium; CFE, colony forming efficiency assay; TUNEL, terminal deoxyribonucleotidyl transferase-mediated dUTP-digoxigenin nick-end labelling

* Corresponding author. Research Unit for Rare Diseases, Clinic of Paediatrics and Adolescent Medicine, 1st Faculty of Medicine, Charles University, Ke Karlovu 2, 128 08 Prague 2, Czech Republic.

E-mail address: kristyna.brejchova@lf1.cuni.cz (K. Brejchova).

<https://doi.org/10.1016/j.exer.2018.06.019>

Received 10 March 2018; Received in revised form 4 June 2018; Accepted 16 June 2018

Available online 19 June 2018

0014-4835/ © 2018 Elsevier Ltd. All rights reserved.

are damaged or the process of corneal epithelial cell renewal is disrupted (Shortt et al., 2014; Schwab and Isseroff, 2000; Tsai et al., 2000). On the other hand, it has been suggested that the leading causes of LSCD are infection (e.g. trachoma) and trauma, which are often reported outside North America (Schwab and Isseroff, 2000) and outside Europe.

Current treatments for LSCD involve the transplantation of *ex vivo* cultured limbal epithelial cells (LECs) that form a confluent sheet of cells on the ocular surface (Shortt et al., 2014; Tsai et al., 2000). Two basic methods are used: explant culture, where limbal cells migrate out from a limbal tissue biopsy, and suspension culture of single cells prepared by enzymatic digestion of the limbal surface, in which the limbal cells are typically co-cultured with feeder cells (Shortt et al., 2007). Currently, there is a range of parallel protocols for the *ex vivo* expansion of LECs using different sera, including fetal bovine serum (FBS), autologous serum (Pellegrini et al., 2014; Zakaria et al., 2014) as well as serum substitutes, such as human platelet lysates (hPL), which is a source of platelet-derived growth factor, insulin-like growth factor-1, transforming growth factor- β 1 and epidermal growth factor (EGF), (Eppley et al., 2004). Also protocols with no serum addition are used (Nakamura et al., 2004, 2006; Notara et al., 2007; Pellegrini et al., 1997; Rama et al., 2010; Tsai et al., 2000). Apart from serum and serum substitutes other medium components are used such as various animal-derived hormones and growth factors (Shortt et al., 2007). From all these possibilities, complex medium (COM) is generally accepted for LSCs cultivation and media of very similar composition are regularly used (Pellegrini et al., 2018; Ramirez et al., 2015). Most often, lethally irradiated mouse fibroblast cells are used as a feeder layer but using no feeder layer has also been demonstrated as an alternative possibility for explant cultures (Jeon et al., 2013; Pellegrini et al., 2014). Diverse scaffolds (amniotic membrane, fibrin, contact lenses, etc.) are employed for the application of LECs on the ocular surface (Di Girolamo et al., 2009; Rama et al., 2001; Zakaria et al., 2014).

The conditions employing complex media containing xenogeneic (FBS) or otherwise problematic components (cholera toxin) (Yu et al., 2016) have successfully been used in some countries (Ramirez et al., 2015). However, the use of such substances or even cells presents the risk of transmitting various pathogens and potentially eliciting an immunological response in clinical applications (Llames et al., 2015; Shahdadfar et al., 2012). In the present study, we compare the properties of LEC cultures *ex vivo* expanded in two completely xeno-free culture media (human serum medium - hSM and human platelet lysate medium - hPLM) with the complex medium used as a gold standard. The aim was to ascertain whether by us tested conditions are at least of the same or better efficiency with respect to promoting LECs growth, stemness maintenance and progress of differentiation or unwanted support of other cell type growth on a substrate appropriate for transfer to the patient's eye. Fibrin tissue glue was used as a substrate for LEC culture as it promotes cell growth, maintains LECs stemness, and enables easy transfer to the patient's eye, (Forni et al., 2013; Talbot et al., 2006), and has an advantage over amniotic membrane to present no risk of viral agent transmission, nor necessity of costly donor screening and donor dependent variation in quality.

2. Materials and methods

2.1. Donor corneal tissue

The study adhered the tenets set out in the Declaration of Helsinki. Donor tissue procurement fulfilled all Czech legal requirements, including the absence of the donor in the National register of persons opposed to the post-mortem withdrawal of tissues and organs. On the use of the corneoscleral rim based on Czech legislation on specific health services (Law Act No. 372/2011 Coll.), informed consent is not required if the presented data are anonymized in the form. Thirty-six corneoscleral rims were obtained from cadaveric donor corneas stored

for 2–20 days (mean storage time: 9.7 ± 4.2 days) in Eusol-C preservation medium (Alchimia, srl., Ponte San Nicolò, Italy) until cornea grafting at University Hospital Kralovske Vinohrady, Prague, or the General University Hospital in Prague. The donor age (mean \pm standard deviation) was 60.7 ± 7.7 years (range 38–72 years).

2.2. Preparation of limbal explants and substrates

Thirty-six corneoscleral rims were divided into two groups: 18 were cultured on polystyrene (plastic) plates and the other 18 in the fibrin-coated wells of 24-well plates (TPP Techno Plastic Products AG, Trasadingen, Switzerland). The corneoscleral rims were washed three times in Dulbecco's modified Eagle's medium (DMEM)/F12 (1:1, GlutaMAX) containing $100\times$ Antibiotic-Antimycotic (AA, Thermo Fisher Scientific, Waltham, MA, USA). Excess of scleral and corneal tissue was removed and each corneoscleral rim was cut into 12 pieces.

In the no-fibrin group, the explants were plated individually in 24-well plates with or without Nunc Thermanox Coverslips (Thermo Fisher Scientific) placed on the bottom of the wells. The cultures grown on coverslips were used for immunostaining.

In the fibrin group, all 12 explants from each rim were grown in fibrin-coated wells prepared as described previously (Sheth et al., 2015). Briefly, fibrin sealant (TISSEEL Lyo, Baxter, Vienna, Austria) was prepared by dissolving the sealer protein concentrate in aprotinin solution. Thrombin solution was prepared by dissolving human thrombin with calcium chloride solution. Each of the solutions were transferred into 15-ml tubes and mixed with the appropriate volumes of phosphate-buffered saline (PBS) to obtain a thrombin and fibrinogen concentration of 10 U/ml and 10 mg/ml, respectively. Equal volumes (150 μ l) of each solution were gently mixed in each well by stirring using a pipette tip. Trituration was avoided as it leads to bubble formation. Any occasionally formed bubbles were ruptured with a surgical needle.

Prior to cell characterization, confluent cultures grown on fibrin were incubated in 5 ml of 1.04 U/mg Dispase II (Thermo Fisher Scientific) for 30 min at 37 °C in a water bath to dissolve the fibrin gel. After the Dispase II had been removed, the LEC cultures were treated with 2 ml non-animal trypsin enzyme (TrypLE Select, Thermo Fisher Scientific) for up to 25 min under the same conditions to yield single-cell suspensions. The cells were counted using a haemocytometer (OPTING Servis, Ostrava, the Czech Republic) and the 5×10^4 cells per slide for immunostaining, 2×10^3 cells per well of 6-well plate for colony forming efficiency assay (CFE) and remaining amount of cells for gene expression analyses were used.

2.3. Cell culture media

All explants from both groups were cultured for 2–4 weeks in three media: COM [1:1 DMEM/F12, 10% FBS, 1% AA, 10 ng/ml recombinant EGF, 0.5% insulin-transferrin-selenium (Thermo Fisher Scientific), 5 μ g/ml hydrocortisone, 10 μ g/ml adenine hydrochloride and 10 ng/ml cholera toxin (Sigma-Aldrich, Darmstadt, Germany)] and xeno-free media supplemented either with 10% pooled human serum or with 10% GroPro Cell Culture Growth Supplement Human Platelet Lysate (Zen-Bio, Research Triangle Park, NC, USA) as a serum substitute. Both xeno-free media were supplemented with 1% AA. The cultures were incubated at 37 °C in 5% CO₂. The culture media were changed every 2–3 days. Tranexamic acid (160 μ l/ml, Sigma-Aldrich) was added at every medium change to prevent fibrin gel digestion during prolonged culture.

2.4. Morphology and cell growth

The expanded LECs were monitored and the beginning of cell migration, reaching confluence and cell morphology were evaluated under an inverted microscope (Olympus CX41, Olympus, Tokyo, Japan). The LEC culture was considered successful when more than

80% confluence was reached. The percentage of successful cultures was calculated based on the number of all explants used. The elapsed time from explant planting to the culture growth onset and to reaching confluence was determined in successful cultures.

2.5. Preparation of 3T3 feeder layers

The 3T3 cell line was maintained using DMEM, 10% FBS and 1% AA (Thermo Fisher Scientific). At 70–80% confluence, 3T3 cells were treated with 12 µg/ml mitomycin-C Kyowa (NORDIC Pharma, Prague, the Czech Republic) for 2 h at 37 °C under 5% CO₂ to arrest cell growth. After incubation, the cells were washed with PBS three times, trypsinized for 2–4 min, and 3 × 10⁵ cells per well were distributed into 6-well plates. The cells were used within 24 h of preparation.

2.6. Colony forming efficiency assay

The clonal growth ability of the cultured cells was determined using the CFE. LEC cultures reaching at least 80% confluence were washed twice with PBS and trypsinized to obtain single-cell suspensions. The cells were counted by haemocytometer, and 2000 cells were seeded in 6-well plates containing a growth-arrested 3T3 feeder layer. The LECs were kept at 37 °C and 5% CO₂ in COM and were observed using an inverted light microscope. After 10–12 days of cultivation, colonies were fixed with cold methanol for 30 min at –20 °C. Subsequently, the cells were rehydrated with PBS and stained with 2% rhodamine solution (Sigma-Aldrich) for 5 min at 37 °C. Finally, the plates were photographed and analysed using image management software (NIS Elements; Laboratory Imaging, Prague, the Czech Republic). The colonies were counted and the CFE was calculated using the following equation (Barrandon and Green, 1987):

$$CFE (\%) = \frac{\text{number of colonies}}{\text{number of seeded cells}} \times 100$$

2.7. Immunocytochemistry

Cells obtained from cultures grown on fibrin were isolated as described above, and cytospin slides of each sample were prepared by centrifuging 5 × 10⁴ cells per slide at 100 × g for 5 min and stored at –20 °C. Immunocytochemical (ICC) staining was performed to evaluate the presence of putative LESC markers [the p63α isotype encoded by the tumour protein *P63* gene – *TP63*, ATP-binding cassette subfamily B member 5 (*ABCB5*) and a ring finger protein, *Bmi-1*, encoded by the *BMI1* proto-oncogene]; markers of differentiated corneal epithelium – keratin 3 and 12 (*K3/12*), and cell proliferation marker *Ki-67*. In brief, LEC cultures on both Thermanox coverslips and cytospin slides were fixed in 4% paraformaldehyde in PBS at room temperature for 10 min, and the cell membranes were permeabilized with 0.33% Triton X-100 (Sigma-Aldrich). The cell cultures intended for *Ki-67* staining were treated for 1 h at room temperature with blocking solution (2.5% bovine serum albumin) supplemented with 0.33% Triton X-100 (Sigma-Aldrich) to uncover hidden nuclear antigens. The remaining slides were treated with blocking solution only, as Triton X-100 can damage the epitopes of the other investigated markers. The cells were incubated with primary antibodies (Table 1) for 1 h at room temperature,

Table 1
Primary antibodies.

Primary antibody	Cat. no.	Antibody registry	Dilution	Company
Rabbit polyclonal anti-human p63α	4892	AB_2270728	1:50	Cell Signalling Technology, Danvers, MA, USA
Mouse monoclonal anti-human ABCB5 (clone 5H3C6)	MABC711	–	1:50	Merck Millipore, Darmstadt, Germany
Rabbit polyclonal anti-human <i>Bmi-1</i>	ab38295	AB_725719	1:400	Abcam, Cambridge, UK
Mouse monoclonal anti-human anti <i>K3/12</i> (clone AE5)	10R-C168a	AB_1284037	1:200	Fitzgerald Industries International, Acton, MA, USA
Mouse monoclonal anti- <i>Ki-67</i> (clone MIB-1)	M7240	AB_2142367	1:50	DAKO Cytomation, Glostrup, Denmark

followed by incubation with secondary antibodies conjugated with fluorescent dye: Alexa Fluor 488-conjugated goat anti-rabbit immunoglobulin G (IgG), Alexa Fluor 488-conjugated goat anti-mouse IgG (cat. no. A11034 and A11029, respectively) and Alexa Fluor 594-conjugated goat anti-rabbit IgG (cat. no. A11037) (all Thermo Fisher Scientific). The samples were mounted with Vectastain mounting medium with 4', 6-diamidino-2-phenylindole (DAPI) as a counterstain (Vector Laboratories, Burlingame, CA, USA) and examined by fluorescence microscopy (Olympus BX51; Olympus) at ×100 and ×200 magnification. At least 1000 cells were evaluated to calculate the percentage of positive cells.

2.8. Detection of apoptosis

The presence of apoptotic cells was identified using In Situ Cell Death Detection Kit, Fluorescein [terminal deoxynucleotidyl transferase-mediated dUTP-digoxigenin nick-end labelling (TUNEL)]; Roche Applied Science, Mannheim, Germany). LECs were fixed in 4% paraformaldehyde and permeabilized (0.33% Triton X-100) prior using the kit according to the manufacturer's instructions. Samples were mounted with VECTASHIELD mounting medium with DAPI (Vector Laboratories). The fluorescein label incorporated at the sites of damaged DNA was visualized by a fluorescence microscope. At least 1000 cells were examined to calculate the percentage of apoptotic cells.

2.9. RNA extraction, reverse transcription and quantitative real-time polymerase chain reaction (qPCR)

The expression of the *TP63*, *ABCB5*, *BMI1*, *keratins 15* and *3* (*K15*, *K3*) genes was detected using qPCR. Total RNA was extracted from all LEC cultures cultivated on plastic and fibrin using TRI Reagent (Molecular Research Center, Cincinnati, OH, USA) according to the manufacturer's instructions. The details of RNA isolation and reverse transcription have been described previously (Trosan et al., 2012). Briefly, 1 µg RNA was treated with deoxyribonuclease I (Promega Corporation, Fitchburg, WI, USA) and used for subsequent reverse transcription. The first-strand complementary DNA was synthesized using random hexamers (Promega) in a total reaction volume of 25 µl using M-MLV Reverse Transcriptase (Promega).

The qPCR was performed in a LightCycler 480 Real-Time PCR system (Roche, Basel, Switzerland). The sequences of the primers used are summarised in Table 2. The sequence specificity of all primers was confirmed via BLAST (<http://www.ncbi.nlm.nih.gov/blast/>). Conventional reverse transcription PCR was performed to confirm that only a single band was obtained. The PCR products were electrophoresed on 1% agarose gels containing GelRed Nucleic Acid Gel Stain (Biotium, Fremont, CA, USA). The qPCR parameters included initial denaturation at 95 °C for 3 min, 40 cycles of denaturation at 95 °C for 20 s, annealing at 60 °C for 30 s and elongation at 72 °C for 15 s. Fluorescence was monitored at 55–95 °C at 0.5 °C intervals for 10 s. Each experiment was performed in triplicate. A relative quantification model was used to calculate the expression of the target gene in comparison to that of glyceraldehyde-3-phosphate dehydrogenase (*GAPDH*), which was used as the endogenous control.

Table 2
Primers used for qPCR.

Primer	Sequence (5'→3')	GenBank accession number	Product size (bp)
<i>GAPDH</i>	GAAGGGGTCATTGATGGCAAC GGGAAGGTGAAGGTCGGAGTC	NM_001289746.1	108
<i>TP63</i>	GAGGTTGGGCTGTTTCATCAT GAGGAGAATTCGTGGAGCTG	NM_001114980.1	174
<i>BMI1</i>	GCTCGCATTCAATTTCTGCT ACACACATCAGGTGGGGATT	NM_005180.8	163
<i>K15</i>	CTACTTACCGCAGCCTGCTC CCACTTGGCCTGATGAGAGT	NM_002275.3	218
<i>K3</i>	GGATGTGGACAGTGCCTATATG AGATAGCTCAGCGTCGTAGAG	NM_057088.2	106

2.10. Statistical analysis

Statistical analysis was performed using Microsoft Excel 2010 and R Statistical Software (<https://www.r-project.org>). One-way analysis of variance (ANOVA) was used to analyse the significance of inter-group variation in the number of successful explants, contamination with fibroblast-like cells, marker staining and gene expression. Then, the Student *t*-test and Wilcoxon test were used to determine inter-pair significance and the *p*-value. $p < 0.05$ was considered statistically significant.

3. Results

3.1. Limbal epithelial cell growth and morphology

LECs grown on both plastic and fibrin were tightly packed in all three media, displaying cuboidal morphology and a high nucleocytoplasmic ratio. No difference in morphology between the experimental groups was observed (Fig. 1A).

Among the 233 explants plated on plastic, 79.7%, 65.5% and 57.3% of explants cultivated in COM, hSM and hPLM, respectively, gave rise to confluent cultures. The 138 explants plated on fibrin yielded similar percentages of successful cultures (COM, 73.4%; hSM, 72.7%; hPLM, 67.2%). There were no statistically significant inter-group differences (Fig. 1B).

When counted from growing explants, the cultures in hSM on plastic with no substrate had delayed growth onset compared to those in COM ($p < 0.001$) and hPLM ($p < 0.001$). On fibrin, LEC expansion in hPLM was delayed compared to both COM ($p < 0.001$) and hSM ($p < 0.01$). LECs cultured in COM and hSM on fibrin expanded significantly earlier ($p < 0.01$ and $p < 0.001$, respectively) and reached confluence more rapidly ($p < 0.001$) than cells cultured in the same media on plastic. On plastic, LECs cultured in COM were confluent significantly earlier than those in hSM ($p < 0.01$) and were harvested earlier than cultures in hPLM ($p < 0.001$). A similar trend was observed in the cultures cultivated on fibrin (Fig. 1C).

Fibroblast-like cell contamination (Fig. 1D) was observed under all tested conditions. It was more prominent in the explants grown on fibrin, although a significant difference was observed for COM only (plastic versus fibrin, $p < 0.01$). There was 0.5%, 8.2% and 21.2% fibroblast-like cell contamination in the cultures grown in COM, hSM and hPLM, respectively, on plastic. A significant increase was demonstrated only for cultures in hPLM compared to COM ($p < 0.05$). For cells expanded on fibrin, 17.7%, 15.4% and 47.6% of cultures in COM, hSM and hPLM, respectively, were contaminated, but only for cultures in hPLM compared to hSM the contamination was statistically significantly different ($p < 0.05$) (Fig. 1E).

3.2. Presence of limbal stem cell markers

Immunostaining for the limbal stem cell markers p63 α , ABCB5 and

Bmi-1 was detected in most of the cultured cells in all six conditions (Fig. 2). The average positive cell counts are shown in [supplementary fig. 1](#). There was a statistically higher percentage of p63 α -positive cells when LECs were cultured on plastic in COM as compared to hSM ($p < 0.05$) and hPLM ($p < 0.001$). On fibrin, there were significantly more p63 α -positive cells in comparison with plastic (hSM, $p < 0.01$; hPLM, $p < 0.001$). Compared to plastic, there were significantly more ABCB5-positive cells on fibrin cultivated in COM ($p < 0.001$), hSM ($p < 0.05$) and hPLM ($p < 0.01$) (Fig. 2, [supplementary fig. 1](#)). Co-localized p63 α and ABCB5 staining was observed in 82–91% of LECs cultivated on fibrin, whereas there was 41–66% co-localization in LECs cultured on plastic (data not shown). Bmi-1 staining was present in most of the cells across all experimental groups (75–97%), with no statistically significant difference (Fig. 2, [supplementary fig. 1](#)). No staining was present in negative controls, from which the primary antibody had been omitted.

The *TP63* gene expression of p63 α isotype was not statistically different among all groups, except for the cells cultivated in hSM, where its expression was significantly higher in LECs cultured on plastic compared to that grown on fibrin ($p < 0.05$) (Fig. 3B). *BMI1* expression was higher in LECs cultivated in COM on fibrin compared with LECs cultured in hSM ($p < 0.01$) and hPLM ($p < 0.01$) on fibrin, and was higher in cultures grown in COM on plastic when compared to LECs cultured in hPLM ($p < 0.05$) on plastic (Fig. 3B). No statistically significant difference was observed in expression of *K15* among all groups. Slightly higher expression of *K15* was observed only in cells cultured in hSM on plastic (Fig. 3B).

3.3. Presence of differentiated corneal epithelial cells

The number of differentiated K3/12-positive cells varied, being on average 15–43% in all cultures cultivated on both substrates in all media (Fig. 2, [supplementary fig. 1](#)). A significantly lower percentage of K3/12-positive cells was found only in cultures grown on plastic in hSM compared to hPLM ($p < 0.05$). These cultures also had significantly fewer K3/12-positive cells than cultures in hSM on fibrin ($p < 0.01$). Fewer K3/12-positive cells were also detected in LECs cultured on fibrin in COM compared to hSM ($p < 0.01$). *K3* gene expression was higher in LECs grown on plastic than on fibrin; however, only for cultures in COM ($p < 0.05$) and hSM ($p < 0.05$) a significant difference was observed, (Fig. 3B). The cultures on fibrin in hPLM had significantly higher *K3* expression when compared with that in COM ($p < 0.001$) and hSM ($p < 0.001$).

3.4. Cell proliferation

Cell proliferation was slightly lower in the cultures grown on plastic than on fibrin (Fig. 2, [supplemental fig. 1](#)); there was a significant difference only between cultures in COM ($p < 0.01$) and hSM ($p < 0.01$). Significantly increased number of proliferating cells was also found in cultures in hSM on fibrin compared to that in hPLM on fibrin ($p < 0.05$).

3.5. Apoptosis

There was no significant difference in the presence of apoptotic cells in cultures grown in all conditions. Apoptotic cells (TUNEL-stained) were rarely detected in cultures in hSM and hPLM on both substrates (up to 1%); however, there were slightly more apoptotic cells (up to 3%) in the cultures cultivated on plastic in COM (Fig. 2, [supplemental fig. 1](#)).

3.6. Colony forming efficiency assay

The CFE was performed for all experimental groups (Fig. 3A); however, it revealed no statistically significant differences. The average

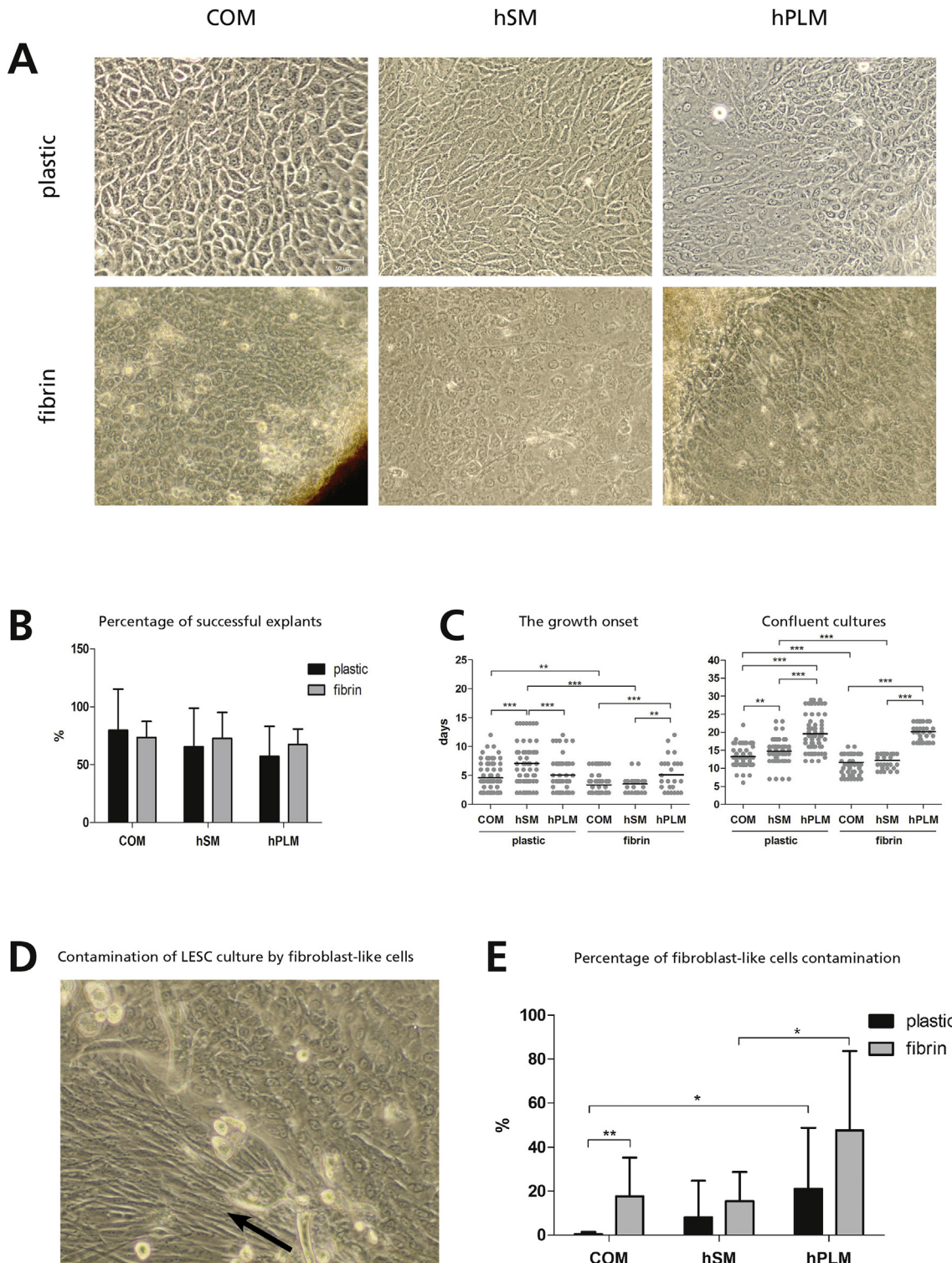


Fig. 1. LEC growth and morphology. Cell morphology in cultures cultivated in COM, hSM and hPLM on plastic or fibrin did not exhibit observable difference (A). Success rate of LEC cultures in relation to number of plated explants (B). The start of outgrowth of LEC cultures from day 0 (plating) until full confluence (harvest) (C). Fibroblast-like cell contamination (D) and the percentage of LEC cultures with contamination (E).

CFE values for cultures grown in COM on plastic were almost the same (3.97%) as that of cultures on fibrin (3.21%). The cultures in xeno-free media had slightly higher CFE on fibrin (hSM, 4.13%; hPLM, 4.48%) than on plastic (hSM, 2.42%; hPLM, 2.92%).

4. Discussion

This study highlights the possibility of using media containing autologous blood products (human serum or human platelet lysate) in combination with acellular substrate (fibrin) as a completely xeno-free condition for preparing LEC graft for patients with LSCD. The explant culture system is most commonly used in clinical studies using LEC

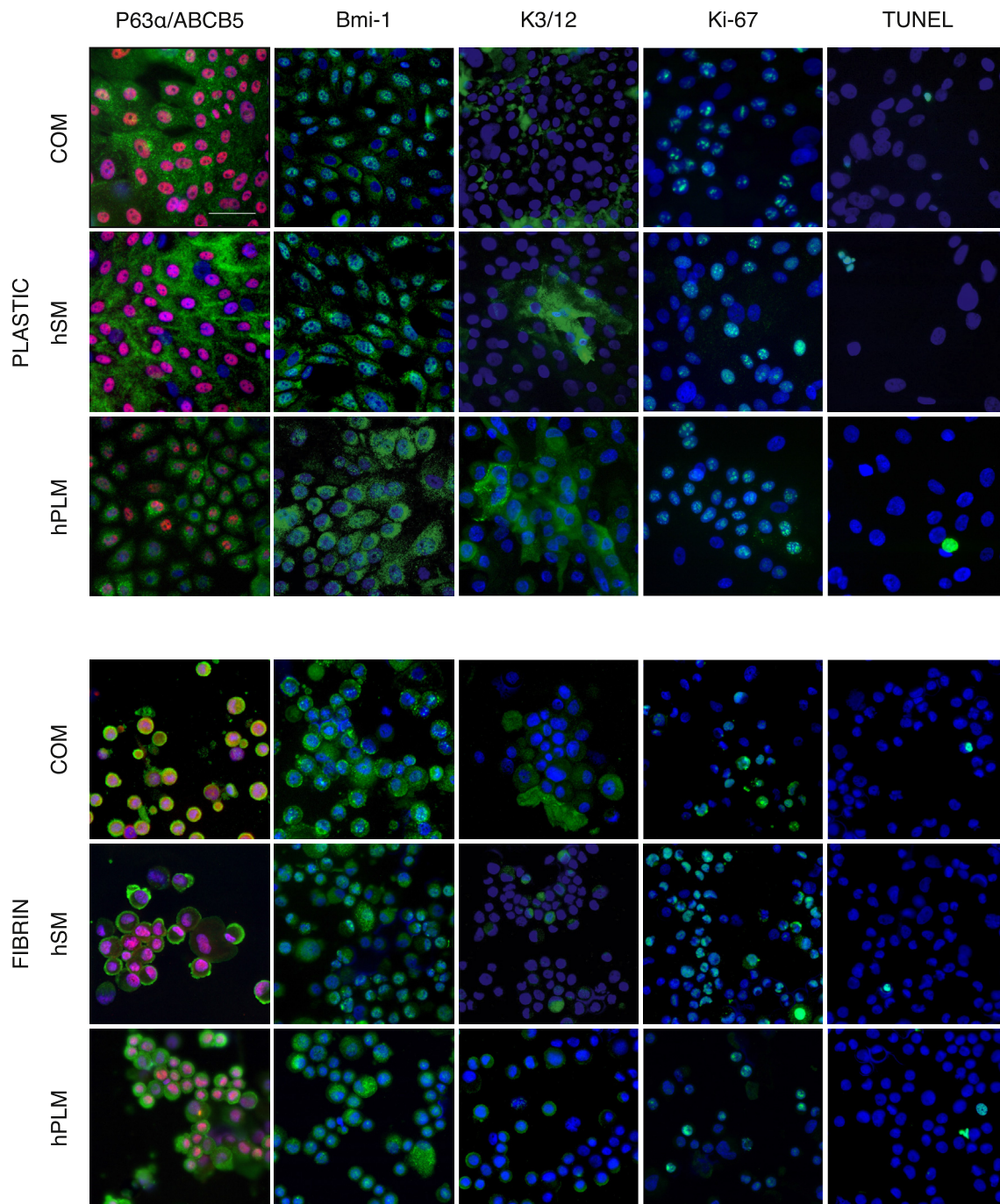


Fig. 2. Immunostaining for putative limbal stem cell markers p63 α (red), ABCB5 (green) and Bmi-1 (green), differentiated corneal epithelial cell marker K3/12 (green) and proliferating cell marker Ki-67 (green) and fluorescent staining of apoptotic LECs (green) cultivated either on plastic or on fibrin substrate in COM, hSM or hPLM. The round morphology of cells cultured previously on fibrin is a consequence of cell preparation for immunocytochemistry experiments by cytospin. Cell nuclei were counterstained with DAPI (blue). Scale bar represents 50 μ m.

grafts (Basu et al., 2012; Koizumi et al., 2001; Utheim et al., 2013). It is an advantageous method due to the maintenance of LESC native niche and no need for feeder layer support (typically, mouse embryonic cells), (Gonzalez and Deng, 2013). However, the lower yield of successfully growing explants (about 40%), (Lopez-Paniagua et al., 2016), represents the disadvantage of this method. In all our experimental conditions, 57% (hPLM, plastic) – 80% (COM, plastic) of explants gave rise to confluent cultures, which corresponds to explant expansion in FBS supplemented complex medium on amniotic membrane (Kethiri et al., 2017) or on plastic (Ghouby-Benallaoua et al., 2011).

The required time for limbal explants to reach confluence in COM

was approximately three weeks in our study, which is in accordance with previous results (Ghouby-Benallaoua et al., 2011; Lopez-Paniagua et al., 2016). However, as far as we know, there are no published studies comparing the cell growth kinetics of complex and xeno-free media employing rigorous statistical approach. The shortest time needed for the growth onset and reaching the confluence was achieved in both hSM and COM on fibrin. This may reflect the fact that fibrin promotes better cell attachment and growth (Reinertsen et al., 2014). On the other hand, cell growth in hPLM on this scaffold was significantly delayed than in COM and hSM, suggesting that hPLM does not support LECs growth rate as efficiently as COM and hSM.

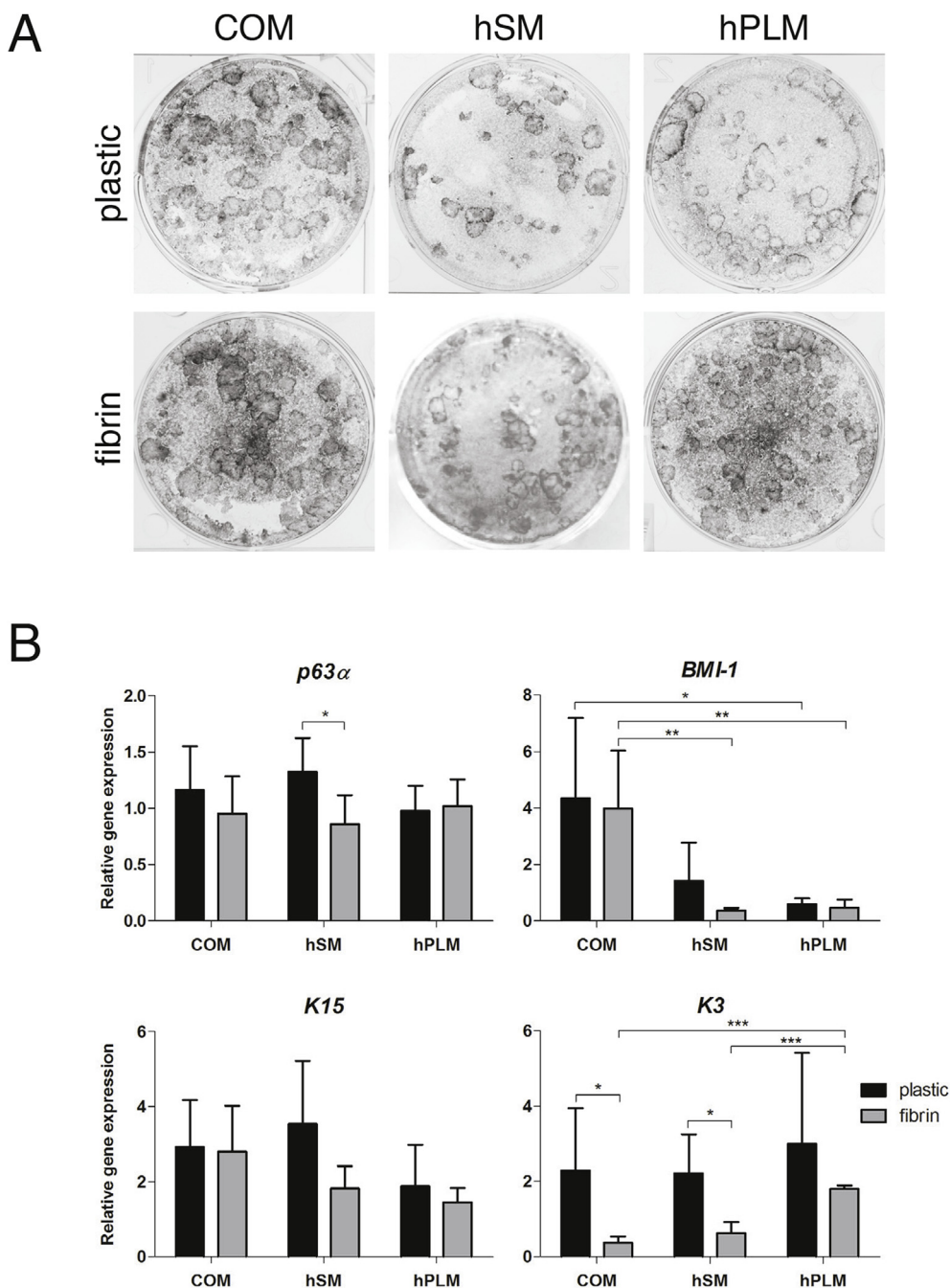


Fig. 3. Colony forming efficiency assay (A). Expression of p63α isotype of *TP63*, *BMI1*, *K15* and *K3* genes (B).

The contamination of cultures by other cell types, particularly stromal fibroblasts (Kethiri et al., 2017; Lopez-Paniagua et al., 2016) represents another challenge for the explant culture model. In our cultures, presence of fibroblast-like cells was observed in all conditions mainly during the later phase of cultivation, similarly as described previously (Kethiri et al., 2017; Polisetty et al., 2008). Generally, the contamination was lower on plastic than on fibrin substrate. However, from a clinical point of view, fibrin but not plastic is a material suitable for cell transfer to ocular surface. Irrespective of the scaffold, the most prominent fibroblast-like cell contamination was detected in cultures grown in hPLM, suggesting that hPL may stimulate their growth more effectively than human serum. The relatively high levels of contamination observed in our experiment could be also a consequence of explant preparation: we used a whole twelfth of the limbus (i.e. with full-thickness stroma). Studies using superficial limbal explants have

reported a lower degree of fibroblast-like cell contamination (Ghoubay-Benallaoua et al., 2011). On the other hand, presence of stromal fibroblast in LEC grafts may not have necessarily negative effect. The direct contact of basal limbal epithelial cells located in limbal crypts and underlying stromal cells (Dziasko et al., 2014) as well as maintenance of LECs in a progenitor-like state based on cross-talks between the LECs and stromal fibroblasts (Notara et al., 2010) has been described previously. Furthermore, the positive effect of stromal stem cells on corneal scarring prevention has been demonstrated on animal model (Basu et al., 2014).

If an LEC graft prepared on fibrin contained more than 3% of p63-positive, holoclone-forming LECs, the transplantation of such a graft achieves a high success rate (about 76%). If not, only 11% of patients develop a stable ocular surface (Rama et al., 2010). High success rate was also reported when amniotic membrane was used for LEC grafts

(Sangwan et al., 2011) or when using complex medium containing either FBS or autologous serum (Nakamura et al., 2006).

The presence of putative stem cell markers p63 α , Bmi-1 and K15 are generally used for evaluation of stemness of LEC cultures (Kramerov et al., 2015; Meyer-Blazejewska et al., 2010; Utheim et al., 2015), and ABCB5 was recently shown to be required for normal LESC function and high success rate of grafting (Ksander et al., 2014). In our study, more than 50% of cells were stained for the used putative stem cell markers in all conditions. This is in agreement with 40–60% p63- and ABCB5-positive cells in LEC cultures grown in COM on plastic (Li et al., 2017; Lopez-Paniagua et al., 2013; Loureiro et al., 2013). There were statistically significantly more p63 α -positive cells in COM compared to xeno-free media on untreated plastic, but we did not find any significant difference in gene *TP63* expression of p63 α isotype in cells grown in these three media. Similarly, Suri et al. did not find any difference in p63 α expression cells cultured in COM with FBS compared to hPL-containing medium (Suri et al., 2016). In agreement with previous results (Forni et al., 2013; Han et al., 2002), our data suggest that the fibrin scaffold maintains LESC stemness, as statistically higher percentages of p63 α - and ABCB5-positive cells were detected on fibrin relative to untreated plastic plates in all three media. LECs cultured in COM on both plastic and fibrin revealed significantly higher expression of another putative stem cells marker - *BMI1* - compared to those cultured in the non-xenogeneic media. The immunostaining, however, did not reveal any statistically significant difference. The discrepancy between the qPCR and immunostaining findings may be explained by the fact that qPCR reflects the relative amount of mRNA while immunofluorescence analyses the number of positive cells and not the amount of protein expressed in each sample. Therefore, the qPCR results cannot be directly compared with the immunostaining findings (Lopez-Paniagua et al., 2013). The expression of *K15* showed no significant difference in LECs grown in any of tested condition. This correlates well with results of others (Ang et al., 2011; Pathak et al., 2016) as well as with expression pattern of p63 α isotype of *TP63* gene shown in this study.

The CFE assay revealed no significant difference among the experimental groups. The total CFE of all tested experimental groups was 2.4–4.5%, which is in agreement with previous reports describing 2–9% stem cells in *ex vivo* cultivated limbal grafts (Lopez-Paniagua et al., 2016; Schwab et al., 2000).

A higher number of K3/12-positive cells during culture indicates increased progression to differentiation into mature corneal epithelial cells *in vitro* (Ghoubay-Benallaoua et al., 2011; Song et al., 2005). About 60–80% K3- and K12-positive cells in COM on untreated plastic has been reported recently (Li et al., 2017; Lopez-Paniagua et al., 2016; Loureiro et al., 2013). We found < 43% K3/12-stained cells in all conditions; cultures in hSM on plastic had the lowest population, about 15% of positive cells. Our findings reveal higher *K3* gene expression in the xeno-free media compared to COM on fibrin as well as in hPLM compared to hSM on both plastic and fibrin, although statistical significance was not proved for all values/groups. This indicates that particularly hPLM, in which hPL is the only supplement, better supports the cell differentiation towards the corneal epithelium phenotype compared to other media. Immunocytochemical analysis revealed a higher percentage of K3/12-stained cells from the cultures in xeno-free media on fibrin than on plastic. Nevertheless, these results were not confirmed by gene expression. Fewer K3-positive cells on fibrin as compared to cells on a non-coated surface has also been reported (Forni et al., 2013). The discrepancy between the immunostaining and gene expression results may be explained by the binding specificity of the antibody used as it binds not only K3 but also K12. Moreover, it is possible that even though a higher percentage of cells grown on fibrin were K3/12-positive, the level of *K3* gene expression was much lower in these cells than in those cultivated on plastic.

The cell cycle marker Ki-67 indicating the population of all dividing cells (Scholzen and Gerdes, 2000) was detected in comparable amounts

in all three media on plastic; nonetheless, the cells grown in COM and hSM on fibrin exhibited significantly higher proliferative activity, which corresponds well with a previous report (Forni et al., 2013).

A low rate of apoptosis observed in our cultures, with no significant difference among the studied conditions, is in agreement with the results of cultures grown in COM and hSM on untreated plates or amniotic membrane (Pathak et al., 2016; Shahdadfar et al., 2012). This contradicts other reports describing an increased number of dying cells in cultures grown on plastic as compared to various biomaterials (Ahmadiankia et al., 2009; Sun et al., 2006).

5. Conclusion

In this study, we demonstrate that from the two non-xenogeneic media, hSM combined with fibrin as a scaffold yields LEC cultures of the same or better quality compared to COM. The use of hPLM showed to be slightly less efficient. Although conditions employing complex media containing xenogeneic or otherwise problematic components have successfully been used in some countries, entirely xeno-free grafts are necessary to ensure maximum patient safety. Our work contributes to the establishment of a standardized protocol, which uses non-xenogeneic culture conditions and assures adequate growth rate and stemness maintenance of LECs. A xeno-free culture protocol would contribute substantially to improving the safety of LEC transplantations in patients with LSCD.

Acknowledgements

This study was supported by Norwegian Financial Mechanism 2009–2014 and the Ministry of Education, Youth and Sports under Project Contract No. MSMT-28477/2014, (7F14156) and by research project BBMRI_CZ LM2015089. PT was supported by SVV, project 260367/2017 and PS by GAUK 250361/2017 and SVV 260367/2017. Institutional support was provided by Progres-Q25 and 26/LF1 and UNCE 204064.

Appendix A. Supplementary data

Supplementary data related to this article can be found at <http://dx.doi.org/10.1016/j.exer.2018.06.019>.

References

- Ahmadiankia, N., Ebrahimi, M., Hosseini, A., Baharvand, H., 2009. Effects of different extracellular matrices and co-cultures on human limbal stem cell expansion *in vitro*. *Cell Biol. Int.* 33, 978–987.
- Ang, L.P., Do, T.P., Thein, Z.M., Reza, H.M., Tan, X.W., Yap, C., Tan, D.T., Beuerman, R.W., 2011. *Ex vivo* expansion of conjunctival and limbal epithelial cells using cord blood serum-supplemented culture medium. *Invest. Ophthalmol. Vis. Sci.* 52, 6138–6147.
- Barrandon, Y., Green, H., 1987. Three clonal types of keratinocyte with different capacities for multiplication. *Proc. Natl. Acad. Sci. U. S. A.* 84, 2302–2306.
- Basu, S., Ali, H., Sangwan, V.S., 2012. Clinical outcomes of repeat autologous cultivated limbal epithelial transplantation for ocular surface burns. *Am. J. Ophthalmol.* 153, 643–650. [e641–642](https://doi.org/10.1016/j.ajo.2012.04.042).
- Basu, S., Hertsberg, A.J., Funderburgh, M.L., Burrow, M.K., Mann, M.M., Du, Y., Lathrop, K.L., Syed-Picard, F.N., Adams, S.M., Birk, D.E., Funderburgh, J.L., 2014. Human limbal biopsy-derived stromal stem cells prevent corneal scarring. *Sci. Transl. Med.* 6, 266ra172.
- Castro-Munozledo, F., Gomez-Flores, E., 2011. Challenges to the study of asymmetric cell division in corneal and limbal epithelia. *Exp. Eye Res.* 92, 4–9.
- Davanger, M., Evensen, A., 1971. Role of the pericorneal papillary structure in renewal of corneal epithelium. *Nature* 229, 560–561.
- Di Girolamo, N., Bosch, M., Zamora, K., Coroneo, M.T., Wakefield, D., Watson, S.L., 2009. A contact lens-based technique for expansion and transplantation of autologous epithelial progenitors for ocular surface reconstruction. *Transplantation* 87, 1571–1578.
- Dziasko, M.A., Armer, H.E., Levis, H.J., Shortt, A.J., Tuft, S., Daniels, J.T., 2014. Localisation of epithelial cells capable of holoclone formation *in vitro* and direct interaction with stromal cells in the native human limbal crypt. *PLoS One* 9, e94283.
- Eppley, B.L., Woodell, J.E., Higgins, J., 2004. Platelet quantification and growth factor analysis from platelet-rich plasma: implications for wound healing. *Plast. Reconstr.*

- Surg. 114, 1502–1508.
- Forni, M.F., Loureiro, R.R., Cristovam, P.C., Bonatti, J.A., Sogayar, M.C., Gomes, J.A., 2013. Comparison between different biomaterial scaffolds for limbal-derived stem cells growth and enrichment. *Curr. Eye Res.* 38, 27–34.
- Ghoubay-Benallaoua, D., Basli, E., Goldschmidt, P., Pecha, F., Chaumeil, C., Laroche, L., Borderie, V., 2011. Human epithelial cell cultures from superficial limbal explants. *Mol. Vis.* 17, 341–354.
- Gonzalez, S., Deng, S.X., 2013. Presence of native limbal stromal cells increases the expansion efficiency of limbal stem/progenitor cells in culture. *Exp. Eye Res.* 116, 169–176.
- Han, B., Schwab, I.R., Madsen, T.K., Isseroff, R.R., 2002. A fibrin-based bioengineered ocular surface with human corneal epithelial stem cells. *Cornea* 21, 505–510.
- Jeon, S., Choi, S.H., Wolosin, J.M., Chung, S.H., Joo, C.K., 2013. Regeneration of the corneal epithelium with conjunctival epithelial equivalents generated in serum- and feeder-cell-free media. *Mol. Vis.* 19, 2542–2550.
- Kethiri, A.R., Basu, S., Shukla, S., Sangwan, V.S., Singh, V., 2017. Optimizing the role of limbal explant size and source in determining the outcomes of limbal transplantation: an in vitro study. *PLoS One* 12, e0185623.
- Koizumi, N., Inatomi, T., Suzuki, T., Sotozono, C., Kinoshita, S., 2001. Cultivated corneal epithelial stem cell transplantation in ocular surface disorders. *Ophthalmology* 108, 1569–1574.
- Kramerov, A.A., Saghizadeh, M., Maguen, E., Rabinowitz, Y.S., Ljubimov, A.V., 2015. Persistence of reduced expression of putative stem cell markers and slow wound healing in cultured diabetic limbal epithelial cells. *Mol. Vis.* 21, 1357–1367.
- Ksander, B.R., Kolovou, P.E., Wilson, B.J., Saab, K.R., Guo, Q., Ma, J., McGuire, S.P., Gregory, M.S., Vincent, W.J., Perez, V.L., Cruz-Guilloty, F., Kao, W.W., Call, M.K., Tucker, B.A., Zhan, Q., Murphy, G.F., Lathrop, K.L., Alt, C., Mortensen, L.J., Lin, C.P., Zieske, J.D., Frank, M.H., Frank, N.Y., 2014. ABCB5 is a limbal stem cell gene required for corneal development and repair. *Nature* 511, 353–357.
- Lehrer, M.S., Sun, T.T., Lavker, R.M., 1998. Strategies of epithelial repair: modulation of stem cell and transit amplifying cell proliferation. *J. Cell Sci.* 111 (Pt 19), 2867–2875.
- Li, Y., Yang, Y., Yang, L., Zeng, Y., Gao, X., Xu, H., 2017. Poly(ethylene glycol)-modified silk fibroin membrane as a Carrier for limbal epithelial stem cell transplantation in a rabbit LSCD model. *Stem Cell Res. Ther.* 8, 256.
- Llames, S., Garcia-Perez, E., Meana, A., Larcher, F., del Rio, M., 2015. Feeder layer cell actions and applications. *Tissue Eng. B Rev.* 21, 345–353.
- Lopez-Paniagua, M., Nieto-Miguel, T., de la Mata, A., Dziasko, M., Galindo, S., Rey, E., Herreras, J.M., Corrales, R.M., Daniels, J.T., Calonge, M., 2016. Comparison of functional limbal epithelial stem cell isolation methods. *Exp. Eye Res.* 146, 83–94.
- Lopez-Paniagua, M., Nieto-Miguel, T., de la Mata, A., Galindo, S., Herreras, J.M., Corrales, R.M., Calonge, M., 2013. Consecutive expansion of limbal epithelial stem cells from a single limbal biopsy. *Curr. Eye Res.* 38, 537–549.
- Loureiro, R.R., Cristovam, P.C., Martins, C.M., Covre, J.L., Sobrinho, J.A., Ricardo, J.R., Hazarbasanov, R.M., Hofling-Lima, A.L., Belfort Jr., R., Nishi, M., Gomes, J.A., 2013. Comparison of culture media for ex vivo cultivation of limbal epithelial progenitor cells. *Mol. Vis.* 19, 69–77.
- Meyer-Blazejewska, E.A., Kruse, F.E., Bitterer, K., Meyer, C., Hofmann-Rummelt, C., Wunsch, P.H., Schlotzer-Schrehardt, U., 2010. Preservation of the limbal stem cell phenotype by appropriate culture techniques. *Invest. Ophthalmol. Vis. Sci.* 51, 765–774.
- Nakamura, T., Inatomi, T., Sotozono, C., Ang, L.P., Koizumi, N., Yokoi, N., Kinoshita, S., 2006. Transplantation of autologous serum-derived cultivated corneal epithelial equivalents for the treatment of severe ocular surface disease. *Ophthalmology* 113, 1765–1772.
- Nakamura, T., Inatomi, T., Sotozono, C., Koizumi, N., Kinoshita, S., 2004. Successful primary culture and autologous transplantation of corneal limbal epithelial cells from minimal biopsy for unilateral severe ocular surface disease. *Acta Ophthalmol. Scand.* 82, 468–471.
- Notara, M., Bullett, N.A., Deshpande, P., Haddow, D.B., MacNeil, S., Daniels, J.T., 2007. Plasma polymer coated surfaces for serum-free culture of limbal epithelium for ocular surface disease. *J. Mater. Sci. Mater. Med.* 18, 329–338.
- Notara, M., Shortt, A.J., Galatowicz, G., Calder, V., Daniels, J.T., 2010. IL6 and the human limbal stem cell niche: a mediator of epithelial-stromal interaction. *Stem Cell Res.* 5, 188–200.
- Pathak, M., Olstad, O.K., Drolsum, L., Moe, M.C., Smorodina, N., Kalasova, S., Jirsova, K., Nicolais, B., Noer, A., 2016. The effect of culture medium and Carrier on explant culture of human limbal epithelium: a comparison of ultrastructure, keratin profile and gene expression. *Exp. Eye Res.* 153, 122–132.
- Pellegrini, G., Ardigo, D., Milazzo, G., Iotti, G., Guatelli, P., Pelosi, D., De Luca, M., 2018. Navigating market authorization: the path holoclar took to become the first stem cell product approved in the european union. *Stem Cells Transl Med* 7, 146–154.
- Pellegrini, G., Rama, P., Di Rocco, A., Panaras, A., De Luca, M., 2014. Concise review: hurdles in a successful example of limbal stem cell-based regenerative medicine. *Stem Cell.* 32, 26–34.
- Pellegrini, G., Traverso, C.E., Franzì, A.T., Zingirian, M., Cancedda, R., De Luca, M., 1997. Long-term restoration of damaged corneal surfaces with autologous cultivated corneal epithelium. *Lancet* 349, 990–993.
- Polisetty, N., Fatima, A., Madhira, S.L., Sangwan, V.S., Vemuganti, G.K., 2008. Mesenchymal cells from limbal stroma of human eye. *Mol. Vis.* 14, 431–442.
- Rama, P., Bonini, S., Lambiase, A., Golisano, O., Paterna, P., De Luca, M., Pellegrini, G., 2001. Autologous fibrin-cultured limbal stem cells permanently restore the corneal surface of patients with total limbal stem cell deficiency. *Transplantation* 72, 1478–1485.
- Rama, P., Matuska, S., Paganoni, G., Spinelli, A., De Luca, M., Pellegrini, G., 2010. Limbal stem-cell therapy and long-term corneal regeneration. *N. Engl. J. Med.* 363, 147–155.
- Ramirez, B.E., Sanchez, A., Herreras, J.M., Fernandez, I., Garcia-Sancho, J., Nieto-Miguel, T., Calonge, M., 2015. Stem cell therapy for corneal epithelium regeneration following good manufacturing and clinical procedures. *BioMed Res. Int.* 2015, 408495.
- Reinertsen, E., Skinner, M., Wu, B., Tawil, B., 2014. Concentration of fibrin and presence of plasminogen affect proliferation, fibrinolytic activity, and morphology of human fibroblasts and keratinocytes in 3D fibrin constructs. *Tissue Eng. Part A* 20, 21–22.
- Sangwan, V.S., Basu, S., Vemuganti, G.K., Sejal, K., Subramaniam, S.V., Bandyopadhyay, S., Krishnaiah, S., Gaddipati, S., Tiwari, S., Balasubramanian, D., 2011. Clinical outcomes of xeno-free autologous cultivated limbal epithelial transplantation: a 10-year study. *Br. J. Ophthalmol.* 95, 1525–1529.
- Shahdadar, A., Haug, K., Pathak, M., Drolsum, L., Olstad, O.K., Johnsen, E.O., Petrovski, G., Moe, M.C., Nicolais, B., 2012. Ex vivo expanded autologous limbal epithelial cells on amniotic membrane using a culture medium with human serum as single supplement. *Exp. Eye Res.* 97, 1–9.
- Sharma, A., Coles, W.H., 1989. Kinetics of corneal epithelial maintenance and graft loss. A population balance model. *Invest. Ophthalmol. Vis. Sci.* 30, 1962–1971.
- Sheth, R., Neale, M.H., Shortt, A.J., Massie, I., Vernon, A.J., Daniels, J.T., 2015. Culture and characterization of oral mucosal epithelial cells on a fibrin gel for ocular surface reconstruction. *Curr. Eye Res.* 40, 1077–1087.
- Shortt, A.J., Bunce, C., Levis, H.J., Blows, P., Dore, C.J., Vernon, A., Secker, G.A., Tuft, S.J., Daniels, J.T., 2014. Three-year outcomes of cultured limbal epithelial allografts in aniridia and Stevens-Johnson syndrome evaluated using the Clinical Outcome Assessment in Surgical Trials assessment tool. *Stem Cells Transl Med* 3, 265–275.
- Shortt, A.J., Secker, G.A., Notara, M.D., Limb, G.A., Khaw, P.T., Tuft, S.J., Daniels, J.T., 2007. Transplantation of ex vivo cultured limbal epithelial stem cells: a review of techniques and clinical results. *Surv. Ophthalmol.* 52, 483–502.
- Schermer, A., Galvin, S., Sun, T.T., 1986. Differentiation-related expression of a major 64K corneal keratin in vivo and in culture suggests limbal location of corneal epithelial stem cells. *J. Cell Biol.* 103, 49–62.
- Scholzen, T., Gerdes, J., 2000. The Ki-67 protein: from the known and the unknown. *J. Cell. Physiol.* 182, 311–322.
- Schwab, I.R., Isseroff, R.R., 2000. Bioengineered corneas—the promise and the challenge. *N. Engl. J. Med.* 343, 136–138.
- Schwab, I.R., Reyes, M., Isseroff, R.R., 2000. Successful transplantation of bioengineered tissue replacements in patients with ocular surface disease. *Cornea* 19, 421–426.
- Song, E., Yang, W., Cui, Z.H., Dong, Y., Sui, D.M., Guan, X.K., Ma, Y.L., 2005. Transplantation of human limbal cells cultivated on amniotic membrane for reconstruction of rat corneal epithelium after alkaline burn. *Chin Med J (Engl)* 118, 927–935.
- Sun, C.C., Su Pang, J.H., Cheng, C.Y., Cheng, H.F., Lee, Y.S., Ku, W.C., Hsiao, C.H., Chen, J.K., Yang, C.M., 2006. Interleukin-1 receptor antagonist (IL-1RA) prevents apoptosis in ex vivo expansion of human limbal epithelial cells cultivated on human amniotic membrane. *Stem Cell.* 24, 2130–2139.
- Suri, K., Gong, H.K., Yuan, C., Kaufman, S.C., 2016. Human platelet lysate as a replacement for fetal bovine serum in limbal stem cell therapy. *Curr. Eye Res.* 41, 1266–1273.
- Talbot, M., Carrier, P., Giasson, C.J., Deschambeault, A., Guerin, S.L., Auger, F.A., Bazin, R., Germain, L., 2006. Autologous transplantation of rabbit limbal epithelia cultured on fibrin gels for ocular surface reconstruction. *Mol. Vis.* 12, 65–75.
- Trosan, P., Svobodova, E., Chudickova, M., Krulova, M., Zajicova, A., Holan, V., 2012. The key role of insulin-like growth factor I in limbal stem cell differentiation and the corneal wound-healing process. *Stem Cell. Dev.* 21, 3341–3350.
- Tsai, R.J., Li, L.M., Chen, J.K., 2000. Reconstruction of damaged corneas by transplantation of autologous limbal epithelial cells. *N. Engl. J. Med.* 343, 86–93.
- Tseng, S.C., 1989. Concept and application of limbal stem cells. *Eye (Lond)* 3 (Pt 2), 141–157.
- Utheim, O., Islam, R., Lyberg, T., Roald, B., Eidet, J.R., de la Paz, M.F., Dartt, D.A., Raeder, S., Utheim, T.P., 2015. Serum-free and xenobiotic-free preservation of cultured human limbal epithelial cells. *PLoS One* 10, e0118517.
- Utheim, T.P., Lyberg, T., Raeder, S., 2013. The culture of limbal epithelial cells. *Meth. Mol. Biol.* 1014, 103–129.
- Yu, M., Bojic, S., Figueiredo, G.S., Rooney, P., de Havilland, J., Dickinson, A., Figueiredo, F.C., Lako, M., 2016. An important role for adenine, cholera toxin, hydrocortisone and triiodothyronine in the proliferation, self-renewal and differentiation of limbal stem cells in vitro. *Exp. Eye Res.* 152, 113–122.
- Zakaria, N., Possemiers, T., Dhuhghail, S.N., Leysens, I., Rozema, J., Koppen, C., Timmermans, J.P., Berneman, Z., Tassignon, M.J., 2014. Results of a phase I/II clinical trial: standardized, non-xenogenic, cultivated limbal stem cell transplantation. *J. Transl. Med.* 12, 58.

References to websites

- R Development Core Team, 2008. R: a language and environment for statistical computing. R Foundation for Statistical Computing, Vienna, Austria ISBN 3-900051-07-0. <http://www.r-project.org>.

Appendix 2

Stadnikova A, **Trosan P**, Skalicka P, Utheim T P, Jirsova K: Interleukin-13 maintains the stemness of conjunctival epithelial cell cultures prepared from human limbal explants. PLoS One. 2019 Feb 11;14(2):e0211861. Doi: 10.1371/journal.pone.0211861. PMID: 30742646.

RESEARCH ARTICLE

Interleukin-13 maintains the stemness of conjunctival epithelial cell cultures prepared from human limbal explants

Andrea Stadnikova¹✉, Peter Trosan¹✉, Pavlina Skalicka², Tor Paaske Utheim^{3,4}, Katerina Jirsova¹✉*

1 Laboratory of the Biology and Pathology of the Eye, Institute of Biology and Medical Genetics, First Faculty of Medicine, Charles University and General University Hospital in Prague, Prague, Czech Republic, **2** Department of Ophthalmology, First Faculty of Medicine, Charles University and General University Hospital in Prague, Prague, Czech Republic, **3** Department of Medical Biochemistry, Oslo University Hospital, Oslo, Norway, **4** Department of Plastic and Reconstructive Surgery, Oslo University Hospital, Oslo, Norway

✉ These authors contributed equally to this work.

* katerina.jirsova@lf1.cuni.cz



OPEN ACCESS

Citation: Stadnikova A, Trosan P, Skalicka P, Utheim TP, Jirsova K (2019) Interleukin-13 maintains the stemness of conjunctival epithelial cell cultures prepared from human limbal explants. PLoS ONE 14(2): e0211861. <https://doi.org/10.1371/journal.pone.0211861>

Editor: Alexander V. Ljubimov, Cedars-Sinai Medical Center, UNITED STATES

Received: October 18, 2018

Accepted: January 23, 2019

Published: February 11, 2019

Copyright: © 2019 Stadnikova et al. This is an open access article distributed under the terms of the [Creative Commons Attribution License](https://creativecommons.org/licenses/by/4.0/), which permits unrestricted use, distribution, and reproduction in any medium, provided the original author and source are credited.

Data Availability Statement: All relevant data are within the paper and its Supporting Information files.

Funding: This study was supported by Norwegian Financial Mechanism 2009-2014 and the Ministry of Education, Youth and Sports under Project Contract No. MSMT-28477/2014, project 7F14156 (AS, PT, KJ) - <http://www.msmt.cz/vyzkum-a-vyvoj-2/projects> and by research project BBMRI_CZ LM2015089 (PT, KJ) - <http://biobanka.lf1.cuni.cz/>. PT was supported by SVV 260367/

Abstract

To use human limbal explants as an alternative source for generating conjunctival epithelium and to determine the effect of interleukin-13 (IL-13) on goblet cell number, mucin expression, and stemness. Human limbal explants prepared from 17 corneoscleral rims were cultured with or without IL-13 (IL-13+ and IL-13-, respectively) and followed up to passage 2 (primary culture [P0]–P2). Cells were characterized by alcian blue/periodic acid–Schiff (AB/PAS) staining (goblet cells); immunofluorescent staining for p63α (progenitor cells), Ki-67 (proliferation), MUC5AC (mucin, goblet cells), and keratin 7 (K7, conjunctival epithelial and goblet cells); and by quantitative real-time polymerase chain reaction for expression of the p63α (*TP63*), *MUC5AC*, *MUC4* (conjunctival mucins), *K3*, *K12* (corneal epithelial cells), and *K7* genes. Clonogenic ability was determined by colony-forming efficiency (CFE) assay. Using limbal explants, we generated epithelium with conjunctival phenotype and high viability in P0, P1, and P2 cultures under IL-13+ and IL-13- conditions, i.e., epithelium with strong K7 positivity, high *K7* and *MUC4* expression and the presence of goblet cells (AB/PAS and MUC5AC positivity; *MUC5AC* expression). p63α positivity was similar in IL-13+ and IL-13- cultures and was decreased in P2 cultures; however, there was increased *TP63* expression in the presence of IL-13 (especially in the P1 cultures). Similarly, IL-13 increased proliferative activity in P1 cultures and significantly promoted P0 and P1 culture CFE. IL-13 did not increase goblet cell number in the P0–P2 cultures, nor did it influence *MUC5AC* and *MUC4* expression. By harvesting unattached cells on day 1 of P1 we obtained goblet cell rich subpopulation showing AB/PAS, MUC5AC, and K7 positivity, but with no growth potential. In conclusion, limbal explants were successfully used to develop conjunctival epithelium with the presence of putative stem and goblet cells and with the ability to preserve the stemness of P0 and P1 cultures under IL-13 influence.

2017 - <http://www.cuni.cz/UK-3362.html> and PS by GAUK 250361/2017 - <https://www.cuni.cz/UK-33.html> and SVV 260367/2017 - <http://www.cuni.cz/UK-3362.html>. Institutional support was provided by Progres-Q25 206025-5 (PT, KJ) - <https://www.cuni.cz/UK-7368.html> and UNCE 204064 (PT) - <https://www.cuni.cz/UK-3761.html>. Oslo University Hospital, Oslo, Norway (TPU) - <https://www.uio.no>. The funders had no role in study design, data collection and analysis, decision to publish, or preparation of the manuscript.

Competing interests: The authors have declared that no competing interests exist.

Introduction

The conjunctiva is composed of a non-keratinizing stratified epithelium with interspersed goblet cells (GCs) and a vascularized stroma. It contributes to the integrity of the ocular surface by producing the mucin component of the tear film, forming a mechanical barrier against pathogens and being a part of the mucosal immune defense system [1–4]. Mucins are high-molecular weight glycoproteins that lubricate the ocular surface and stabilize the ocular film. Human GCs secrete the gel-forming mucin MUC5AC, soluble MUC2, and membrane-associated MUC16. Corneal and conjunctival epithelial cells express the membrane-associated MUC1 and MUC16, while MUC4 is prevalently expressed by conjunctival cells [3, 5].

Corneal epithelium is maintained by limbal stem cells located in palisades of Vogt [6]. Conjunctival stem cells are bipotential and give rise to both epithelial cells and GCs [7]. Stem cells are distributed throughout the conjunctival tissue, with density being highest in the nasal part of the lower fornix and the medial canthus [8, 9], where GC density is also the highest [2]. Differentiation into GCs occurs later during the stem cell life cycle at the stage of transient amplifying cell [7]. GCs can be generated also from limbal epithelial cells influenced by the conjunctival environment [10].

The effect of interleukin-13 (IL-13), a T helper 2-type cytokine [11], on GCs and mucus production in healthy and diseased tissues has been intensively studied in other tissues, for example airway epithelium [12]. In conjunctiva, increase of IL-13 is believed to be involved in the pathogenesis of conjunctival immune diseases involving stimulation of GC numbers, mucus production and fibroblasts proliferation (atopic and vernal keratoconjunctivitis, giant papillary conjunctivitis, mucous membrane pemphigoid) [13–16]. Moreover, it appears that its presence in healthy conjunctival tissue is necessary for GC differentiation and homeostasis [17]. In epidermal tissue, IL-13 could be important for protection against environmental stressors and carcinogenesis [18]. So far, only a few studies have focused on IL-13 and conjunctival tissue prepared *in vitro* [19–22]. In *in vitro* murine experiments, IL-13 stimulated conjunctival GC proliferation [19–21]; however, its effect on MUC5AC is inconsistent; one study showed it had no effect on MUC5AC secretion [20], and another reported a stimulatory effect [19]. The addition of IL-13 to human conjunctival epithelial cell cultures stimulated MUC5AC secretion [22]; however, its effect on GC numbers or MUC5AC expression in human conjunctival tissue prepared *in vitro* has not been studied so far.

Ocular surface deterioration associated with dry eye, conjunctival damage, and scarring is usually accompanied by decreased or even absent GCs and mucin (for review see [3, 23]). Most diseases or conditions affecting the ocular surface are related to the destruction of both the corneal and conjunctival epithelium, i.e., reconstruction in such cases requires the regeneration of both tissues [24]. Experiments on the development of human tissue-engineered conjunctival equivalents have been underway for almost 30 years [25, 26]; the search for convenient cultivation conditions continues because engineering full-fledged conjunctival tissue from two cell types is much more complicated in comparison to that for corneal epithelium composed of only epithelial cells. Thus, so far experimental studies using cultured conjunctival epithelial cells for conjunctival reconstruction prevail [26, 27] and studies in patients are very rare [28]. However, the rationale for improving the culture protocols for human conjunctival epithelial cell sheets is substantiated by their ability to treat limbal stem cell deficiency (LSCD) without the need for immunosuppression in cases where autologous limbal tissue is not available (e.g. bilateral total LSCD) [24, 29–31].

Following the landmark publication by Rama *et al.* published in 2010 [32] demonstrating that the percentage of a marker for undifferentiated cells in transplanted sheets is linked to success following transplantations in patients with LSCD, research on how to support the

maintenance of stemness in cultured sheets intended for ocular surface reconstruction has significantly gained momentum. In light of this, we herein explored to what extent IL-13 could influence the stemness of cultured conjunctival cells. In addition, we tested whether explant culture from human corneoscleral rims could be used for engineering conjunctival epithelium and evaluated the influence of human recombinant IL-13 on GC numbers and mucin expression in the conjunctival cultures.

Materials and methods

Tissue specimens

The study followed the standards of the Ethics Committees of the General Teaching Hospital and the First Faculty of Medicine of Charles University, Prague, Czech Republic (Ethics Committee approval no. 8/14 held on January 23, 2014), and adhered to the tenets set out in the Declaration of Helsinki. We obtained human cadaver corneoscleral rims from 17 donors, which were surplus from surgery and stored in Eusol-C (Alchimia, Padova, Italy), from the Department of Ophthalmology, General University Hospital in Prague, Czech Republic, for the study. On the use of the corneoscleral rims, based on Czech legislation on specific health services (Law Act No. 372/2011 Coll.), informed consent is not required if the presented data are anonymized in the form. The mean donor age \pm standard deviation (SD) was 63.5 ± 6.5 years. The tissue was collected within 24 h from death. After the surgery, the corneoscleral rims were stored in Eusol-C at 4°C until limbal explants were prepared for cultivation. The mean storage time \pm SD (from tissue collection until explantation) was 6.2 ± 3.2 days. Conjunctival impression cytology was performed on two healthy adult volunteers who had provided informed consent (EK-2370/14 S-IV approved on 12/11/2014). Conjunctival tissue with pterygium was harvested from two patients at the Department of Ophthalmology, General University Hospital in Prague, Czech Republic. Patients provided informed consent before the pterygium removal surgery (EK-1570/11 S-IV approved on 10/13/2011).

Limbal explants and cell culture

The surplus cornea and sclera of the corneoscleral rims were cut off, and then the limbal portion, including the residual conjunctival tissue, was cut into 12 pieces (approximately 2×3 mm) and placed corneconjunctival epithelial side down in a 24-well plate (TPP Techno Plastic Products AG, Trasadingen, Switzerland). Six explants were placed directly on the plastic bottom of the plate and six pieces were placed on Thermanox plastic cell culture coverslips (Nunc, Thermo Fisher Scientific, Rochester, NY, USA) for histological or immunohistochemical staining of cultured cells. Each explant was covered with one drop (35 μ l) of complete medium and maintained at 37°C in 5% CO₂. Complete medium was changed every day until cell outgrowth was seen. Then, the tissue was covered with 1 ml complete medium, which was changed three times a week until the cells were 90–100% confluent.

The complete medium consisted of Dulbecco's modified Eagle medium mixed 1:1 with Ham's F12 (DMEM/F12 with GlutaMAX) and supplemented with 10% fetal bovine serum, 1.5 g/l sodium bicarbonate (7.5% solution), 10 mM HEPES, 1 μ g/ml insulin–transferrin–selenium, 1% Antibiotic-Antimycotic solution (100 IU/ml penicillin, 100 μ g/ml streptomycin, 0.25 μ g/ml fungizone), and 10 ng/ml recombinant human epidermal growth factor (all, Gibco, Thermo Fisher Scientific, Paisley, UK). Half of the donor explants were cultured in complete medium supplemented with 10 ng/ml recombinant human IL-13 (BioLegend, San Diego, CA, USA). Similarly, after passage, the cells were cultured in complete medium with (IL-13+) or without IL-13 (IL-13-). At day 1 of passage 1 (P1d1) cultivation, numerous cells with prevalent GC morphology that were only slightly attached and unattached were found on top of the

firmly attached epithelial cells. The unattached cells were harvested on P1d1 and designated the P1d1 subpopulation. When primary (P0) cultures and P1 cultures were 90–100% confluent and when P2 cultures had been cultured for 12–14 days from the beginning of culture, the cells were detached using TrypLE Express (Gibco, Thermo Fisher Scientific). P0 and P1 cells intended for cell passaging were seeded in 24-well plates at concentrations of 1.5×10^4 cells per well. Experiments were run on P0, P1, and P2 cells, and partially on the P1d1 fraction. All experiments were repeated at least three times.

3T3 mouse fibroblast feeder layer

3T3 mouse fibroblasts were cultivated in DMEM supplemented with 10% newborn calf serum and 1% Antibiotic-Antimycotic solution (all, Gibco, Thermo Fisher Scientific). The cultures were maintained at 37°C and 5% CO₂ and passaged after reaching 90% confluence. The mouse fibroblasts were growth-arrested by 2-h incubation with 12 µg/ml Mitomycin-C Kyowa (NORDIC Pharma, Prague, Czech Republic) and plated on a 6-well plate at a density of 2.6×10^5 cells per well.

Cell viability

Cell viability was assessed by staining with 0.4% trypan blue (Gibco, Thermo Fisher Scientific). Unstained live cells and stained dead cells were counted with a hemocytometer under an inverted phase contrast microscope. Cell viability was calculated as follows: viability (%) = live cells/(live + dead cells) × 100.

Colony-forming efficiency (CFE) assay

Cultured cells were detached, centrifuged, single-cell suspended, and plated at a density of 700 or 1000 viable cells per well in 6-well plates containing growth-arrested 3T3 mouse fibroblasts. Similarly, to determine the clonal growth ability of GCs one day after passage, the unattached GC-enriched subpopulations were harvested and plated at a density of 1000 or 2000 viable cells per well. All experiments were performed in triplicate for each donor and condition (i.e., IL-13- and IL-13+). On day 12 or 13 after the cultures were started, the colonies were washed with phosphate-buffered saline (PBS; Gibco, Thermo Fisher Scientific), fixed with ice-cold methanol for 30 min at -20°C, rehydrated in PBS, and stained for 5 min at 37°C with 2% rhodamine B (Merck KGaA, Darmstadt, Germany). After the rhodamine B had been removed, the colonies were washed with tap water until optimal staining intensity was achieved. The plates were photographed, and the total number of colonies was counted using NIS Elements software (Laboratory Imaging, Prague, Czech Republic). The total CFE (%) was calculated as follows: (total number of colonies formed at the end of growth period/total number of viable cells seeded) × 100.

Cytospin

Superfrost Plus slides (Thermo Fisher Scientific, Braunschweig, Germany) and filter paper were placed in the sample chamber of a cytospin centrifuge. Cell aliquots (100 µl) were loaded into each chamber and centrifuged at 180 ×g for 8 min. After centrifugation, the slides were air-dried and stored at -20°C until used.

Alcian blue/periodic acid–Schiff (AB/PAS) staining

At the end of the culture, cells grown on Thermanox coverslips were washed with PBS and fixed (solution of 2 ml glacial acetic acid, 1.9 ml 40% formaldehyde, 29.5 ml 95% ethanol, 10.5

ml distilled water) for 10 min and stored in 70% ethanol at 4°C until used. Cells centrifuged on Superfrost Plus slides were taken out of the -20°C freezer and after 30 min on air fixed and AB/PAS stained. AB/PAS staining for demonstrating GC positivity was performed as follows: Tap water was used to hydrate fixed cells and to wash cells after each step of staining. Cells were stained with alcian blue (pH 2.5, Sigma-Aldrich, St. Louis, MO, USA) for 15 min, treated with freshly prepared 0.5% periodic acid solution for 10 min, stained for 6 min with Schiff's reagent (Sigma-Aldrich; diluted 1:3 in distilled water) and counterstained with hematoxylin solution modified according to Gill III (Merck KGaA) for 5 sec. At the end, the cells were washed with Scott's water (0.2 g sodium bicarbonate, 1 g magnesium sulfate, 100 ml distilled water), air-dried and mounted in Aquatex medium (Merck KGaA). The staining results were as follows: acidic mucins were stained blue, neutral mucins were stained magenta, and acidic and neutral mucins were stained purple [33].

All images were acquired with an Olympus BX51 microscope (Tokyo, Japan), a ProgRes C12 plus camera (Jenoptik Laser, Optik, Systeme GmbH, Jena, Germany), and NIS Elements software (Laboratory Imaging). Specimens harvested by bulbar conjunctival impression cytology and cryosectioned pterygium specimens were used as a positive control for AB/PAS staining. The absolute number of AB/PAS-positive GCs per image area (0.58 mm²) was counted on 10 randomly captured images per well from at least five independent tissue donors, and the final results are expressed as absolute cell numbers per 1 mm². The percentage of AB/PAS-positive GCs in P1d1 population was counted on at least 500 cells/ donor (range 500–2200 cells/ donor).

Impression cytology

Upper bulbar conjunctival impression cytology specimens were obtained from living healthy donors after the application of 0.4% oxybuprocaine hydrochloride eye drops as topical anesthesia [34]. For immunofluorescent staining, cells were harvested using sterile, single-pack Millicell inserts (PICM01250, Millipore, Bedford, MA, USA). The inserts with the impressed cells were stored at -80°C until analysis. For AB/PAS staining, nitro acetate cellulose filter papers (GSWP 0.4700, 0.22- μ m pore size, Millipore) were used for cell harvesting.

Indirect fluorescent immunocytochemistry

The cells that had been cultured on Thermanox slides or centrifuged on Superfrost Plus slides were washed twice with PBS and, according to the primary antibody to be used, fixed in 4% paraformaldehyde for 10 min at room temperature (for keratin 7 [K7], a conjunctival cell keratin [3, 34]; Ki-67, a proliferation marker of a nuclear protein expressed in all phases of the active cell cycle [35]; and p63 α [the p63 α isoform encoded by the tumor protein P63 gene *TP63*], a p53-related nuclear protein included in the regulation of epithelial cell differentiation and proliferation [36] and considered a putative marker of limbal epithelial stem cells and young transient amplifying cells [37, 38]) or in ice-cold methanol for 5 min at -20°C (for MUC5AC, a GC-specific mucin [3]), and thereafter hydrated in PBS. Table 1 lists the details of all primary antibodies. The negative control did not contain primary antibody.

K7 staining and Ki-67 and p63 α double staining. After hydration in PBS and washing three times in 0.5% Tween 20 (Sigma-Aldrich) and three times in PBS, cells were blocked for 1 h in 5% goat serum and 0.3% Triton X-100 (Sigma-Aldrich) diluted in PBS, followed by 1-h incubation at room temperature with primary antibody diluted in 0.1% bovine serum albumin (K7) or blocking solution (Ki-67 and p63 α). Then, the cells were rinsed three times in 0.5% Tween 20 and incubated for 1 h at room temperature with the respective secondary antibody diluted in 0.1% bovine serum albumin (K7) or blocking solution (Ki-67 and p63 α): goat anti-

Table 1. Primary antibodies.

Target protein	Animal	Clone	Manufacturer	Catalog Number	Original concentration	Dilution
K7	mouse	OV-TL 12/30	DAKO Cytomation, Glostrup, Denmark	M7018	243 mg/L	1:50
Ki-67	mouse	MIB-1	DAKO Cytomation, Glostrup, Denmark	M7240	80 mg/L	1:50
p63 α	rabbit	Polyclonal	Cell Signalling Technology, Danvers, MA, USA	4892	17 μ g/ml	1:50
MUC5AC	rabbit	Polyclonal	Thermo Fisher Scientific, Rockford, IL, USA	PA5-34612	1 mg/ml	1:400

<https://doi.org/10.1371/journal.pone.0211861.t001>

mouse Alexa Fluor 488 (1:500, A11029), goat anti-mouse Alexa Fluor 594 (1:500, A11032), and goat anti-rabbit Alexa Fluor 488 (1:500, A11034, all secondary antibodies were from Life Technologies, Eugene, OR, USA). After rinsing three times in 0.5% Tween 20, followed by rinsing in PBS, the cells were mounted with VectaShield-DAPI (4' 6-diamidino-2-phenylindole) (Vector Laboratories, Burlingame, CA, USA) to counterstain nuclear DNA. Staining was performed on two wells per condition (i.e., IL-13-/+).

MUC5AC staining. After hydration in PBS, the cells were blocked for 10 min in 2.5% bovine serum albumin and 0.2% Triton X-100 diluted in PBS, followed by PBS wash and 1-h incubation at room temperature in primary antibody diluted in 0.25% bovine serum albumin and 0.05% Tween 20. Then, the cells were rinsed three times in PBS and incubated for 1 h at room temperature with the secondary antibody goat anti-rabbit Alexa Fluor 488 (1:300, A11034, Life Technologies) diluted in 0.25% bovine serum albumin and 0.05% Tween 20. After rinsing three times in PBS, the cells were mounted with VectaShield-DAPI (Vector Laboratories) to counterstain nuclear DNA.

Immunofluorescence detection of MUC5AC on bulbar conjunctival imprints was performed as described previously [34]. Briefly, primary antibody against MUC5AC and the secondary antibody Alexa Fluor 488 (1:300, A11034, Life Technologies) were diluted in 0.1% bovine serum albumin; after staining, the cells were mounted with VectaShield-DAPI (Vector Laboratories).

Immunofluorescent images were acquired with an Olympus BX51 microscope and CCD-1300 camera (VDS Vosskühler GmbH, Osnabrück, Germany). The images were analyzed with NIS Elements software (Laboratory Imaging). The percentage of positive cells was counted on six randomly captured photographs per well (two wells per condition) from at least four independent tissue donors.

Quantitative real-time polymerase chain reaction (qPCR)

The expression of the *GAPDH* (glyceraldehyde-3-phosphate dehydrogenase), *TP63*, *MUC5AC*, *MUC4* (a conjunctiva-prevalent transmembrane mucin [5, 39]), *K3* and *K12* (keratins of differentiated corneal epithelial cells [40]), and *K7* genes were detected by qPCR. Cells from P0, P1 and P2 cultures were collected and transferred into Eppendorf tubes containing 500 μ l TRI Reagent (Molecular Research Center, Cincinnati, OH, USA), and total RNA was extracted according to the manufacturer's instructions. Total RNA (1 μ g) was treated using deoxyribonuclease I (Promega, Madison, WI, USA) and used for reverse transcription (RT). First-strand complementary DNA (cDNA) was synthesized using M-MLV (Moloney murine leukemia virus) reverse transcriptase and random primers (Promega) in a total reaction volume of 25 μ l. The qPCR was performed in a LightCycler 480 Real-Time PCR system (Roche, Basel, Switzerland).

Table 2. Primers used for quantitative real-time PCR.

Gene (human)	Sequence (5'→3')	GenBank accession number	Product size (bp)
<i>GAPDH</i>	F: GAAGGGGTCATTGATGGCAAC R: GGAAGGTGAAGGTCGGAGTC	NM_001289746.1	108
<i>MUC5AC</i>	F: CCTGCAAGCCTCCAGGTAG R: CTGCTCCACTGGCTTTGG	NM_001304359.1	103
<i>MUC4</i>	F: TCCGTGTCCTGCTGGATAACC R: GTTGCGGCTCAGGAGGACTC	NM_018406.6	104
<i>TP63 (p63α isomers)</i>	F: GAGGTTGGGCTGTTCATCAT R: GAGGAGAATTCTGTGGAGCTG	NM_001114980.1	174
<i>K3</i>	F: GGATGTGGACAGTGCCTATATG R: AGATAGCTCAGCGTCGTAGAG	NM_057088.2	106
<i>K7</i>	F: AGGATGTGGTGGAGGACTTC R: CTTGCTCATGTAGGCAGCAT	NM_005556.3	116
<i>K12</i>	F: CCAGGTGAGGTCAGCGTAGAA R: CCTCCAGGTTGCTGATGAGC	NM_000223.3	352

<https://doi.org/10.1371/journal.pone.0211861.t002>

Table 2 lists the primer sequences used for the amplification. The sequence specificity of the primers was confirmed via Primer-BLAST (National Center for Biotechnology Information). Conventional RT-PCR was performed to confirm that only a single band was obtained. The LightCycler 480 SYBR Green I Master (Roche) was used to perform the qPCR. The qPCR parameters involved denaturation at 95°C for 3 min, then 40 cycles at 95°C for 20 s, annealing at 60°C for 30 s, and elongation at 72°C for 15 s. Fluorescence was monitored at 55–95°C at 0.5°C intervals for 10 s. Triplicate reactions were performed for each sample and gene. A relative quantification model was used to calculate the expression of the target gene in comparison to the endogenous control *GAPDH*.

Statistical analysis

Statistical analysis was carried out with GraphPad Prism (Graphpad Software, La Jolla, CA, USA). Descriptive statistics are reported as N (number of values), the mean ± SD, or the median with quartile range. Data distribution normality was assessed using the D'Agostino and Pearson omnibus normality test. Data sets that passed the normality test were analyzed using a two-tailed unpaired *t*-test (comparison between IL-13- and IL-13+ groups within passages) or one-way analysis of variance that in case of significance was followed by Bonferroni's multiple comparison test (comparison among either IL-13- or IL-13+ groups). Data sets with lower numbers of values were analyzed using the two-tailed Mann-Whitney test (comparison between IL-13- and IL-13+ groups within passages) or Kruskal-Wallis test that in case of significance was followed by Dunn's multiple comparison test (comparison among either IL-13- or IL-13+ groups). P-values < 0.05 were considered statistically significant.

Results

Cell outgrowth from limbal explants mostly began day 4 after culture initiation, and cells were 90–100% confluent at day 9, with no significant differences between the IL-13- and IL-13+ cultures. At the end of the P0 culture, the IL-13- group had significantly higher cell viability (89.06 ± 4.6%, N = 17, P = 0.0468) than the IL-13+ group (83.81 ± 9.4%, N = 17). At P1, IL-13- and IL-13+ cells reached confluence similarly and were harvested on day 9–12. The cell viability at the end of the P1 cultures was 91% (N = 17), with no statistical significance between groups. On P1d1, numerous unattached cells, particularly GCs, were seen in the IL-13- and IL-13+ cultures and were rinsed and evaluated. Their viability in both the IL-13- or IL-13+

groups was significantly lower (about 41%, $N = 12$, $P \leq 0.001$) in comparison to viability of P0–P2 cultures. At P2, cells were harvested on day 12–14 of culture without reaching confluence. The cell viability was about 89% ($N = 10$), with no statistical significance between the IL-13- and IL-13+ groups (Fig 1A).

In P0, the epithelial cell morphology in the IL-13- and IL-13+ groups was cobblestone in shape and with a high nuclear-to-cytoplasmic ratio. Round to oval-shaped GCs were present either as single cells or as groups of cells. Most GCs were interspersed among epithelial cells and protruded above them (Fig 1Ba and 1Be). A mixture of cuboidal and flattened epithelial cells with superficially located GCs appeared at P1 (Fig 1Bb and 1Bf); differentiated flattened epithelial cells with low nuclear-to-cytoplasmic ratio and with superficially located GCs appeared at P2 (Fig 1Bc and 1Bg). On P1d1, many unattached cells were seen in the IL-13- and IL-13+ groups (Fig 1Bd and 1Bh).

Characterization of cultured cells: Keratins

Strong K7 immunostaining clearly showed conjunctival epithelial cells and GCs in IL-13- and IL-13+ cultures at the end of the P0, P1, and P2 cultivation periods and in the P1d1 GC-enriched population (Fig 2A). There were >99% K7-positive cells in the P0 and P1 IL-13- and IL-13+ groups and in the P2 IL-13+ group; K7 positivity was 80% only in the P2 IL-13- group (Fig 2B, descriptive statistics in S1 Table). K7 positivity increased significantly in the P1 IL-13+ ($P < 0.05$) and P2 IL-13+ ($P \leq 0.01$) groups in comparison to the P0 IL-13+ group.

Gene expression was measured for the *K7*, *K3*, and *K12* genes. Strong K7 expression was present in IL-13- and IL-13+ conditions and in all evaluated groups (Fig 3A). The median values of K7 expression were higher in all passages of IL-13+ cells, and that in the P1 IL-13+ group was significantly different ($P = 0.0317$) compared to the P1 IL-13- group. In the IL-13+ cultures, K7 expression was significantly higher ($P < 0.05$) at the end of P2 compared to P0. *K3* and *K12* genes were expressed in all tested groups (Fig 3B and 3C, respectively) but at much lower levels, especially low expression was seen for *K3*. S2 Table presents the descriptive statistics of *K7*, *K3*, and *K12* gene expression in the P0, P1, and P2 groups.

Characterization of cultured cells: Mucins

AB/PAS staining revealed the presence of single and grouped GCs in all groups under IL-13- or IL-13+ conditions (Fig 4A). Pure neutral mucins and a mixture of neutral and acidic mucins were produced in the P0, P1, and P2 cultures and within the P1d1 GC-enriched sub-population. The presence of only acidic mucins in GCs was very rare. Bulbar conjunctival impression cytology specimens and cryosectioned pterygium specimens served as a positive control for AB/PAS staining (Fig 4B). AB/PAS-positive GCs were counted and are expressed as medians of absolute cell numbers/mm². The absolute number of GCs in the P1 IL-13- group was significantly higher ($P = 0.0411$) than that in the P1 IL-13+ group. Among the IL-13- groups, significantly higher numbers of GCs were present at P1 ($P \leq 0.01$) in comparison to P0; among the IL-13+ groups, there were significantly higher numbers of GCs at P2 ($P \leq 0.01$) in comparison to P0 (Fig 4C). S3 Table shows the descriptive statistics of the AB/PAS-positive GCs.

P1d1 GC-enriched population showed AB/PAS-positivity in 27.6% of cells in IL-13- group and 24.4% of cells in IL-13+ group with no significant difference between groups (Fig 4D). S4 Table shows the descriptive statistics of the AB/PAS-positive GCs in P1d1 population.

MUC5AC immunostaining confirmed the presence of single and grouped GCs in all tested groups (Fig 5A). Cells harvested by bulbar impression cytology and pterygium sections were used as positive controls for MUC5AC staining (Fig 5B). qPCR confirmed *MUC5AC* gene

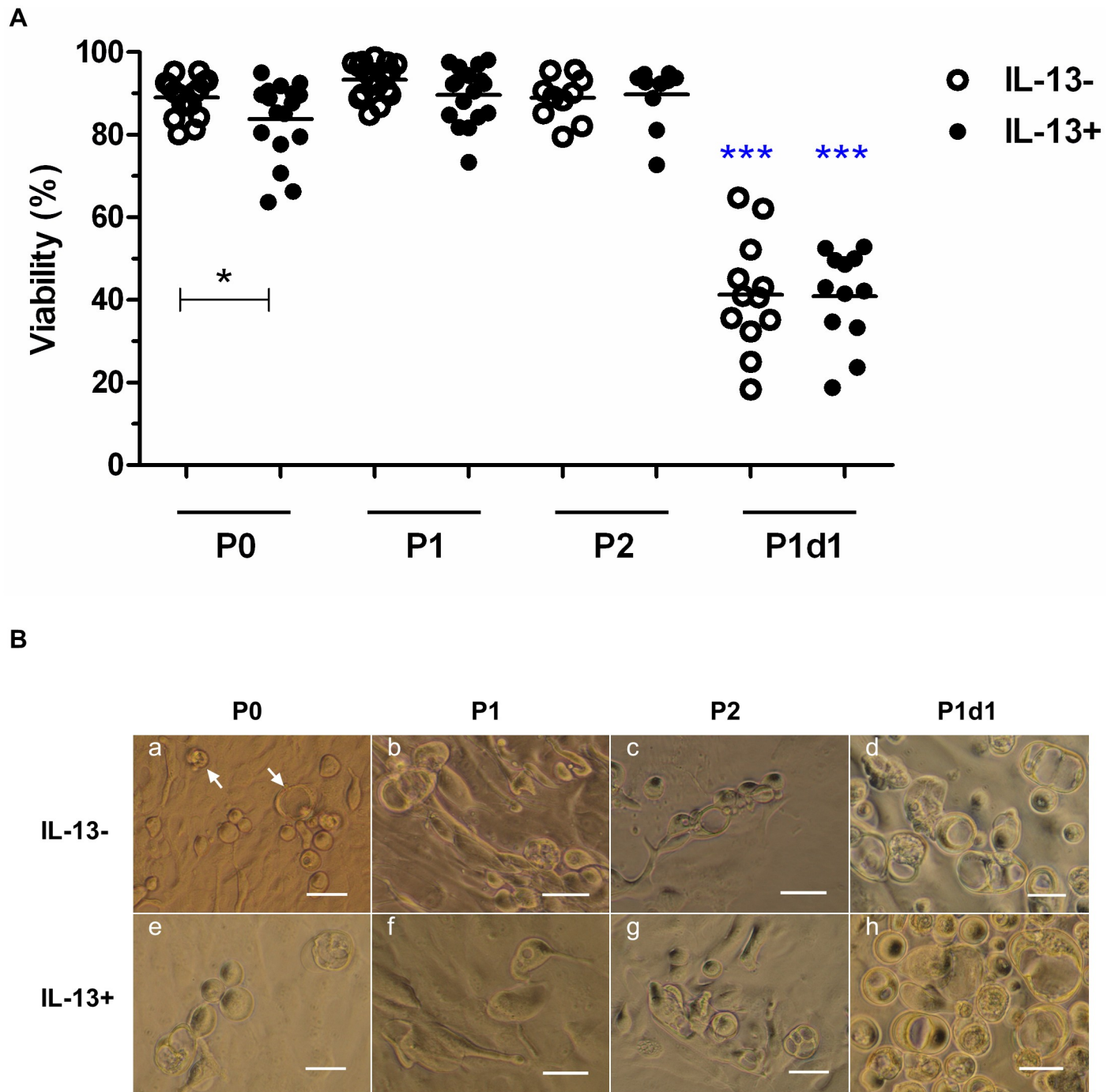


Fig 1. The viability and morphology of IL-13- or IL-13+ cell cultures. (A) Percentages of cell viability at the end of cultivation of P0, P1, and P2 cultures and percentages of cell viability of the unattached GC-enriched subpopulation harvested on P1d1. Cell viability data are presented in a vertical scatter plot graph with line indicating mean. * $P < 0.05$, *** $P \leq 0.001$. Blue asterisks indicate significant decrease of viability in P1d1 IL-13- or P1d1 IL-13+ group vs. P0, P1, and P2 IL-13- or IL-13+ groups, respectively. (B) Cell morphology at the end of cultivation of P0, P1, and P2 cultures observed under inverted phase contrast microscope. P1d1 images show no attached GC-enriched subpopulations. White arrows show examples of GCs. Scale bars: 50 μ m.

<https://doi.org/10.1371/journal.pone.0211861.g001>

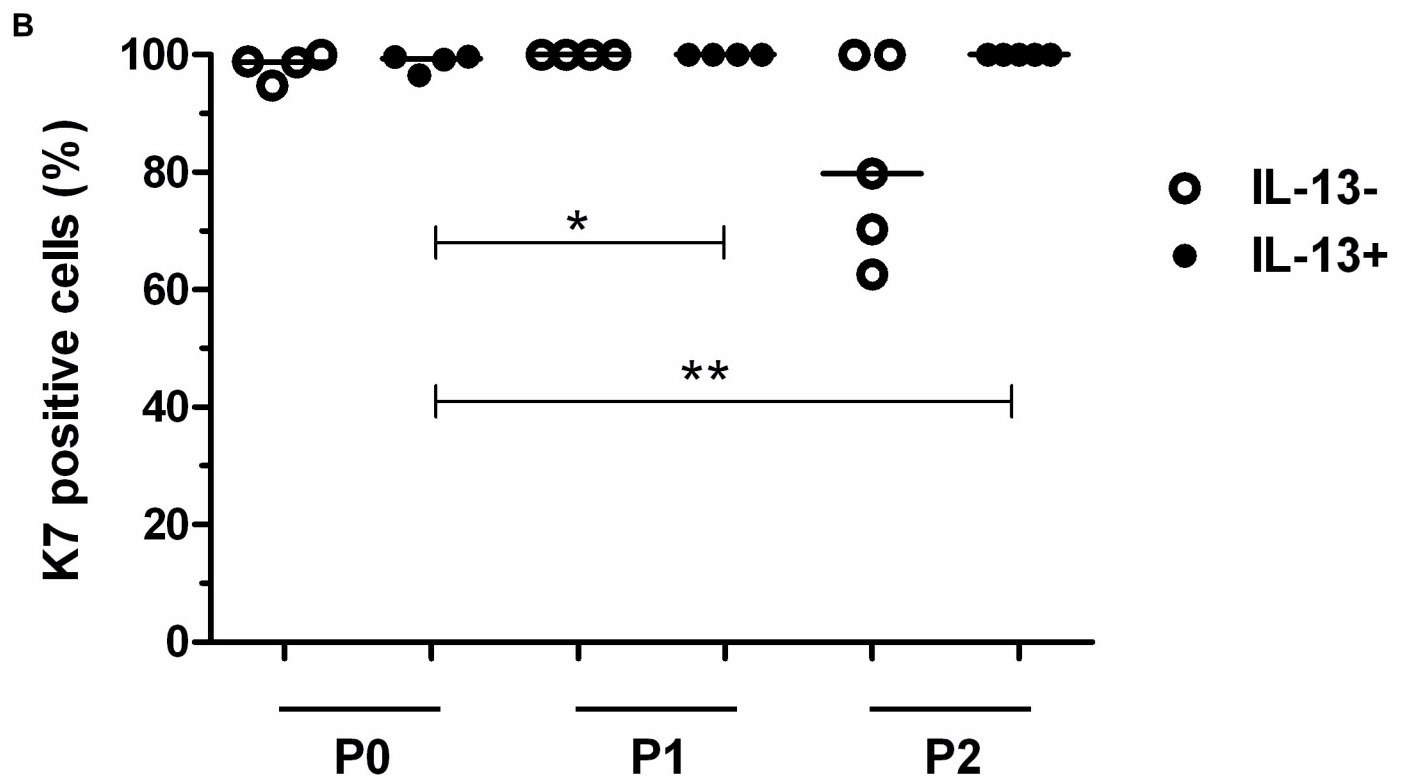
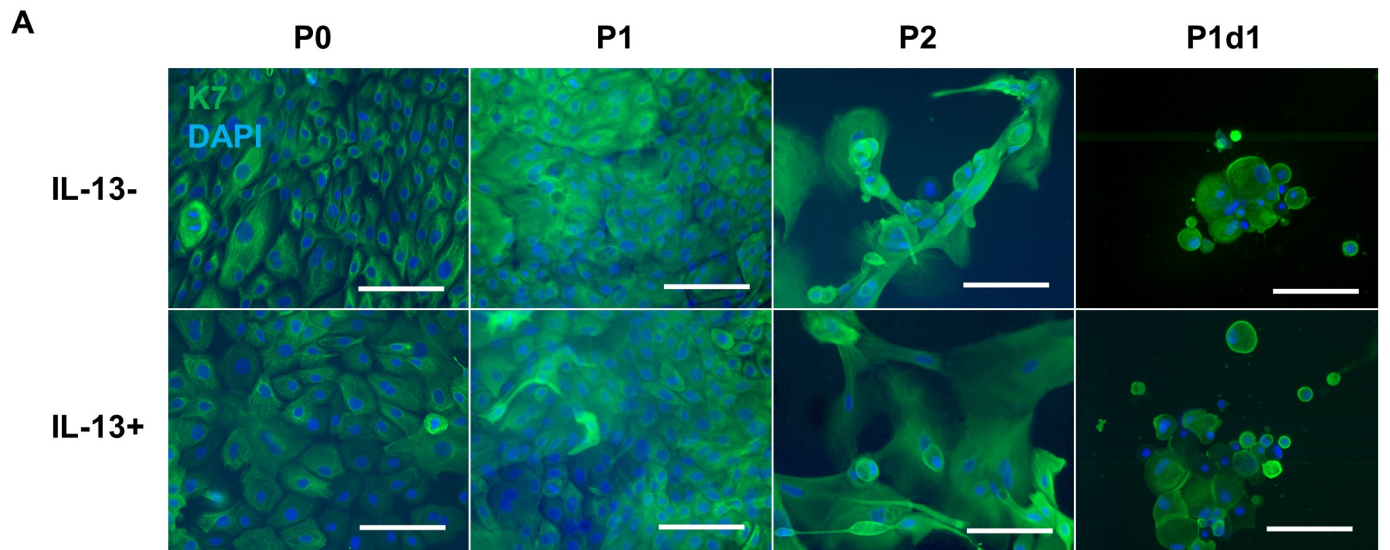


Fig 2. Immunofluorescent staining of K7 in IL-13- or IL-13+ cell cultures. P0 cells originating from limbal explants, P1 and P2 cells (all fixed at the end of cultivation), and the unattached GC-enriched subpopulation (P1d1, harvested on day 1 after passage of primary cells) were analyzed by immunofluorescent staining. (A) K7, green; DAPI-counterstained nuclei, blue; scale bars: 100 μ m. (B) Distribution of percentages in P0, P1, and P2 groups for K7 positivity. All data of positive percentages are presented in the vertical scatter plot graph with line indicating median. * $P < 0.05$, ** $P \leq 0.01$.

<https://doi.org/10.1371/journal.pone.0211861.g002>

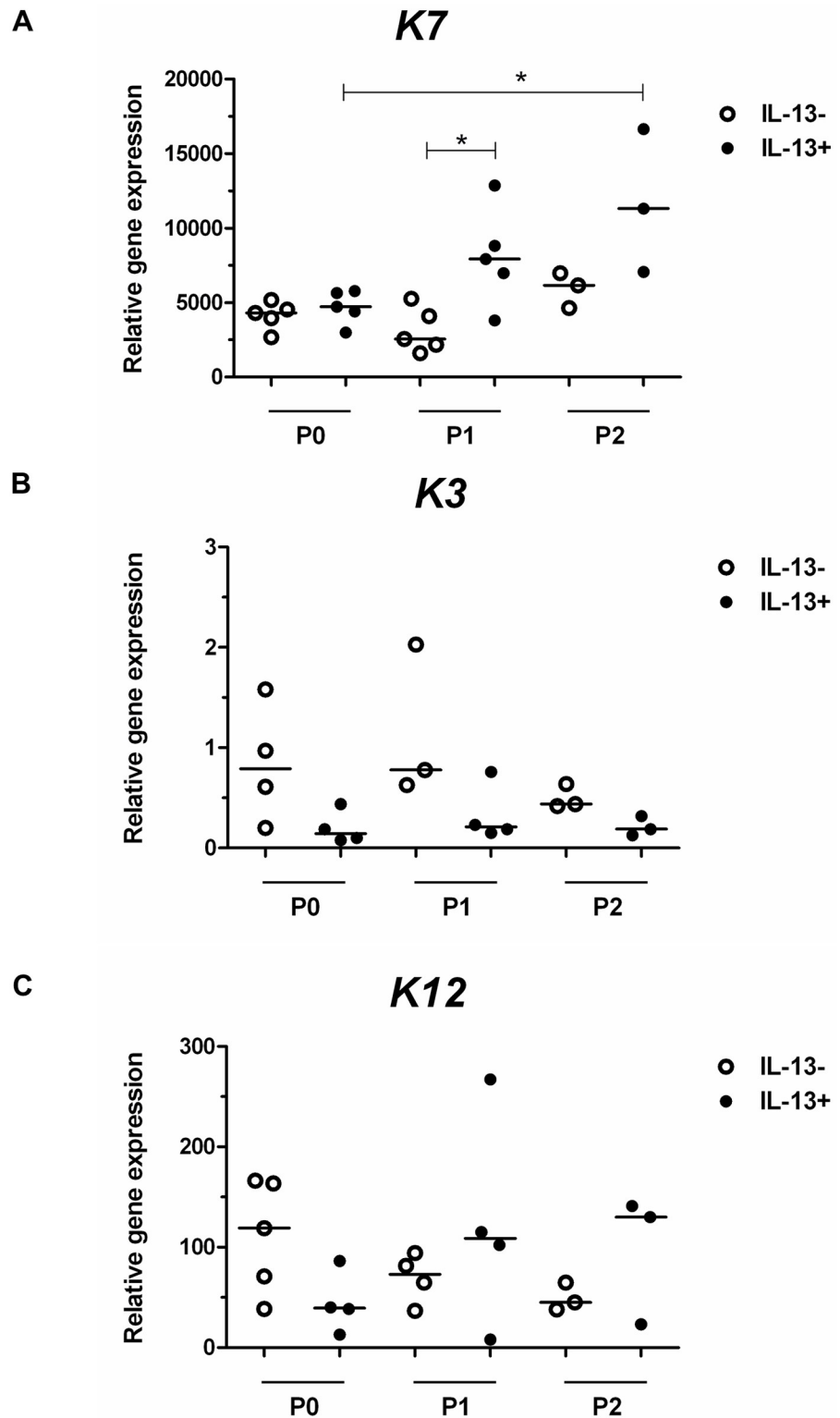


Fig 3. Relative expression of *K7*, *K3*, and *K12* genes in IL-13- or IL-13+ cell cultures. At the end of cultivation, P0 cells originating from limbal explants and passaged cells (P1 and P2) were analyzed for *K7* (A), *K3* (B), and *K12* (C) gene expression by qPCR. All data are presented in a vertical scatter plot graph with line indicating median. * $P < 0.05$.

<https://doi.org/10.1371/journal.pone.0211861.g003>

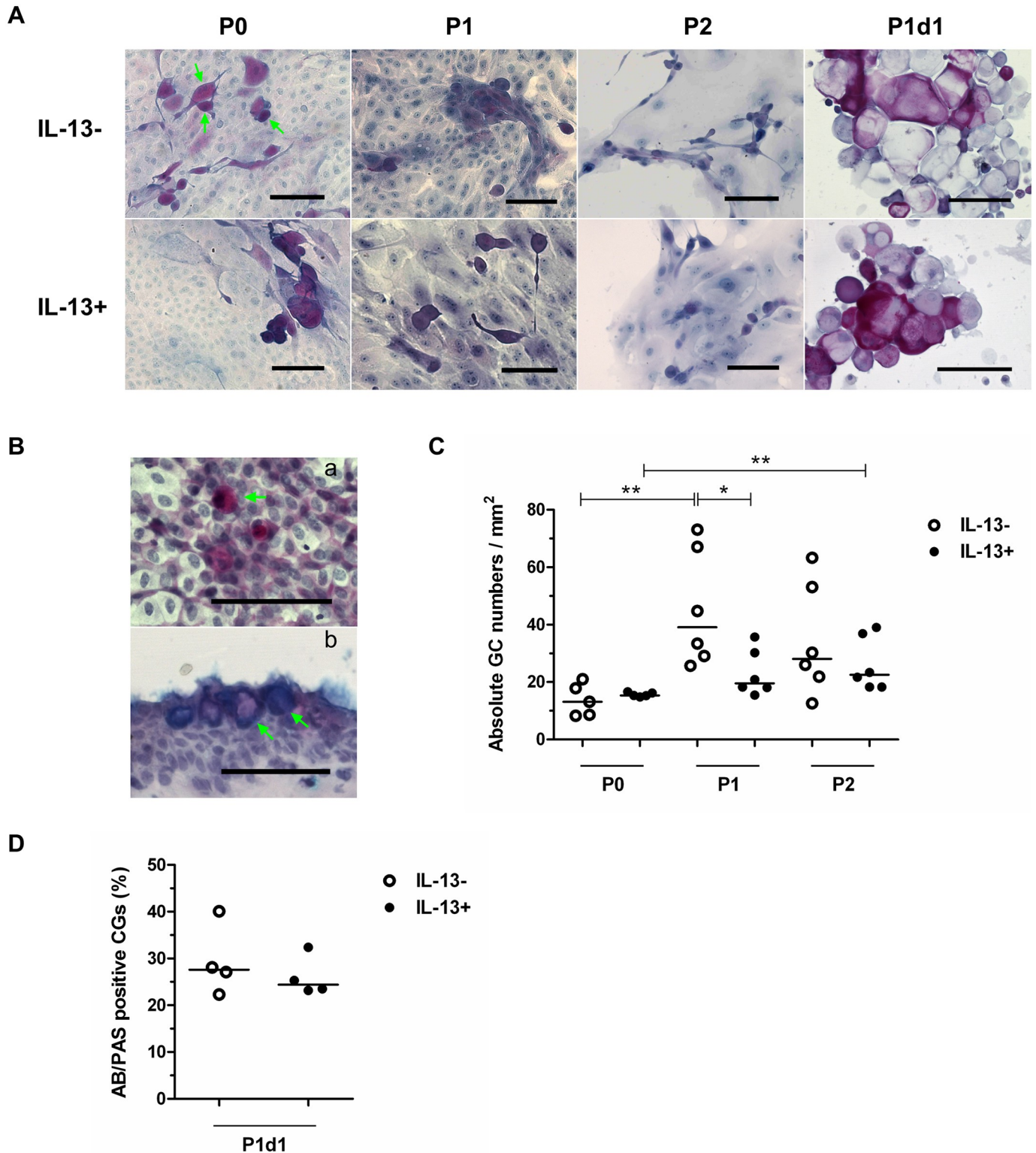


Fig 4. AB/PAS staining of GCs in IL-13- or IL-13+ cell cultures and P1d1 subpopulation. (A) P0 cells originating from limbal explants, P1 and P2 cells (all fixed at the end of cultivation), and the unattached GC-enriched subpopulation (P1d1, harvested on day 1 after passage of primary cells) were analyzed by AB/PAS staining. Green arrows indicate examples of GCs. (B) AB/PAS-positive GCs on the surface of the conjunctiva (impression cytology) (a) and on pterygium cryosections (b) were used as a positive control. Green arrows indicate examples of GCs. (C) Distribution of absolute numbers of AB/PAS-positive GCs in individual groups presented in a vertical scatter plot graph with line indicating median. (D) Distribution of percentages of AB/PAS-positive GCs in individual groups of P1d1 subpopulation presented in a vertical scatter plot graph with line indicating median. * $P < 0.05$, ** $P \leq 0.01$. Scale bars: 100 μ m.

<https://doi.org/10.1371/journal.pone.0211861.g004>

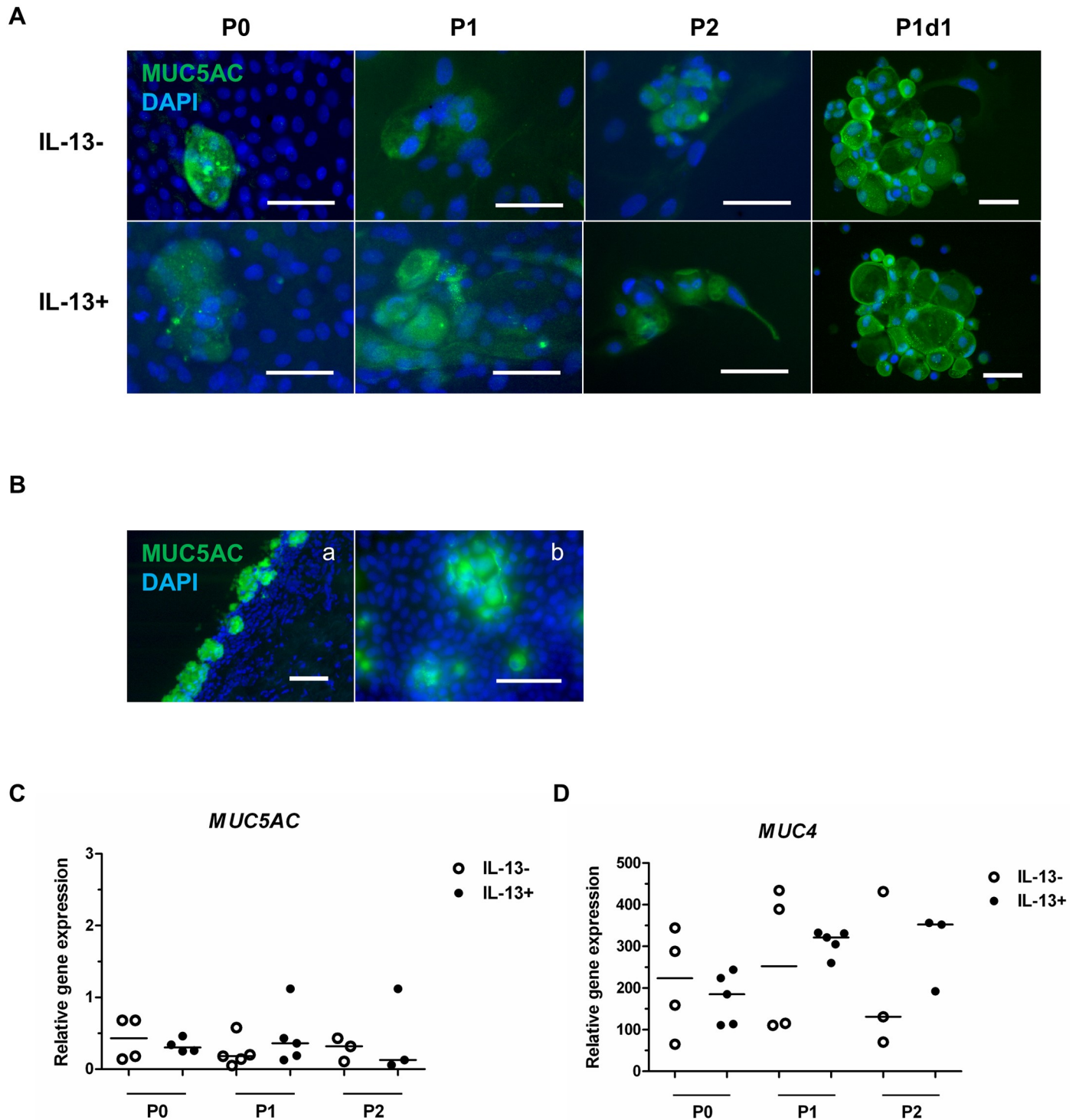


Fig 5. Immunofluorescent staining of MUC5AC and relative expression of *MUC5AC* and *MUC4* genes in IL-13- or IL-13+ cell cultures. (A) P0 cells originating from limbal explants, P1 and P2 cells (all fixed at the end of cultivation), and the unattached GC-enriched subpopulation (P1d1, harvested on day 1 after passage of primary cells) were analyzed by immunofluorescent staining for MUC5AC (green). Nuclei were counterstained with DAPI (blue). (B) MUC5AC staining of GCs on pterygium cryosection (a) and upper bulbar conjunctival impression cytology (b). qPCR analysis of the relative gene expression of (C) *MUC5AC* and (D) *MUC4*. All data are presented in vertical scatter plot graphs with line indicating median. Scale bars: 50 μ m.

<https://doi.org/10.1371/journal.pone.0211861.g005>

expression, which was present in all evaluated groups but was not statistically significant among groups (Fig 5C, S2 Table). *MUC4* was expressed in all groups under IL-13- and IL-13+ conditions but with no statistical significance among groups (Fig 5D, S2 Table).

Characterization of cultured cells: Proliferation and stemness

Ki-67 and p63 α immunostaining demonstrated a high percentage of positivity, particularly in the P0 and P1 groups, and a low percentage of positivity in the P2 groups (Fig 6A). The P0 IL-13- (53%) and P1 IL-13+ (51%) groups had the highest Ki-67 and p63 α double positivity, while expression was lowest (<4%) in the P2 IL-13- ($P \leq 0.01$) and IL-13+ ($P < 0.05$) groups. Between the P0, P1, and P2 IL-13- and IL-13+ groups, P1 IL-13+ cells had significantly higher ($P = 0.0286$) Ki-67 and p63 α double positivity (Fig 6Ba, S1 Table).

A similar pattern of antigen expression was seen for Ki-67 staining versus Ki-67 and p63 α double staining; indicating almost 100% Ki-67 co-localization with p63 α in P0, P1, and P2 cells (Fig 6Bb, S1 Table).

p63 α immunostaining was present in around 90% of cells in the P0 and P1 groups, with a significant decrease ($P < 0.05$) in p63 α positivity to 12% in the P2 IL-13- group and to 38% in the P2 IL-13+ group. No difference was seen between the P0, P1, and P2 IL-13- and IL-13+ groups (Fig 6Bc, S1 Table).

TP63 gene expression was present in all evaluated groups under the IL-13- and IL-13+ conditions (Fig 6C, S2 Table). All IL-13+ groups had higher median *TP63* expression, with the P1 IL-13+ group having significantly higher median *TP63* expression ($P = 0.0159$) than the P1 IL-13- group.

Colony-forming efficiency

The P0 IL-13- group had about 1% total CFE; that of the P0 IL-13+, P1 IL-13-, and P1 IL-13+ groups were about 8%, 0.5%, and 2%, respectively; in the P2 and P1d1 IL-13- and IL-13+ groups, the total CFE was <0.5% (Fig 7). Statistical analysis of the CFE data demonstrated higher growth potential in P0 IL-13- ($P \leq 0.01$) or IL-13+ cultures ($P \leq 0.001$) compared to that of consequent passages, especially P2. The P0 IL-13+ group had significantly higher growth potential ($P = 0.0048$) compared to the P0 IL-13- group. Similarly, the P1 IL-13+ group had significantly higher growth potential ($P = 0.037$) than the P1 IL-13- group (Fig 7B, S5 Table).

Discussion

We successfully prepared conjunctival epithelium using limbal explants from surplus tissue from human corneoscleral rims. The cultured epithelium was composed of K7-positive epithelial cells and GCs; additionally, the GCs showed AB/PAS and MUC5AC positivity and *MUC5AC* expression. Previously published studies have reported inconsistent results, as they have demonstrated either presence or absence of GCs in cultures derived from human limbal cells [7, 41]. Conjunctival cultures did not contain GCs if explants were obtained <3 mm from the limbus [42], but GCs were present in cultures if the biopsy was obtained 3–5 mm from the corneoscleral rim [43].

Although the number of GCs in our cultures appears low, about 13–15 GCs/mm², they are markedly higher compared to the 0.5–0.6 GCs/mm² reported by Ang *et al.*, who used explants from the superior bulbar region [44], and lie between the GC levels obtained by Pellegrini *et al.* in non-confluent and confluent cultures, respectively [7]. Using flow cytometry, Lužnik *et al.* reported a relatively high percentage of GCs (9–11% based on serum concentration) [41] in limbal explant cultures, which could be an interesting result; unfortunately, their results are

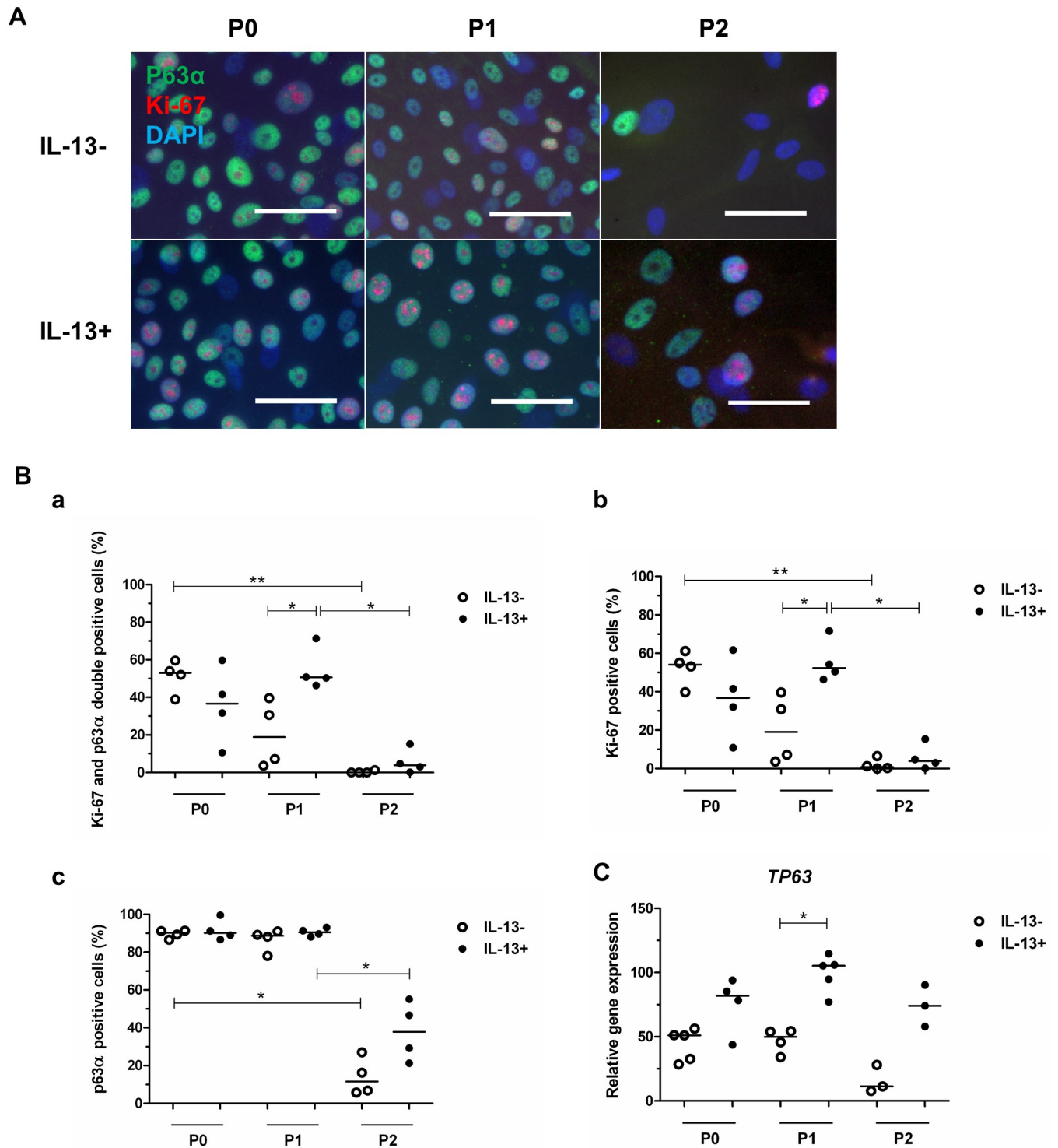


Fig 6. Immunofluorescent Ki-67 and p63 α double staining and the relative *TP63* gene expression in IL-13- or IL-13+ cell cultures. (A) At the end of cultivation, P0 cells originating from limbal explants and P1 and P2 cells were analyzed by immunofluorescent staining for Ki-67 (red) and p63 α (green); nuclei were counterstained with DAPI (blue). Scale bars: 50 μ m. (B) Distribution of percentages in P0, P1, and P2 groups for Ki-67 and p63 α double staining (a), and Ki-67 (b) and p63 α (c) immunostaining. (C) qPCR analysis of relative *TP63* gene expression. All data are presented in vertical scatter plot graphs with line indicating median. * $P < 0.05$, ** $P \leq 0.01$.

<https://doi.org/10.1371/journal.pone.0211861.g006>

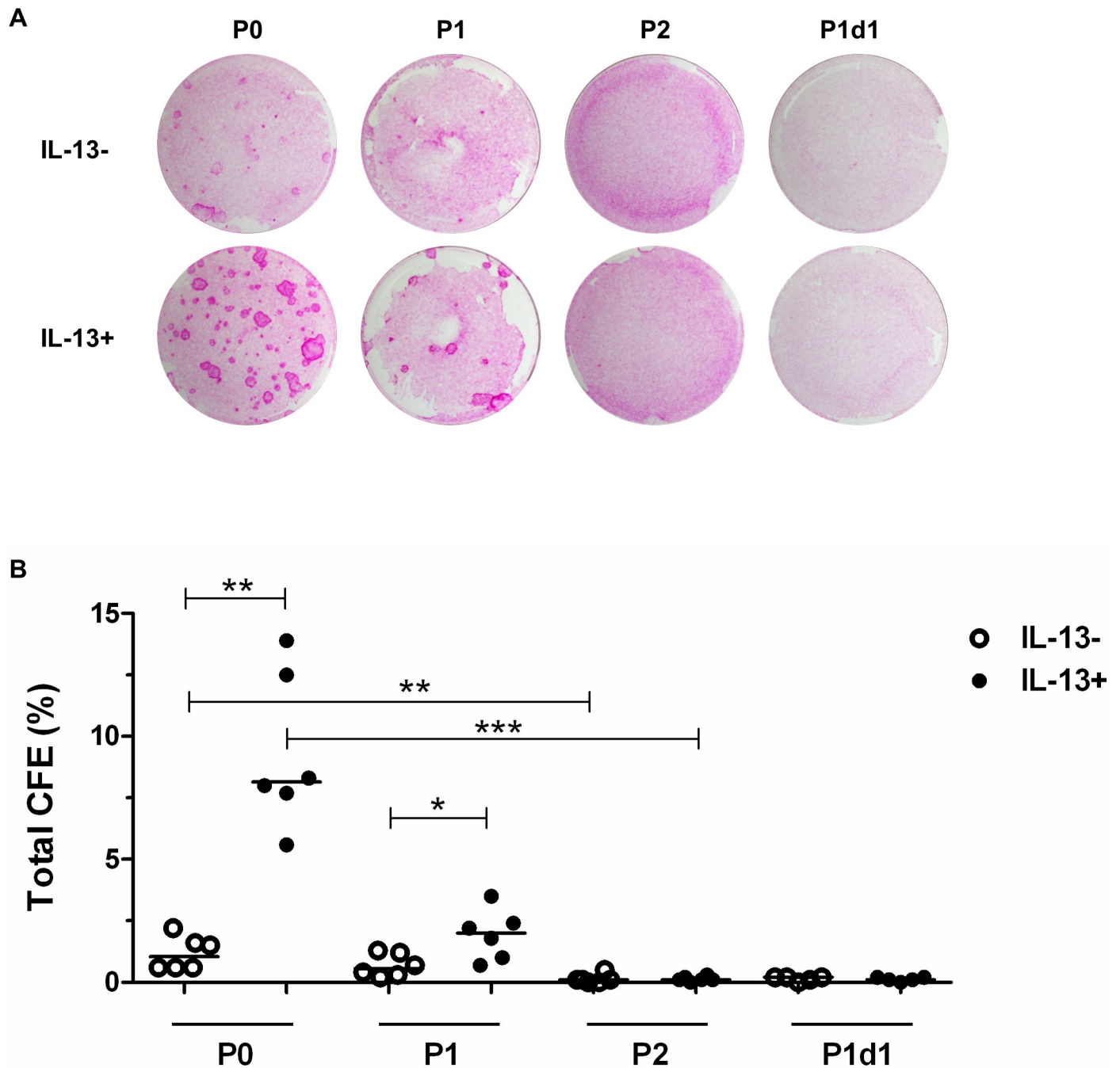


Fig 7. Comparison of total CFE. At the end of cultivation, P0 cells from limbal explants, P1 and P2 cells, and the unattached GC-enriched subpopulation (P1d1, harvested on day 1 after passage of primary cells) were cultured with growth-arrested 3T3 mouse fibroblasts to compare their growth ability under IL-13- and IL-13+ conditions. All total CFE data are presented in vertical scatter plot graphs with line indicating median. *P < 0.05, **P ≤ 0.01, ***P ≤ 0.001. (A) Colonies grown in CFE assay and stained with 2% rhodamine B (day 12). (B) Distribution of total CFE percentages of the P0, P1, P2, and P1d1 groups.

<https://doi.org/10.1371/journal.pone.0211861.g007>

expressed as the mean ± standard error of the mean, which does not adequately describe the actual dispersion of values [45]. Moreover, their error bars are quite large despite the standard error of the mean, which presumes large variability in the distribution. Concerning the P1 cultures, the P1 IL-13- group had more GCs, i.e., 39 GCs/mm², and the P1 IL-13+ group had

similar GC numbers, i.e., 19 GCs/mm², as compared to the P1 control group of human conjunctival epithelial cells of Schrader *et al.* [43].

The positive influence of IL-13 on GC numbers [19, 20] and MUC5AC secretion has previously been reported [22]. In the present study, we did not observe differences in the number of AB/PAS-positive GCs between the P0 IL-13- and IL-13+ cultures. From this point of view, IL-13 in our P0 cultures did not influence the number of GCs as compared to two studies in mice [19, 20], which achieved the proliferation of conjunctival GCs. However, the two studies describe cultures that are far from the natural GC-to-epithelial cell ratio [7], as the reported GC content was incredibly high, showing GC presence in cultures as high as 100% [19] and 85% [20]. Differences between animal and human studies are not surprising, as it has been proposed that human conjunctival GCs are post-mitotic terminally differentiated cells [7], while mouse conjunctival GCs have mitotic activity [8]. Surprisingly, not only did IL-13 not increase GC numbers in our cultures, there were significantly more AB/PAS-positive GCs in the P1 IL-13- group. Thus, it appears that IL-13 prevents the differentiation of young transient cells into GCs, and this finding might support the fact that IL-13 maintained stemness in our cultures. Here, we evaluated for the first time the relationship between IL-13 and the gene expression of the human conjunctival mucins *MUC5AC* and *MUC4*, and found that, at the end of the P0, P1, and P2 cultures, IL-13 did not alter their expression.

The determination of GC numbers was done using AB/PAS staining because it is easier to distinguish individual GCs within cell clusters with AB/PAS staining than with MUC5AC staining; additionally, histological staining yielded better information on the morphology of our cultures. On P1d1 under IL-13- and IL-13+ conditions, we observed cells with typical GC morphology, and these spontaneously unattached cells were collected and characterized by AB/PAS and MUC5AC staining. AB/PAS staining revealed about 28% and 24% of positive cells in IL-13- and IL-13+ group, respectively. This P1d1 GC-enriched subpopulation did not exhibit clonogenic ability, which is consistent with the proposal that human conjunctival GCs are terminally differentiated [7], especially if they produce MUC5AC [3, 46]. Moreover, the GC lifespan in culture appeared quite short, as we observed floating detached GCs daily. The lifespan of conjunctival GCs has not been studied so far; however, for example, intestinal GC turnover is 3–7 days [47].

The presence of the conjunctival cell marker K7 throughout the cultivation is consistent with the conjunctival, but not corneal phenotype of epithelial cells [3, 34]. Moreover, our results clearly show that K7 was present in both conjunctival cell types, i.e., in epithelial cells and GCs. In the present study, the IL-13+ cell cultures had significantly higher K7 expression and more histologically stained GCs in P2 cells compared to P0 cells. This finding is consistent with the increasing differentiation observed throughout P0, P1, and P2.

As we cultured limbal explants that are primarily considered as a source for corneal tissue, we tested our cultures for the cornea-specific genes *K3* and *K12*, which confirmed their expression. We also showed that IL-13 does not alter their expression significantly. However, the difference between *K3* (very low) and *K12* (higher) expression was present. Although *K3* and *K12* form a pair at a protein level, at the mRNA level, they are encoded by different genes and located at different chromosomes. Moreover, their expression is induced by two different PAX6 isoforms and enhanced by different factors [48]. Therefore, the difference between the expressions of these two genes is possible, and lower relative gene expression of *K3* versus *K12* in corneal, limbal and conjunctival tissue was shown [48]. Human conjunctival epithelium contains ectopically residing clusters of K12-positive epithelial cells [49], conjunctival cultures initiated from cells from the proximity of the limbal area express *K3* and *K12* [42], and corneal and conjunctival lineages both come from PAX6 ectodermal origin [50]. Thus, the mixed expression of corneal and conjunctival markers in our limbal tissue-derived cultures is not

surprising. However, due to the predominant expression of *K7* over *K12* and *K3*, we believe that our cultures differentiated primarily to the conjunctival phenotype, which is also supported by the expression of conjunctiva-prevalent *MUC4* and GCs presence. Previously, we found that *K7*-positivity in human limbal explant cultures also appeared but it was lower to *K3*- and *K12*-positivity [51]. Tissue with conjunctival markers cultured from human limbal explants has been also prepared by Luznik *et al.* [41]. They found that higher percentage of used human serum lead to higher expression of *K7* and *MUC5AC* in limbal explant cultures. Thus, the appearance of conjunctival markers in our cultures could also be associated with usage of serum (FBS). For example, one of active serum components, nerve growth factor (NGF) increases the presence of GCs and *MUC5AC* expression in mouse limbal cultures [10] and increases goblet cell number and their differentiation in human conjunctival cultures [52]. However, the concentration of NGF in serum is much lower (pg/ml) compared to efficient NGF concentration used *in vitro* (ng/ml) [52, 53].

Currently, p63 α is considered the most important marker characterizing limbal stem cells and young transient amplifying cells that give rise to holoclones and meroclones, respectively [37, 38]. Clinical results have shown that limbal transplants containing >3% p63-bright cells led to successful corneal epithelial regeneration in a higher percentage of eyes with limbal stem cell deficiency (78%) than transplants with \leq 3% p63-bright cells (11%) [32]. In the present study, the P0 and P1 cultures contained very high percentages of p63 α -positive cells (about 90%), although the IL-13- and IL-13+ groups were not significantly different; however, the IL-13+ groups had increased *TP63* expression, especially the P1 groups, and demonstrating that IL-13 maintained the stemness of the cultures. p63 α is expressed in cells with high proliferative potential that are slow-cycling *in vivo* but extensively proliferating *in vitro* [38]. p63 α and Ki-67 double staining showed the number of p63 α -positive cells that had proliferated at the end of the culture period, and double staining positivity was highest in the P0 IL-13- (53%) and P1 IL-13+ groups (51%). The P1 IL-13- group had a higher percentage of Ki-67-positive proliferating cells (19%) than conjunctival cultures seeded in plasma or cryoprecipitate scaffolds (P1, ~11%) [22] and a lower percentage than that in P1 cells in another study (39%) [54]. The increased Ki-67 positivity (52%) in the P1 IL-13+ groups demonstrates the effect of IL-13 on epithelial cell proliferation.

Our P0 IL-13- cultures had comparable clonogenic ability (1%) with those of some areas of human conjunctival tissue [9, 54] and limbal explants [55]. IL-13 can inhibit or stimulate colony formation depending on cell type and dose [56, 57]. In the P0 IL-13+ cultures, clone-forming ability increased to 8%, which was even higher than that of cultures from the human inferior forniceal and medial canthal areas [9]. The higher clonogenic capacity of IL-13-stimulated epithelial cells in P0 and P1 corresponds with the same tendency shown in *TP63* expression, particularly in P1. Of note, IL-13 also preserved *K7* expression in our cultures. Thus, it appears IL-13 has a two-fold effect; the maintenance of stemness and the support of differentiation. Differentiation of limbal epithelial cells requires asymmetric cell division [58]. Therefore, the more stem cells present in the cell culture, the more differentiated cells will be generated (IL-13+ cultures). Conversely, if the number of stem cells decreases during cultivation, the number of differentiated cells will also decrease as terminally differentiated cells do not have the proliferation activity (IL-13- cultures).

In conclusion, we have cultured human limbal explants prepared from corneoscleral rims and engineered epithelium with a predominant conjunctival phenotype with the presence of stem/progenitor/proliferating cells and a relatively high density of GCs. We show that IL-13 maintains the stemness of the cultures by increasing their clonal ability and *TP63* expression. IL-13 also preserved the expression of conjunctiva-specific keratin (*K7*) during passage, with no other significant changes in conjunctival mucin expression, GC number, and cornea-

specific keratins. Moreover, we have isolated a subpopulation containing GCs and have demonstrated that mucin-producing GCs are terminally differentiated cells with no proliferative potential. For the first time, we raise the possibility of using corneoscleral rims as an alternative source for engineering a conjunctival epithelium that can be used for further research on GCs and for treating patients with ocular surface disorders.

Supporting information

S1 Table. Descriptive statistics of indirect fluorescent immunocytochemistry.
(DOCX)

S2 Table. Descriptive statistics of relative gene expression.
(DOCX)

S3 Table. Descriptive statistics of absolute GC numbers per mm².
(DOCX)

S4 Table. Descriptive statistics of AB/PAS-positive GCs in P1d1 subpopulation.
(DOCX)

S5 Table. Descriptive statistics of total CFE.
(DOCX)

Acknowledgments

The 3T3 cell line was a kind gift from Prof. Vladimir Holan, Czech Academy of Sciences, Prague, Czech Republic. We thank V. Vesela, M.D., and S. Kalasova for their excellent technical assistance in the preparation of the specimens.

Author Contributions

Conceptualization: Andrea Stadnikova, Peter Trosan, Tor Paaske Utheim, Katerina Jirsova.

Formal analysis: Andrea Stadnikova, Peter Trosan.

Funding acquisition: Katerina Jirsova.

Investigation: Andrea Stadnikova, Peter Trosan.

Methodology: Andrea Stadnikova, Peter Trosan.

Resources: Pavlina Skalicka.

Supervision: Katerina Jirsova.

Validation: Andrea Stadnikova, Peter Trosan, Katerina Jirsova.

Visualization: Andrea Stadnikova, Peter Trosan.

Writing – original draft: Andrea Stadnikova, Peter Trosan.

Writing – review & editing: Andrea Stadnikova, Peter Trosan, Tor Paaske Utheim, Katerina Jirsova.

References

1. Siebelmann S, Gehlsen U, Huttmann G, Koop N, Bolke T, Gebert A, et al. Development, alteration and real time dynamics of conjunctiva-associated lymphoid tissue. *PLoS One*. 2013; 8(12):e82355. <https://doi.org/10.1371/journal.pone.0082355> PMID: 24376530.

2. Kessing SV. Mucous gland system of the conjunctiva. A quantitative normal anatomical study. *Acta Ophthalmol (Copenh)*. 1968; Suppl 95:1+. PMID: [4170134](#).
3. Gipson IK. Goblet cells of the conjunctiva: A review of recent findings. *Prog Retin Eye Res*. 2016; 54:49–63. <https://doi.org/10.1016/j.preteyeres.2016.04.005> PMID: [27091323](#).
4. Dua HS, Gomes JA, Jindal VK, Appa SN, Schwarting R, Eagle RC Jr., et al. Mucosa specific lymphocytes in the human conjunctiva, corneoscleral limbus and lacrimal gland. *Curr Eye Res*. 1994; 13(1):87–93. PMID: [7908866](#).
5. Gipson IK. Distribution of mucins at the ocular surface. *Exp Eye Res*. 2004; 78(3):379–88. PMID: [15106916](#).
6. Li W, Hayashida Y, Chen YT, Tseng SC. Niche regulation of corneal epithelial stem cells at the limbus. *Cell Res*. 2007; 17(1):26–36. <https://doi.org/10.1038/sj.cr.7310137> PMID: [17211449](#).
7. Pellegrini G, Golisano O, Paterna P, Lambiase A, Bonini S, Rama P, et al. Location and clonal analysis of stem cells and their differentiated progeny in the human ocular surface. *J Cell Biol*. 1999; 145(4):769–82. PMID: [10330405](#).
8. Wei ZG, Cotsarelis G, Sun TT, Lavker RM. Label-retaining cells are preferentially located in fornical epithelium: implications on conjunctival epithelial homeostasis. *Invest Ophthalmol Vis Sci*. 1995; 36(1):236–46. PMID: [7822151](#).
9. Stewart RM, Sheridan CM, Hiscott PS, Czanner G, Kaye SB. Human Conjunctival Stem Cells are Predominantly Located in the Medial Canthal and Inferior Forniceal Areas. *Invest Ophthalmol Vis Sci*. 2015; 56(3):2021–30. <https://doi.org/10.1167/iovs.14-16266> PMID: [25722207](#).
10. Li W, Sun X, Wang Z, Li R, Li L. The effect of nerve growth factor on differentiation of corneal limbal epithelial cells to conjunctival goblet cells in vitro. *Mol Vis*. 2010; 16:2739–44. PMID: [21179428](#).
11. Junttila IS. Tuning the Cytokine Responses: An Update on Interleukin (IL)-4 and IL-13 Receptor Complexes. *Front Immunol*. 2018; 9:888. <https://doi.org/10.3389/fimmu.2018.00888> PMID: [29930549](#).
12. Gour N, Wills-Karp M. IL-4 and IL-13 signaling in allergic airway disease. *Cytokine*. 2015; 75(1):68–78. <https://doi.org/10.1016/j.cyto.2015.05.014> PMID: [26070934](#).
13. Garcia-Posadas L, Contreras-Ruiz L, Soriano-Romani L, Dartt DA, Diebold Y. Conjunctival Goblet Cell Function: Effect of Contact Lens Wear and Cytokines. *Eye Contact Lens*. 2016; 42(2):83–90. <https://doi.org/10.1097/ICL.000000000000158> PMID: [26067396](#).
14. Fukuda K, Kumagai N, Fujitsu Y, Nishida T. Fibroblasts as local immune modulators in ocular allergic disease. *Allergol Int*. 2006; 55(2):121–9. <https://doi.org/10.2332/allergolint.55.121> PMID: [17075248](#).
15. Saw VP, Offiah I, Dart RJ, Galatowicz G, Dart JK, Daniels JT, et al. Conjunctival interleukin-13 expression in mucous membrane pemphigoid and functional effects of interleukin-13 on conjunctival fibroblasts in vitro. *Am J Pathol*. 2009; 175(6):2406–15. <https://doi.org/10.2353/ajpath.2009.090579> PMID: [19910508](#).
16. Leonardi A, Motterle L, Bortolotti M. Allergy and the eye. *Clin Exp Immunol*. 2008; 153 Suppl 1:17–21. <https://doi.org/10.1111/j.1365-2249.2008.03716.x> PMID: [18721324](#).
17. De Paiva CS, Raince JK, McClellan AJ, Shanmugam KP, Pangelinan SB, Volpe EA, et al. Homeostatic control of conjunctival mucosal goblet cells by NKT-derived IL-13. *Mucosal Immunol*. 2011; 4(4):397–408. <https://doi.org/10.1038/mi.2010.82> PMID: [21178983](#).
18. Dalessandri T, Crawford G, Hayes M, Castro Seoane R, Strid J. IL-13 from intraepithelial lymphocytes regulates tissue homeostasis and protects against carcinogenesis in the skin. *Nat Commun*. 2016; 7:12080. <https://doi.org/10.1038/ncomms12080> PMID: [27357235](#).
19. Tukler Henriksson J, Coursey TG, Corry DB, De Paiva CS, Pflugfelder SC. IL-13 Stimulates Proliferation and Expression of Mucin and Immunomodulatory Genes in Cultured Conjunctival Goblet Cells. *Invest Ophthalmol Vis Sci*. 2015; 56(8):4186–97. <https://doi.org/10.1167/iovs.14-15496> PMID: [26132778](#).
20. Contreras-Ruiz L, Ghosh-Mitra A, Shatos MA, Dartt DA, Masli S. Modulation of conjunctival goblet cell function by inflammatory cytokines. *Mediators Inflamm*. 2013; 2013:636812. <https://doi.org/10.1155/2013/636812> PMID: [24453426](#).
21. Garcia-Posadas L, Hodges RR, Diebold Y, Dartt DA. Context-Dependent Regulation of Conjunctival Goblet Cell Function by Allergic Mediators. *Sci Rep*. 2018; 8(1):12162. <https://doi.org/10.1038/s41598-018-30002-x> PMID: [30111832](#).
22. Garcia-Posadas L, Soriano-Romani L, Lopez-Garcia A, Diebold Y. An engineered human conjunctival-like tissue to study ocular surface inflammatory diseases. *PLoS One*. 2017; 12(3):e0171099. <https://doi.org/10.1371/journal.pone.0171099> PMID: [28248962](#).
23. Lavker RM, Tseng SC, Sun TT. Corneal epithelial stem cells at the limbus: looking at some old problems from a new angle. *Exp Eye Res*. 2004; 78(3):433–46. PMID: [15106923](#).

24. Utheim TP. Limbal epithelial cell therapy: past, present, and future. *Methods Mol Biol.* 2013; 1014:3–43. https://doi.org/10.1007/978-1-62703-432-6_1 PMID: 23690002.
25. Tsai RJ, Tseng SC. Substrate modulation of cultured rabbit conjunctival epithelial cell differentiation and morphology. *Invest Ophthalmol Vis Sci.* 1988; 29(10):1565–76. PMID: 3049430.
26. Eidet JR, Dartt DA, Utheim TP. Concise Review: Comparison of Culture Membranes Used for Tissue Engineered Conjunctival Epithelial Equivalents. *J Funct Biomater.* 2015; 6(4):1064–84. <https://doi.org/10.3390/jfb6041064> PMID: 26690486.
27. Schrader S, Notara M, Beaconsfield M, Tuft SJ, Daniels JT, Geerling G. Tissue engineering for conjunctival reconstruction: established methods and future outlooks. *Curr Eye Res.* 2009; 34(11):913–24. <https://doi.org/10.3109/02713680903198045> PMID: 19958107.
28. Ang LP, Tan DT, Cajucom-Uy H, Beuerman RW. Autologous cultivated conjunctival transplantation for pterygium surgery. *Am J Ophthalmol.* 2005; 139(4):611–9. <https://doi.org/10.1016/j.ajo.2004.10.056> PMID: 15808155.
29. Tanioka H, Kawasaki S, Yamasaki K, Ang LP, Koizumi N, Nakamura T, et al. Establishment of a cultivated human conjunctival epithelium as an alternative tissue source for autologous corneal epithelial transplantation. *Invest Ophthalmol Vis Sci.* 2006; 47(9):3820–7. <https://doi.org/10.1167/iovs.06-0293> PMID: 16936093.
30. Ang LP, Tanioka H, Kawasaki S, Ang LP, Yamasaki K, Do TP, et al. Cultivated human conjunctival epithelial transplantation for total limbal stem cell deficiency. *Invest Ophthalmol Vis Sci.* 2010; 51(2):758–64. <https://doi.org/10.1167/iovs.09-3379> PMID: 19643956.
31. Di Girolamo N, Bosch M, Zamora K, Coroneo MT, Wakefield D, Watson SL. A contact lens-based technique for expansion and transplantation of autologous epithelial progenitors for ocular surface reconstruction. *Transplantation.* 2009; 87(10):1571–8. <https://doi.org/10.1097/TP.0b013e3181a4bbf2> PMID: 19461496.
32. Rama P, Matuska S, Paganoni G, Spinelli A, De Luca M, Pellegrini G. Limbal stem-cell therapy and long-term corneal regeneration. *N Engl J Med.* 2010; 363(2):147–55. <https://doi.org/10.1056/NEJMoa0905955> PMID: 20573916.
33. Myers R. Special Stain Techniques for the Evaluation of Mucins. <https://www.leicabiosystems.com/pathologyleaders/special-stain-techniques-for-the-evaluation-of-mucins/>.
34. Jirsova K, Dudakova L, Kalasova S, Vesela V, Merjava S. The OV-TL 12/30 clone of anti-cytokeratin 7 antibody as a new marker of corneal conjunctivalization in patients with limbal stem cell deficiency. *Invest Ophthalmol Vis Sci.* 2011; 52(8):5892–8. <https://doi.org/10.1167/iovs.10-6748> PMID: 21693612.
35. Gerdes J, Lemke H, Baisch H, Wacker HH, Schwab U, Stein H. Cell cycle analysis of a cell proliferation-associated human nuclear antigen defined by the monoclonal antibody Ki-67. *J Immunol.* 1984; 133(4):1710–5. PMID: 6206131.
36. Parsa R, Yang A, McKeon F, Green H. Association of p63 with proliferative potential in normal and neoplastic human keratinocytes. *J Invest Dermatol.* 1999; 113(6):1099–105. <https://doi.org/10.1046/j.1523-1747.1999.00780.x> PMID: 10594758.
37. Di Iorio E, Barbaro V, Ruzza A, Ponzin D, Pellegrini G, De Luca M. Isoforms of DeltaNp63 and the migration of ocular limbal cells in human corneal regeneration. *Proc Natl Acad Sci U S A.* 2005; 102(27):9523–8. <https://doi.org/10.1073/pnas.0503437102> PMID: 15983386.
38. Pellegrini G, Dellambra E, Golisano O, Martinelli E, Fantozzi I, Bondanza S, et al. p63 identifies keratinocyte stem cells. *Proc Natl Acad Sci U S A.* 2001; 98(6):3156–61. <https://doi.org/10.1073/pnas.061032098> PMID: 11248048.
39. Inatomi T, Spurr-Michaud S, Tisdale AS, Zhan Q, Feldman ST, Gipson IK. Expression of secretory mucin genes by human conjunctival epithelia. *Invest Ophthalmol Vis Sci.* 1996; 37(8):1684–92. PMID: 8675412.
40. Dyrland TF, Poulsen ET, Scavenius C, Nikolajsen CL, Thogersen IB, Vorum H, et al. Human cornea proteome: identification and quantitation of the proteins of the three main layers including epithelium, stroma, and endothelium. *J Proteome Res.* 2012; 11(8):4231–9. <https://doi.org/10.1021/pr300358k> PMID: 22698189.
41. Luznik Z, Hawlina M, Malicev E, Bertolin M, Kopitar AN, Ihan A, et al. Effect of Cryopreserved Amniotic Membrane Orientation on the Expression of Limbal Mesenchymal and Epithelial Stem Cell Markers in Prolonged Limbal Explant Cultures. *PLoS One.* 2016; 11(10):e0164408. <https://doi.org/10.1371/journal.pone.0164408> PMID: 27723792.
42. Madhira SL, Vemuganti G, Bhaduri A, Gaddipati S, Sangwan VS, Ghanekar Y. Culture and characterization of oral mucosal epithelial cells on human amniotic membrane for ocular surface reconstruction. *Mol Vis.* 2008; 14:189–96. PMID: 18334934.

43. Schrader S, Notara M, Tuft SJ, Beaconsfield M, Geerling G, Daniels JT. Simulation of an in vitro niche environment that preserves conjunctival progenitor cells. *Regen Med.* 2010; 5(6):877–89. <https://doi.org/10.2217/rme.10.73> PMID: 21082888.
44. Ang LP, Tan DT, Seah CJ, Beuerman RW. The use of human serum in supporting the in vitro and in vivo proliferation of human conjunctival epithelial cells. *Br J Ophthalmol.* 2005; 89(6):748–52. <https://doi.org/10.1136/bjo.2004.055046> PMID: 15923513.
45. Curran-Everett D. Explorations in statistics: standard deviations and standard errors. *Adv Physiol Educ.* 2008; 32(3):203–8. <https://doi.org/10.1152/advan.90123.2008> PMID: 18794241.
46. Liu CY. Wakayama symposium: role of canonical Notch signaling in conjunctival goblet cell differentiation and dry eye syndrome. *BMC Ophthalmol.* 2015; 15 Suppl 1:152. <https://doi.org/10.1186/s12886-015-0136-6> PMID: 26818247.
47. Birchenough GM, Johansson ME, Gustafsson JK, Bergstrom JH, Hansson GC. New developments in goblet cell mucus secretion and function. *Mucosal Immunol.* 2015; 8(4):712–9. <https://doi.org/10.1038/mi.2015.32> PMID: 25872481.
48. Sasamoto Y, Hayashi R, Park SJ, Saito-Adachi M, Suzuki Y, Kawasaki S, et al. PAX6 Isoforms, along with Reprogramming Factors, Differentially Regulate the Induction of Cornea-specific Genes. *Sci Rep.* 2016; 6:20807. <https://doi.org/10.1038/srep20807> PMID: 26899008.
49. Kawasaki S, Tanioka H, Yamasaki K, Yokoi N, Komuro A, Kinoshita S. Clusters of corneal epithelial cells reside ectopically in human conjunctival epithelium. *Invest Ophthalmol Vis Sci.* 2006; 47(4):1359–67. <https://doi.org/10.1167/iops.05-1084> PMID: 16565369.
50. Koroma BM, Yang JM, Sundin OH. The Pax-6 homeobox gene is expressed throughout the corneal and conjunctival epithelia. *Invest Ophthalmol Vis Sci.* 1997; 38(1):108–20. PMID: 9008636.
51. Pathak M, Olstad OK, Drolsum L, Moe MC, Smorodina N, Kalasova S, et al. The effect of culture medium and carrier on explant culture of human limbal epithelium: A comparison of ultrastructure, keratin profile and gene expression. *Exp Eye Res.* 2016; 153:122–32. <https://doi.org/10.1016/j.exer.2016.09.012> PMID: 27702552.
52. Lambiase A, Micera A, Pellegrini G, Merlo D, Rama P, De Luca M, et al. In vitro evidence of nerve growth factor effects on human conjunctival epithelial cell differentiation and mucin gene expression. *Invest Ophthalmol Vis Sci.* 2009; 50(10):4622–30. <https://doi.org/10.1167/iops.08-2716> PMID: 19407015.
53. Lambiase A, Bonini S, Bonini S, Micera A, Magrini L, Bracci-Laudiero L, et al. Increased plasma levels of nerve growth factor in vernal keratoconjunctivitis and relationship to conjunctival mast cells. *Invest Ophthalmol Vis Sci.* 1995; 36(10):2127–32. PMID: 7657550.
54. Garcia-Posadas L, Arranz-Valsero I, Lopez-Garcia A, Soriano-Romani L, Diebold Y. A new human primary epithelial cell culture model to study conjunctival inflammation. *Invest Ophthalmol Vis Sci.* 2013; 54(10):7143–52. <https://doi.org/10.1167/iops.13-12866> PMID: 24106119.
55. Lopez-Paniagua M, Nieto-Miguel T, de la Mata A, Dziasko M, Galindo S, Rey E, et al. Comparison of functional limbal epithelial stem cell isolation methods. *Exp Eye Res.* 2016; 146:83–94. <https://doi.org/10.1016/j.exer.2015.12.002> PMID: 26704459.
56. Xi X, Schlegel N, Caen JP, Minty A, Fournier S, Caput D, et al. Differential effects of recombinant human interleukin-13 on the in vitro growth of human haemopoietic progenitor cells. *Br J Haematol.* 1995; 90(4):921–7. PMID: 7669673.
57. Jacobsen SE, Okkenhaug C, Veiby OP, Caput D, Ferrara P, Minty A. Interleukin 13: novel role in direct regulation of proliferation and differentiation of primitive hematopoietic progenitor cells. *J Exp Med.* 1994; 180(1):75–82. PMID: 7516418.
58. Gomez-Flores E, Sanchez-Guzman E, Castro-Munozledo F. Asymmetrical cell division and differentiation are not dependent upon stratification in a corneal epithelial cell line. *J Cell Physiol.* 2011; 226(3):700–9. <https://doi.org/10.1002/jcp.22380> PMID: 20717959.

Appendix 3

Trosan P, Javorkova E, Zajicova A, Hajkova M, Hermankova B, Kossl J, Krulova M, Holan V: The supportive role of insulin-like growth factor-I in the differentiation of murine mesenchymal stem cells into corneal-like cells. *Stem Cells Dev.* 2016 Jun 1;25(11):874-81. Doi: 10.1089/scd.2016.0030. PMID: 27050039.

The Supportive Role of Insulin-Like Growth Factor-I in the Differentiation of Murine Mesenchymal Stem Cells into Corneal-Like Cells

Peter Trosan,¹⁻³ Eliska Javorkova,^{1,2} Alena Zajicova,¹ Michaela Hajkova,^{1,2} Barbora Hermankova,^{1,2} Jan Kossl,^{1,2} Magdalena Krulova,^{1,2} and Vladimir Holan^{1,2}

This study was focused on characterizing the differentiation of bone marrow-derived mesenchymal stem cells (MSCs) into corneal-like cells. Mouse MSCs were isolated from the bone marrow, grown in cell culture for 3 weeks, and purified using a magnetic activated cell sorter. Purified MSCs were cultured with an extract prepared from excised corneas and in the presence or absence of insulin-like growth factor-I (IGF-I). Analysis by quantitative real-time polymerase chain reaction showed that the expression of corneal specific markers, such as cytokeratin 12 (K12), keratocan, and lumican, was already induced after a 3-day cultivation and gradually increased during the 10-day incubation of MSCs with the extract. The presence of IGF-I significantly increased differentiation. Immunofluorescence analysis of differentiated MSCs showed positive results for the K12 protein. The morphology of the differentiated cells and the expression of cell surface markers CD45, CD11b, CD73, CD44, and CD105 were comparable in the control and differentiated MSCs. Proliferative activity was even higher in differentiated cells than in untreated MSCs. Both untreated and differentiated MSCs inhibited the production of interleukin-2 and interferon- γ in spleen cells stimulated with Concanavalin A. The results thus show that MSCs cultured in the presence of corneal extract and IGF-I efficiently differentiate into corneal-like cells. The differentiated cells possess characteristics of corneal epithelial cells and keratocytes, while at the same time maintaining MSC properties.

Introduction

SEVERE INJURIES OR DAMAGE of the ocular surface can lead to limbal stem cell deficiency (LSCD). In such cases, as the cornea cannot heal properly, corneal transparency is decreased and the defect cumulates in a loss of vision. The only way to treat such defects is transplantation of limbal stem cells (LSCs) from the healthy eye [1–3] or from an unrelated donor. If the LSCD is bilateral, autologous LSCs are not available and allogeneic LSCs have to be used. However, the use of allogeneic cells requires strong immunosuppression, and treatment results are not always satisfactory [4,5]. To overcome these problems, various other types of autologous stem cells have been proposed and tested [6–8]. Among them, mesenchymal stem cells (MSCs) are the most promising and prospective cell type.

MSCs represent a population of multipotent stem cells that can be obtained relatively easily from various sources. They can be isolated in a sufficient amount from bone

marrow or adipose tissue and are able to differentiate into a number of various cell types, including those that form bone, cartilage, muscle, fat, and other connective tissues [9], or can even transdifferentiate into other cell types, including corneal epithelial cells [7,10]. Furthermore, MSCs possess potent immunosuppressive and immunoregulatory properties [11,12] and are a source of numerous growth and trophic factors [13,14]. All these properties contribute to their therapeutic potential and make them promising candidate for cell populations for ocular surface regeneration. Indeed, numerous studies have demonstrated the ability of MSCs to treat damaged ocular surface and LSCD [7,15,16].

Although the ability of MSCs to differentiate into corneal cells is still a matter of debate [17], many authors clearly demonstrated the expression of markers of corneal epithelial cells or keratocytes in differentiated MSCs under selective conditions. For example, Du *et al.* [18] used reduced-serum medium supplemented with ascorbate and insulin for differentiation, Park *et al.* [19] cultured MSCs in keratocyte-

¹Department of Transplantation Immunology, Institute of Experimental Medicine, Academy of Sciences of the Czech Republic, Prague, Czech Republic.

²Department of Cell Biology, Faculty of Science, Charles University, Prague, Czech Republic.

³Laboratory of the Biology and Pathology of the Eye, First Faculty of Medicine, Institute of Inherited Metabolic Disorders, General University Hospital in Prague, Charles University in Prague, Prague, Czech Republic.

conditioned medium, and the medium from LSC cultures was used by Gu *et al.* [10]. In other studies, the coculture of MSCs with corneal epithelial cells or with corneal stromal cells induced the expression of corneal epithelial cell-associated markers [20,21].

In our previous study, we found that insulin-like growth factor-I (IGF-I) supports the differentiation of LSCs into corneal-like cells [22]. In the present study, we tested whether mouse bone marrow-derived MSCs have the potential to differentiate into corneal epithelial cells using the extract from the cornea, and whether the differentiation process is increased in the presence of IGF-I. We also evaluated the characteristics of MSCs differentiated with corneal extract and IGF-I and compared them to the untreated MSCs.

Materials and Methods

Animals

Mice of both sexes of the inbred strain BALB/c at the age of 2–4 months were used in the experiments. The animals were obtained from the breeding unit of the Institute of Molecular Genetics, Prague. The use of animals was approved by the local Animal Ethics Committee of the Institute of Experimental Medicine, Prague. The animals were treated in accordance with the Principles of Laboratory Animal Care.

Isolation, culture, and purification of MSCs

MSCs were isolated from the bone marrow of BALB/c mice. The bone marrow was flushed out from the femurs and tibias, and a single-cell suspension was prepared with a tissue homogenizer. The cells were seeded at a concentration of 4×10^6 cells/mL in Dulbecco's modified Eagle's medium (DMEM; Sigma) containing 10% fetal calf serum (Gibco BRL), antibiotics (100 U/mL of penicillin and 100 μ g/mL of streptomycin), and 10 mM HEPES buffer (after this referred to as complete DMEM) in 75-cm² tissue culture flasks (Trasadingen). After 72-h cultivation, the nonadherent cells were removed by washing and the remaining adherent cells were cultured with a regular exchange of medium and held to optimal cell concentration for an additional 2–3 weeks at 37°C in an atmosphere of 5% CO₂. The adherent cells were harvested by 5-min incubation with 1 mL of 0.5% trypsin and gently scrapped. The cell suspension was incubated for 15 min with CD11b MicroBeads and CD45 MicroBeads (Miltenyi Biotec) according to the manufacturer's instructions and immunodepleted CD11b⁺ and CD45⁺ cells using a magnetic activated cell sorter (AutoMACS; Miltenyi Biotec). The remaining CD11b⁻ and CD45⁻ cells were evaluated in terms of their purity and differentiation potential.

Phenotypic characterization of MSCs by flow cytometry

Untreated and differentiated MSCs were washed in phosphate-buffered saline (PBS) containing 0.5% bovine serum albumin and incubated for 30 min on ice with the following anti-mouse monoclonal antibodies (mAbs): allophycocyanin (APC)-labeled anti-CD44 (clone IM7; BD PharMingen), phycoerythrin (PE)-labeled anti-CD105 (clone MJ7/18; eBioscience), APC-labeled anti-CD11b (clone M1/70; BioLegend), fluorescein isothiocyanate-labeled anti-CD45 (clone 30-

F11; BioLegend), or PE-labeled anti-CD73 (clone: TY/11.8; eBioscience). Dead cells were stained using Hoechst 33258 fluorescent dye (Invitrogen) added to the samples 10 min before flow cytometry analysis. Data were collected using an LSR II cytometer (BD Biosciences) and analyzed using a FlowJo software (Tree Star).

Differentiation of MSCs to adipocytes and osteoblasts

MSCs were cultured for 2–3 weeks and separated by magnetic cell sorting. The cells were cultured in a complete DMEM supplemented with specific adipogenic (containing 0.1 mM dexamethasone, 0.5 mM 3-isobutyl-1-methyl xanthine, 0.1 mM indomethacine, and 0.5 mg/mL of insulin) or osteogenic (0.1 mM dexamethasone, 0.1 mM L-ascorbic acid, and 10 mM β -glycerophosphate disodium salt pentahydrate) reagents [23]. Cell differentiation was confirmed by staining with Oil Red O or Alizarin Red S.

Preparing the corneal extract

The corneas were harvested and cut into small pieces in serum-free DMEM (one cornea/125 μ L of medium) postmortem. The samples were frozen at -80°C and thawed/frozen in three cycles for 10 min each. The extracts were filtered through a 0.22 μ m filter and stored at -80°C until used.

Differentiation of MSCs

MSCs were cultured for 3, 7, or 10 days in complete DMEM with extract from the corneas and in the absence or presence of IGF-I (20 ng/mL; PeproTech). The concentration of the extract in the culture medium was 20% and increased to 40% during the culturing and exchange of the medium. The culture medium was exchanged every 2–3 days.

Detecting gene expression

The expression of genes for K12, keratocan, and lumican in cultured MSCs was detected using a quantitative real-time polymerase chain reaction (qPCR). The following primers were used for amplification: K12 (sense: GTGAGTCCGC TGGTGGTAAC, antisense: CATCAGCACAGCAGGAA GTG), keratocan (sense: TCCCCCATCAACTTATTTTAGC, antisense: AGTTTGGGGTTGCCATTACA), lumican (sense: GGATGGCAATCCTCTCACTC, antisense: TCATTTGCT ACACGTAGACACTCAT), and GAPDH (sense: AGAACA TCATCCCTGCATCC, antisense: ACATTGGGGGTAGG AACAC). Untreated or differentiated cells were transferred into Eppendorf tubes containing 500 μ L of TRI Reagent (Molecular Research Center), and the total RNA was extracted according to the manufacturer's instructions. One microgram of RNA was treated with deoxyribonuclease I (Promega) and used for subsequent reverse transcription. The first-strand cDNA was synthesized using random hexamers (Promega) in a total reaction volume of 25 μ L using M-MLV Reverse Transcriptase (Promega). qPCR was performed in a StepOnePlus real-time PCR system (Applied Biosystems) as previously described [22]. The PCR parameters included denaturation at 95°C for 3 min, 40 cycles at 95°C for 20 s, annealing at 60°C for 30 s, and elongation at 72°C for 30 s. Fluorescence data were collected at each cycle after an elongation step at 80°C for

5 s and were analyzed using StepOne Software version 2.2.3 (Applied Biosystems). Each individual experiment was done in triplicate. A relative quantification model was applied to calculate the expression of the target gene in comparison to GAPDH used as an endogenous control.

Determining metabolic cell activity

The metabolic activity of living cells was determined by the WST-1 assay. The assay is based on the ability of living cells to cleave tetrazolium salts by mitochondrial dehydrogenases into water soluble formazan, which is then measured by spectrophotometry. MSCs (2×10^5 cells/mL) were cultured in complete DMEM with or without extract from the corneas and IGF-I in 24-well tissue culture plates (Corning) for 7 days at 37°C in an atmosphere of 5% CO₂. WST-1 reagent (Roche) (10 µL/100 µL of the medium) was added to each well and the plates were incubated for another 4 h to form formazan [24]. Formazan-containing medium (100 µL) was transferred from each well into the 96-well tissue culture plates (Corning) and the absorbance was measured using a Sunrise Remote ELISA Reader (Grödig) at a wavelength of 450 nm.

Immunostaining with anti-K12 antibody

Corneal cells (prepared by trypsinization of corneal tissue) and untreated or differentiated MSCs (3.7×10^5 cells/mL) were fixed for 20 min with 4% paraformaldehyde and

permeabilized for 10 min with 0.1% Triton X-100. The samples were incubated with goat polyclonal anti-K12 antibody (Santa Cruz Biotechnology) for 1 h at room temperature and then with a secondary donkey anti-goat IgG antibody conjugated with Alexa Flour 594 (Invitrogen). The cells were rinsed with PBS containing 0.05% TWEEN and fixed on glass slides with Mowiol 4-88 (Calbiochem) in the presence of the nuclear dye 4',6-diamidino-2-phenylindole (DAPI). Visualization of the fluorescent label was performed using a fluorescent microscope (Leica).

Immunostaining with phalloidin

Untreated or differentiated MSCs (2.5×10^5 cells/mL) were fixed for 20 min with 4% paraformaldehyde and permeabilized for 10 min with 0.1% Triton X-100. The samples were then incubated with Phalloidin conjugated with Alexa Fluor 568 (Invitrogen) for 1 h at room temperature. Cell nuclei were stained with DAPI for 1 min and samples were mounted with VECTASHIELD. Visualization of the fluorescent label was performed using a fluorescent microscope (Leica).

Comparing the immunosuppressive properties of untreated and differentiated MSCs

Spleen cells (0.6×10^6 /mL) from BALB/c mice were stimulated with Concanavalin A (ConA; Sigma-Aldrich), as described previously [25]. Cells were cultured in a volume of

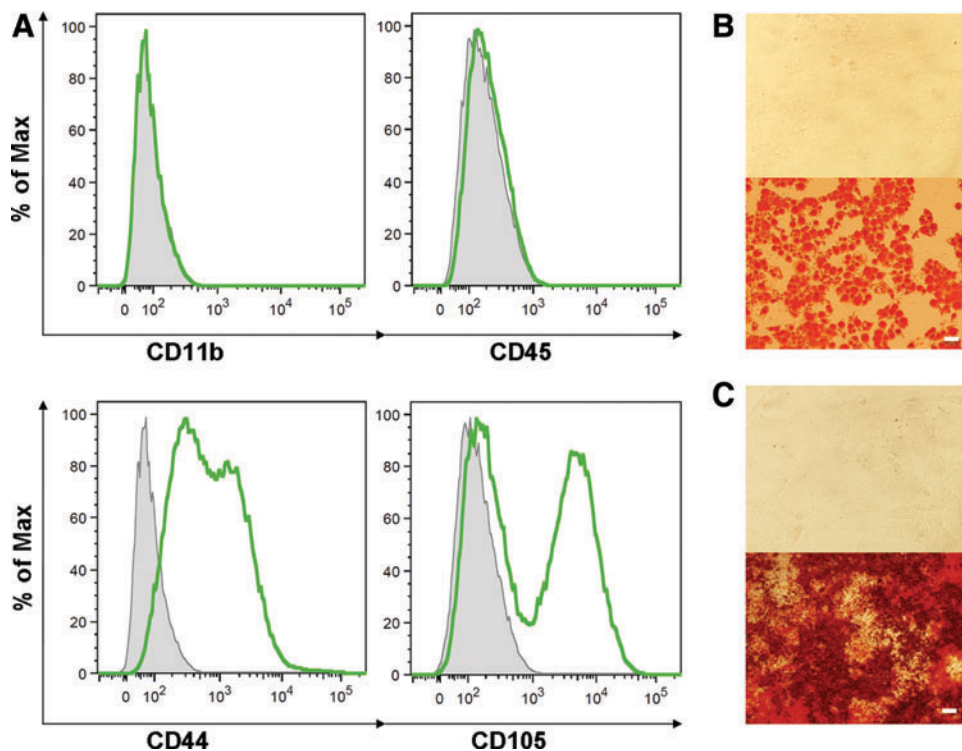


FIG. 1. Characterization of untreated bone marrow-derived MSCs. (A) Flow cytometry analysis of CD11b, CD45, CD44, and CD105 markers are expressed by MSCs (green curve) in comparison with unlabeled MSCs (gray-tinted curve). One of three similar experiments is shown. (B) The ability of MSCs to undergo adipogenic differentiation. The cultures without (upper panel) or with the addition of differentiation agents (lower panel) were stained with Oil Red O (scale bar represents 50 µm, original magnification: 200×). (C) The ability of MSCs to undergo osteogenic differentiation. The cultures without (upper panel) or with the addition of differentiation agents (lower panel) were stained with Alizarin Red S (scale bar represents 250 µm, original magnification: 40×). MSCs, mesenchymal stem cells. Color images available online at www.liebertpub.com/scd

0.4 mL of complete DMEM in 48-well tissue culture plates (Corning) alone or were stimulated with 1 μ g/mL of ConA. Untreated or differentiated MSCs were added to these cultures at a lymphocyte/MSC ratio of 8:1. Supernatants were harvested after a 24-h incubation for interleukin-2 (IL-2) determination and after a 48-h incubation period for interferon- γ (IFN- γ) determination. The concentrations of cytokines in the supernatants were determined by ELISA using cytokine-specific capture and detection mAbs purchased from BD Pharmingen and following the manufacturer's instructions.

Statistical analysis

The statistical significance of differences between individual groups was calculated using the Student's *t*-test. A value of $P < 0.05$ was considered statistically significant.

Results

Characterization of MSCs

The purified cells had a uniform spindle-shaped morphology. The purity and phenotypic markers of MACS-separated MSCs were evaluated by flow cytometry. The results showed that MSCs were positive for CD44 and CD105, but negative for CD11b and CD45 (Fig. 1A). In addition, the MSCs were characterized by their ability to undergo specific adipogenic (Fig. 1B) and osteogenic differentiation (Fig. 1C). These observations showed that the adherent MACS-separated bone marrow-derived cells possess the phenotype and differentiation characteristics of MSCs.

Differentiation of MSCs

The MSCs were cultured in the absence or presence of the corneal extract and with or without recombinant IGF-I (20 ng/mL) for 3, 7, or 10 days. The expression of genes for cornea-associated markers was determined by qPCR. Figure 2 shows that the expression of genes for K12, keratocan, and lumican was already upregulated 3 days after the culture with the extract. Adding IGF-I to the culture medium significantly increased the expression of the tested genes.

The differentiation potential of the MSCs was confirmed by immunostaining for the K12 protein using anti-K12 antibody. As demonstrated in Fig. 3, the K12 protein was clearly detected in the MSCs differentiated with the extract (Fig. 3B) and with the extract and IGF-I (Fig. 3C). Untreated MSCs were used as a negative control for K12 expression (Fig. 3D), while isolated corneal epithelial cells served as a positive control (Fig. 3A).

Morphology, growth, and gene expression of differentiated MSCs

The morphology of the untreated and differentiated MSCs is shown in Fig. 4. Both cell types had a typical fibroblast-like shape and adhered to plastic and glass surfaces. The expression of cell surface markers CD45, CD11b, CD73, CD44, and CD105 was determined by flow cytometry. The analysis revealed that both cell types had a similar expression profile (Fig. 5). Results from the WST-1 assay showed that differentiated MSCs have rather better proliferation activity than untreated cells (Fig. 6).

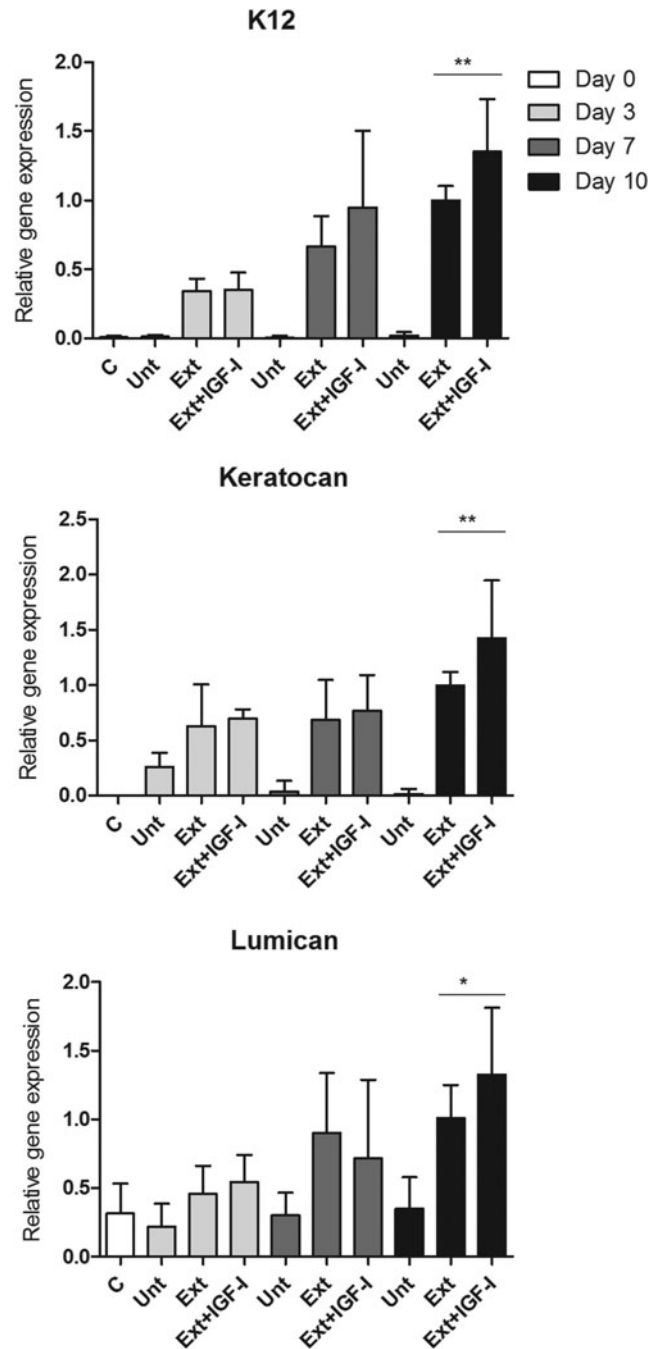
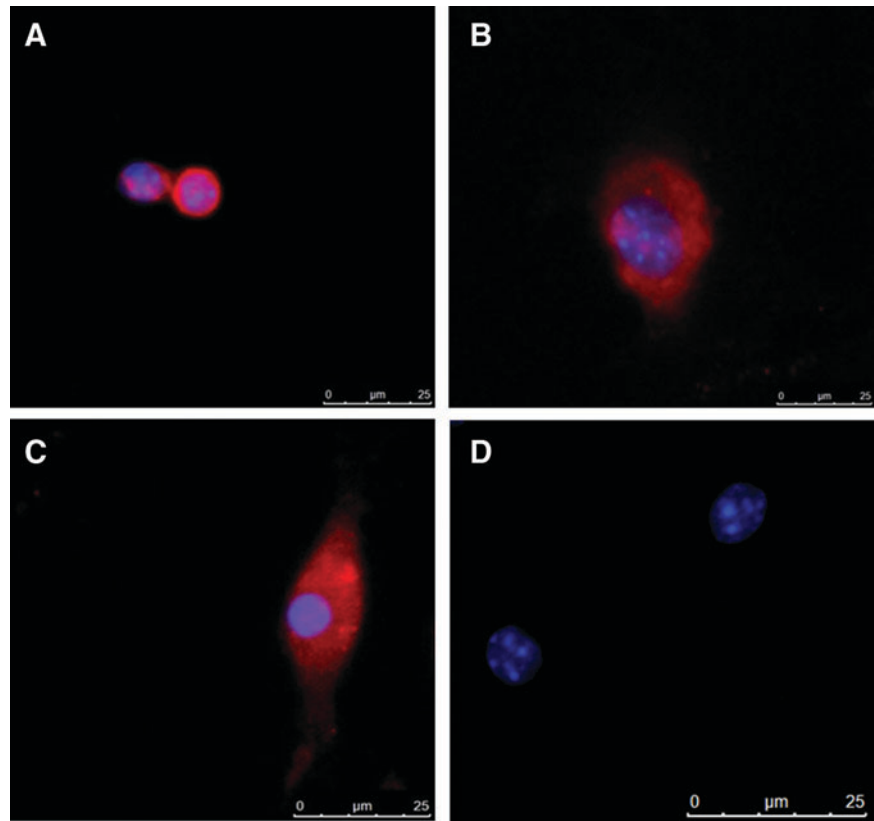


FIG. 2. The expression of genes for K12, keratocan, and lumican in untreated and differentiated MSCs was determined by qPCR. The cells were cultured for 3, 7, or 10 days untreated (Unt), with the extract from the corneas (Ext) and in the presence of the extract and IGF-I (Ext+IGF-I). Each bar represents mean \pm SD from four to five determinations. The asterisks represent statistically significant (* $P < 0.05$, ** $P < 0.01$) difference in the gene expression between MSCs treated only with the extract or with the extract and IGF-I. Freshly purified MSCs are marked as a control (C). IGF-I, insulin-like growth factor-I; qPCR, quantitative real-time polymerase chain reaction.

FIG. 3. Immunostaining for K12 protein in corneal cells and untreated or differentiated MSCs. Single cell suspensions of corneal cells (**A**), MSCs cultured with the extract (**B**), or with the extract and IGF-I (**C**), or untreated MSCs (**D**) were stained with a goat antibody against mouse K12. The nuclei were stained with DAPI (*blue*). One representative experiment of four similar ones is shown. DAPI, 4',6-diamidino-2-phenylindole. Color images available online at www.liebertpub.com/scd



Immunosuppressive properties of untreated and differentiated MSCs

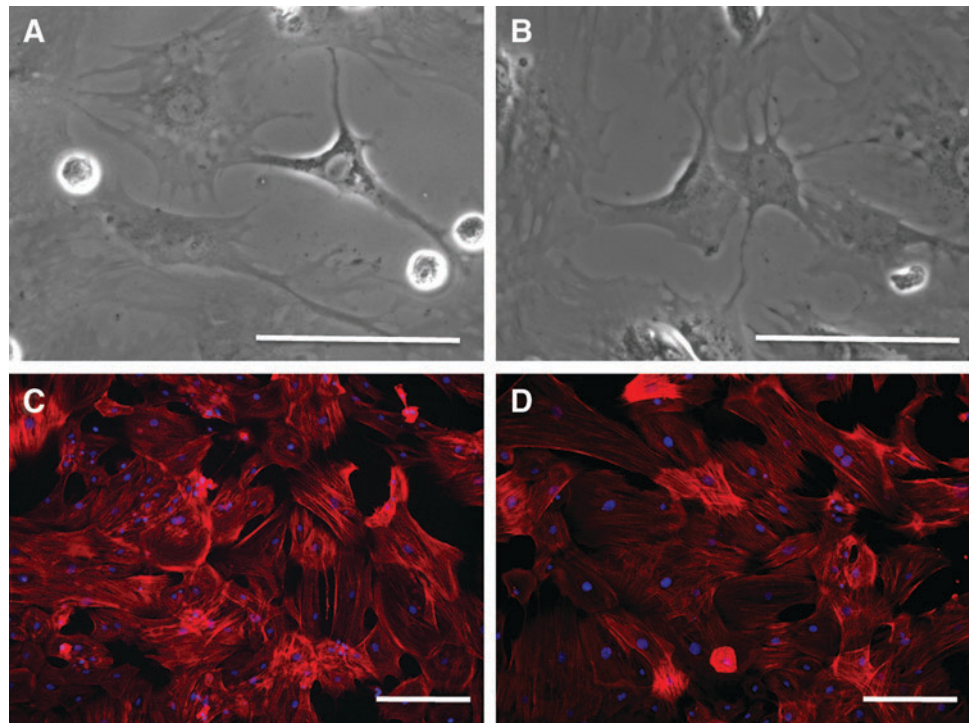
Spleen cells were stimulated with T-cell mitogen ConA in the absence or presence of untreated or differentiated MSCs (the ratio of lymphocytes to MSCs was 8:1). The production of IL-2 and IFN- γ was determined in the supernatants by ELISA.

As demonstrated in Fig. 7, both cell types significantly inhibited production of tested pro-inflammatory cytokines.

Discussion

The integrity of the cornea is ensured by a population of stem cells that reside in the limbus. When the cornea is

FIG. 4. Comparison of morphology of untreated and differentiated MSCs. The growing untreated MSCs (**A**, **C**) or MSCs treated for 10 days with the extract and IGF-I (**B**, **D**) are shown. The cells for the light microscopy analysis (**A**, **B**) remained unstained, the cells for the immunofluorescence analysis were stained with phalloidin for F-actin (*red filaments*) (**C**, **D**). The nuclei were stained with DAPI (*blue*). One representative experiment of three similar ones is shown. Scale bars represent 25 μ m. Color images available online at www.liebertpub.com/scd



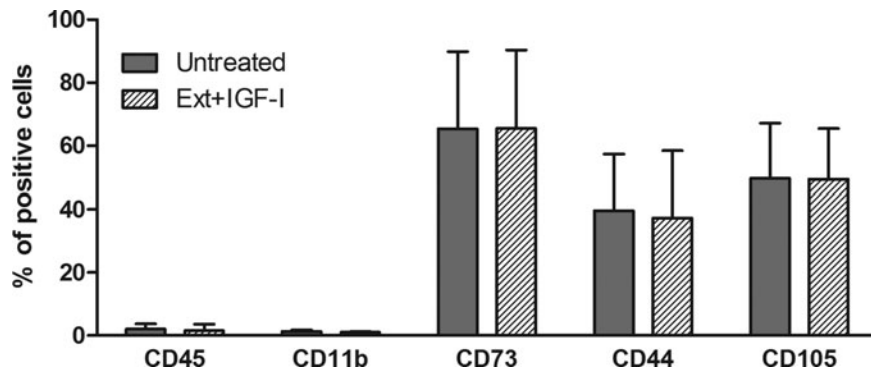


FIG. 5. Comparison of the expression of cell surface markers in untreated and differentiated MSCs. Flow cytometry analysis of CD45, CD11b, CD73, CD44, and CD105 markers expressed in untreated (Unt) or differentiated (Ext+IGF-I) MSCs is demonstrated. Each bar represents mean \pm SD from three determinations.

injured, LSCs start to proliferate, differentiate, and migrate to the site of injury. To treat corneal defects in patients with unilateral LSCD, LSCs can be isolated from healthy eyes, propagated in vitro, and using an appropriate scaffold transferred to treat the damaged cornea [2,26]. However, LSC therapy is limited by the low number of cells available and harmful immunological rejection if the cells are transplanted from a genetically unrelated donor. Therefore, other sources of autologous stem cells have been tested. These include conjunctival epithelial stem cells [8], oral mucosal cells [6], dental pulp stem cells [27], hair follicle stem cells [28], or various types of MSCs [7,15,29].

One of the properties required for stem cells used in the treatment of LSCD is their capability to differentiate into corneal cells. Therefore, in the present study, we characterized mouse bone marrow-derived MSCs and tested their ability to differentiate into cells expressing cornea-associated markers, which were not detected in untreated MSCs.

MSCs isolated by a negative sorting from the population of adherent bone marrow cells were positive for CD44 and CD105 and negative for CD11b and CD45, as described earlier [30]. In addition, these cells effectively differentiated into adipocytes and osteoblasts, thus fulfilling the basic criteria for definition of MSCs [31]. Based on screening the gene expression in untreated MSCs, we identified three

genes, which were not (*K12*, keratocan) or only weakly (lumican) expressed in unstimulated MSCs.

Previous studies have demonstrated the effects of the coculture of MSCs with corneal cells in limbal or corneal cell-conditioned medium on the differentiation of MSCs into keratocytes [18,19] or cells with markers and characteristics of corneal epithelial cells [10,20,21,32]. In the present study, we used the extract from corneas for differentiation of MSCs. We observed that already after a 3-day culture of the MSCs in the presence of the extract, the cells started to express corneal markers and their expression gradually increased. This observation is in accordance with the above studies showing the expression of corneal markers in MSCs cultured in the presence of corneal cells or in corneal cell-conditioned medium. In our previous study, we found that IGF-I plays an important role in the differentiation of LSCs into corneal epithelial cells. IGF-I, which is highly expressed in the cornea after the injury, migrates to the limbus where it binds to its receptor and triggers the differentiation process of LSCs [22]. Huang *et al.* [33] demonstrated that IGF-I can dose-dependently stimulate the proliferation of MSCs, upregulate the expression of CXCR4, and accelerate their migration. It has been also observed that IGF-I is secreted by MSCs after their therapeutic administration [34–36]. Therefore, we tested whether IGF-I could also play a role in the differentiation of MSCs into corneal-like cells. Adding IGF-I into MSC cultures with extract from the corneas significantly increased the expression of genes for *K12*, keratocan, and lumican. IGF-I alone had no effect on the expression of these genes (data not shown).

Purified bone marrow MSCs have fibroblastic morphology. Differentiated MSCs did not change their morphology and remained in fibroblastic shape, which is comparable to previous results [20,32]. Both untreated and differentiated MSCs adhered to plastic and glass surfaces. Comparing the expression of cell surface markers did not reveal differences between untreated and differentiated cells. A similar conclusion was reached in the study where unstimulated MSCs and MSCs stimulated with a cocktail of pro-inflammatory cytokines were tested for the expression of endothelial, stromal, and adhesive markers [37]. In accordance with other studies on the proliferative and metabolic activity of differentiated cells [33,38,39], we found that MSCs differentiated with corneal extract and IGF-I have comparable or even slightly enhanced metabolic activity to untreated cells.

MSCs possess potent immunosuppressive properties and inhibit the production of various pro-inflammatory cytokines

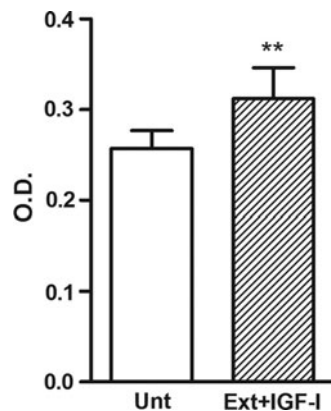


FIG. 6. Comparison of the metabolic activity of the untreated (Unt) and differentiated (Ext+IGF-I) MSCs. WST-1 reagent was added to the cell cultures for 4 h to form formazan. The absorbance was measured using a Sunrise Remote ELISA Reader at a wavelength of 450 nm. Each bar represents mean \pm SD from three determinations (** $P < 0.01$).

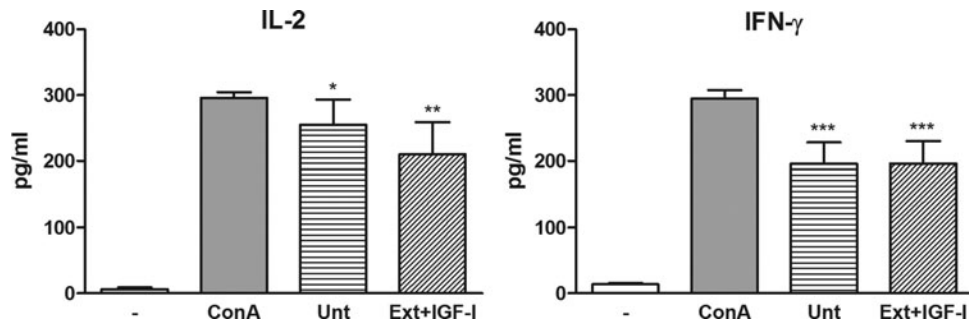


FIG. 7. Comparison of the immunosuppressive properties of untreated and differentiated MSCs. Spleen cells were cultured unstimulated or were stimulated with ConA in the presence of untreated (Unt) or differentiated (Ext+IGF-I) MSCs. The production of IL-2 and IFN- γ was determined in the supernatants after a 24 h (IL-2) or 48 h (IFN- γ) incubation period by ELISA. Each bar represents mean \pm SD from three determinations (* P < 0.05, ** P < 0.01, *** P < 0.001). ConA, concanavalin A; IL-2, interleukin-2; IFN- γ , interferon- γ .

[24,40]. In the present study, we confirmed the suppressive potential of unstimulated MSCs and we showed that differentiated MSCs inhibit the production of IFN- γ and IL-2, similar to untreated MSCs.

In conclusion, we showed that IGF-I supports differentiation of mouse bone marrow-derived MSCs into cells expressing markers of corneal cells. Differentiated MSCs expressed markers of both corneal epithelial cells and keratocytes. This observation makes them a promising source of stem cells for the regeneration of damaged or diseased cornea. In addition, the differentiated cells maintain characteristics of unstimulated MSCs and suppress the production of pro-inflammatory cytokines by activated T lymphocytes.

Acknowledgments

This work was supported by projects 889113 and 80815 from the Grant Agency of Charles University, grant 14-12580S from the Grant Agency of the Czech Republic, and by the projects CZ.1.05/1.1.00/02.0109, CZ.2.16/3.1.00/21528, SVV 260206, UNCE 204013, NPUI LO1309, and NPUI LO1508 and also by funding from the Norwegian Financial Mechanism 2009–2014 and the Ministry of Education, Youth and Sports under project contract no. MSMT-28477/2014, project 7F14156.

Author Disclosure Statement

No competing financial interests exist.

References

- Pellegrini G, CE Traverso, AT Franzi, M Zingirian, R Cancedda and M De Luca. (1997). Long-term restoration of damaged corneal surfaces with autologous cultivated corneal epithelium. *Lancet* 349:990–993.
- Rama P, S Matuska, G Paganoni, A Spinelli, M De Luca and G Pellegrini. (2010). Limbal stem-cell therapy and long-term corneal regeneration. *N Engl J Med* 363:147–155.
- Marchini G, E Pedrotti, M Pedrotti, V Barbaro, E Di Iorio, S Ferrari, M Bertolin, B Ferrari, M Passilongo, A Fasolo and D Ponzin. (2012). Long-term effectiveness of autologous cultured limbal stem cell grafts in patients with limbal stem cell deficiency due to chemical burns. *Clin Exp. Ophthalmol* 40:255–267.
- Miri A, B Al-Deiri and HS Dua. (2010). Long-term outcomes of autolimbal and allolimbal transplants. *Ophthalmology* 117:1207–1213.
- Pellegrini G, P Rama, A Di Rocco, A Panaras and M De Luca. (2014). Concise review: hurdles in a successful example of limbal stem cell-based regenerative medicine. *Stem Cells* 32:26–34.
- Inatomi T, T Nakamura, N Koizumi, C Sotozono, N Yokoi and S Kinoshita. (2006). Midterm results on ocular surface reconstruction using cultivated autologous oral mucosal epithelial transplantation. *Am J Ophthalmol* 141:267–275.
- Ma Y, Y Xu, Z Xiao, W Yang, C Zhang, E Song, Y Du and L Li. (2006). Reconstruction of chemically burned rat corneal surface by bone marrow-derived human mesenchymal stem cells. *Stem Cells* 24:315–321.
- Sangwan VS, GK Vemuganti, S Singh and D Balasubramanian. (2003). Successful reconstruction of damaged ocular outer surface in humans using limbal and conjunctival stem cell culture methods. *Biosci Rep* 23:169–174.
- Caplan AI. (1991). Mesenchymal stem cells. *J Orthop Res* 9:641–650.
- Gu SF, CZ Xing, JY Han, MOM Tso and J Hong. (2009). Differentiation of rabbit bone marrow mesenchymal stem cells into corneal epithelial cells in vivo and ex vivo. *Mol Vis* 15:99–107.
- Abumaree M, M Al Jumah, RA Pace and B Kalionis. (2012). Immunosuppressive properties of mesenchymal stem cells. *Stem Cell Rev* 8:375–392.
- Le Blanc K, L Tammik, B Sundberg, SE Haynesworth and O Ringden. (2003). Mesenchymal stem cells inhibit and stimulate mixed lymphocyte cultures and mitogenic responses independently of the major histocompatibility complex. *Scand J Immunol* 57:11–20.
- Oh JY, MK Kim, MS Shin, WR Wee and JH Lee. (2009). Cytokine secretion by human mesenchymal stem cells cocultured with damaged corneal epithelial cells. *Cytokine* 46:100–103.
- Uccelli A, L Moretta and V Pistoia. (2008). Mesenchymal stem cells in health and disease. *Nat Rev Immunol* 8:726–736.
- Ye J, K Yao and JC Kim. (2006). Mesenchymal stem cell transplantation in a rabbit corneal alkali burn model: engraftment and involvement in wound healing. *Eye (Lond)* 20:482–490.
- Holan V and E Javorkova. (2013). Mesenchymal stem cells, nanofiber scaffolds and ocular surface reconstruction. *Stem Cell Rev* 9:609–619.

17. Harkin DG, L Foyn, LJ Bray, AJ Sutherland, FJ Li and BG Cronin. (2015). Concise reviews: can mesenchymal stromal cells differentiate into corneal cells? A systematic review of published data. *Stem Cells* 33:785–791.
18. Du YQ, DS Roh, ML Funderburgh, MM Mann, KG Marra, JP Rubin, XA Li and JL Funderburgh. (2010). Adipose-derived stem cells differentiate to keratocytes in vitro. *Mol Vis* 16:2680–2689.
19. Park SH, KW Kim, YS Chun and JC Kim. (2012). Human mesenchymal stem cells differentiate into keratocyte-like cells in keratocyte-conditioned medium. *Exp Eye Res* 101:16–26.
20. Jiang TS, L Cai, WY Ji, YN Hui, YS Wang, D Hu and J Zhu. (2010). Reconstruction of the corneal epithelium with induced marrow mesenchymal stem cells in rats. *Mol Vis* 16:1304–1316.
21. Nieto-Miguel T, S Galindo, R Reinoso, A Corell, M Martino, JA Perez-Simon and M Calonge. (2013). In vitro simulation of corneal epithelium microenvironment induces a corneal epithelial-like cell phenotype from human adipose tissue mesenchymal stem cells. *Curr Eye Res* 38:933–944.
22. Trosan P, E Svobodova, M Chudickova, M Krulova, A Zajicova and V Holan. (2012). The key role of insulin-like growth factor I in limbal stem cell differentiation and the corneal wound-healing process. *Stem Cells Dev* 21:3341–3350.
23. Tropel P, D Noel, N Platet, P Legrand, AL Benabid and F Berger. (2004). Isolation and characterisation of mesenchymal stem cells from adult mouse bone marrow. *Exp Cell Res* 295:395–406.
24. Zajicova A, K Pokorna, A Lencova, M Krulova, E Svobodova, S Kubinova, E Sykova, M Pradny, J Michalek, *et al.* (2010). Treatment of ocular surface injuries by limbal and mesenchymal stem cells growing on nanofiber scaffolds. *Cell Transplant* 19:1281–1290.
25. Holan V, K Pokorna, J Prochazkova, M Krulova and A Zajicova. (2010). Immunoregulatory properties of mouse limbal stem cells. *J Immunol* 184:2124–2129.
26. Ramirez BE, A Sanchez, JM Herreras, I Fernandez, J Garcia-Sancho, T Nieto-Miguel and M Calonge. (2015). Stem cell therapy for corneal epithelium regeneration following good manufacturing and clinical procedures. *Biomed Res Int* 2015:408–495.
27. Syed-Picard FN, Y Du, KL Lathrop, MM Mann, ML Funderburgh and JL Funderburgh. (2015). Dental pulp stem cells: a new cellular resource for corneal stromal regeneration. *Stem Cells Transl Med* 4:276–285.
28. Meyer-Blazejewski EA, MK Call, O Yamanaka, H Liu, U Schlotzer-Schrehardt, FE Kruse and WW Kao. (2011). From hair to cornea: toward the therapeutic use of hair follicle-derived stem cells in the treatment of limbal stem cell deficiency. *Stem Cells* 29:57–66.
29. Holan V, P Trosan, C Cejka, E Javorkova, A Zajicova, B Hermankova, M Chudickova and J Cejkova. (2015). A Comparative study of the therapeutic potential of mesenchymal stem cells and limbal epithelial stem cells for ocular surface reconstruction. *Stem Cells Transl Med* 4:1052–1063.
30. Javorkova E, P Trosan, A Zajicova, M Krulova, M Hajkova and V Holan. (2014). Modulation of the early inflammatory microenvironment in the alkali-burned eye by systemically administered interferon-gamma-treated mesenchymal stromal cells. *Stem Cells Dev* 23:2490–2500.
31. Dominici M, K Le Blanc, I Mueller, I Slaper-Cortenbach, F Marini, D Krause, R Deans, A Keating, D Prockop and E Horwitz. (2006). Minimal criteria for defining multipotent mesenchymal stromal cells. The international society for cellular therapy position statement. *Cytotherapy* 8:315–317.
32. Rohaina CM, KY Then, AMH Ng, WHWA Halim, AZM Zahidin, A Saim and RBH Idrus. (2014). Reconstruction of limbal stem cell deficient corneal surface with induced human bone marrow mesenchymal stem cells on amniotic membrane. *Transl Res* 163:200–210.
33. Huang YL, RF Qiu, WY Mai, J Kuang, XY Cai, YG Dong, YZ Hu, YB Song, AP Cai and ZG Jiang. (2012). Effects of insulin-like growth factor-1 on the properties of mesenchymal stem cells in vitro. *J Zhejiang Univ Sci B* 13:20–28.
34. Tao ZW, LG Li, ZH Geng, T Dang and SJ Zhu. (2010). Growth factors induce the improved cardiac remodeling in autologous mesenchymal stem cell-implanted failing rat hearts. *J Zhejiang Univ Sci B* 11:238–248.
35. Xu M, R Uemura, Y Dai, Y Wang, Z Pasha and M Ashraf. (2007). In vitro and in vivo effects of bone marrow stem cells on cardiac structure and function. *J Mol Cell Cardiol* 42:441–448.
36. Nagaya N, K Kangawa, T Itoh, T Iwase, S Murakami, Y Miyahara, T Fujii, M Uematsu, H Ohgushi, *et al.* (2005). Transplantation of mesenchymal stem cells improves cardiac function in a rat model of dilated cardiomyopathy. *Circulation* 112:1128–1135.
37. Najar M, G Raicevic, HF Kazan, C De Bruyn, D Bron, M Toungouz and L Lagneaux. (2012). Immune-related antigens, surface molecules and regulatory factors in human-derived mesenchymal stromal cells: the expression and impact of inflammatory priming. *Stem Cell Rev Rep* 8: 1188–1198.
38. Ren J, WK Samson and JR Sowers. (1999). Insulin-like growth factor I as a cardiac hormone: physiological and pathophysiological implications in heart disease. *J Mol Cell Cardiol* 31:2049–2061.
39. Kaplan RC, HD Strickler, TE Rohan, R Muzumdar and DL Brown. (2005). Insulin-like growth factors and coronary heart disease. *Cardiol Rev* 13:35–39.
40. Di Nicola M, C Carlo-Stella, M Magni, M Milanese, PD Longoni, P Matteucci, S Grisanti and AM Gianni. (2002). Human bone marrow stromal cells suppress T-lymphocyte proliferation induced by cellular or nonspecific mitogenic stimuli. *Blood* 99:3838–3843.

Address correspondence to:

Peter Trosan, MSc

Laboratory of the Biology and Pathology of the Eye

First Faculty of Medicine

Institute of Inherited Metabolic Disorders

General University Hospital in Prague

Charles University in Prague

Ke Karlovu 2

Prague 2 128 08

Czech Republic

E-mail: peter.trosan@lf1.cuni.cz

Received for publication February 1, 2016

Accepted after revision April 5, 2016

Prepublished on Liebert Instant Online April 6, 2016

Appendix 4

Smeringaiova I, **Trosan P**, Mrstinova MB, Matecha J, Burkert J, Bednar J, Jirsova K: Comparison of impact of two decontamination solutions on the viability of the cells in human amnion. Cell Tissue Bank. 2017 Sep;18(3):413-423. Doi: 10.1007/s10561-017-9636-3. PMID: 28677080.

Comparison of impact of two decontamination solutions on the viability of the cells in human amnion

Ingrida Smeringaiova  · Peter Trosan · Miluse Berka Mrstinova · Jan Matecha · Jan Burkert · Jan Bednar · Katerina Jirsova

Received: 4 January 2017 / Accepted: 6 June 2017
© Springer Science+Business Media B.V. 2017

Abstract Human amniotic membrane (HAM) is used as an allograft in regenerative medicine or as a source of pluripotent cells for stem cell research. Various decontamination protocols and solutions are used to sterilize HAM before its application, but little is known about the toxicity of disinfectants on HAM cells. In this study, we tested two decontamination solutions, commercial (BASE-128) and laboratory decontamination solution (LDS), with an analogous content of antimycotic/antibiotics for their cytotoxic effect on HAM epithelial (EC) and mesenchymal stromal cells (MSC). HAM was processed in a standard way, placed on nitrocellulose scaffold, and decontaminated, following three protocols: (1) 6 h, 37 °C; (2) 24 h, room temperature; (3) 24 h, 4 °C. The viability of EC was assessed via trypan blue staining.

The apoptotic cells were detected using terminal deoxynucleotidyl transferase dUTP nick end labelling (TUNEL). The mean % (\pm SD) of dead EC (%DEC) from six fresh placentas was 12.9 ± 18.1 . Decontamination increased %DEC compared to culture medium. Decontamination with BASE-128 for 6 h, 37 °C led to the highest EC viability (81.7%). Treatment with LDS at 24 h, 4 °C resulted in the lowest EC viability (55.9%) in the set. MSC were more affected by apoptosis than EC. Although the BASE-128 expresses lower toxicity compared to LDS, we present LDS as an alternative decontamination solution with a satisfactory preservation of cell viability. The basic formula of LDS will be optimised by enrichment with nutrient components, such as glucose or vitamins, to improve cell viability.

I. Smeringaiova · P. Trosan · J. Bednar · K. Jirsova (✉)
Laboratory of the Biology and Pathology of the Eye,
Institute of Inherited Metabolic Disorders, First Faculty of
Medicine, Charles University and General University
Hospital in Prague, Ke Karlovu 2, 128 08 Prague,
Czech Republic
e-mail: katerina.jirsova@lf1.cuni.cz

M. B. Mrstinova · J. Matecha
Department of Obstetrics and Gynaecology, Second
Faculty of Medicine, Charles University, Prague,
Czech Republic

J. Burkert · K. Jirsova
Department of Transplantation and Tissue Bank, Motol
University Hospital, Prague, Czech Republic

Keywords Amniotic membrane · Decontamination solution · Viability · Apoptosis · Epithelial and mesenchymal cells

Introduction

The human placenta at term has two distinguishable fetal membranes that develop separately: the amniotic membrane (HAM) on the fetal surface of placenta and the chorionic membrane underneath the HAM. The two membranes remain separable due to the existence of a spongy layer in between. HAM

consists of a monolayer of epithelial cells (EC), which resides on a resistant basement membrane, and of a mesenchymal layer at the bottom. The latter can be subdivided into the acellular compact layer, the fibroblast layer with sparsely distributed mesenchymal stromal cells (MSC), and the acellular spongy layer, contiguous with the chorionic membrane (Bourne 1960, 1962; Dua et al. 2004; Lindenmair et al. 2012).

Different mechanisms of action, such as wound-healing, anti-scarring, anti-angiogenic, anti-inflammatory, antimicrobial effects and low antigenicity, have been attributed to the soluble bioactive compounds—cytokines, growth factors, vasoactive peptides etc., produced by HAM resident cells (Gruss and Jirsch 1978; Akle et al. 1981; Dua et al. 2004).

The HAM is most often used as a temporary biologic dressing in ophthalmology, but also in plastic surgery, dermatology and gynaecology (King et al. 2007; Mamede et al. 2012; Malhotra and Jain 2014). The HAM is elastic and translucent and is devoid of nerves, smooth muscle cells, lymph and blood vessels. Beside its clinical use, HAM is used in tissue engineering as a cheap and flexible biological 3D-cell carrier for cell migration, differentiation and delivery of *in vitro* cultured cells into ocular wound (Ishino et al. 2004; Gholipourmalekabadi et al. 2016).

The HAM is available without an ethical conflict, typically procured after caesarean section delivery and decontaminated with solutions containing antibiotics and antimycotics (AA). HAM is manually dissected under sterile conditions, thoroughly washed from blood clots and debris. During HAM preparation AA solutions may be used for repeated rinsing of tissue prior to storage. Alternatively, gamma irradiation is used for HAM sterilization (Singh et al. 2007; von Versen-Hoeynck et al. 2008; Riau et al. 2010).

Despite its putative advantages over preserved HAM, such as preservation of viable cells, the transplantation of fresh HAM (tissue not subjected to preservation, used within 14 days) has not been yet established. Some attempts have been made in this matter (Ganatra and Durrani 1996; Mejía et al. 2000; Adds et al. 2001), however, there is a lack of proper evidence for its safe clinical use, without risk of transmission of infection to a patient (Khokhar et al. 2001). In most western countries, fresh HAM is not permitted for use. Donor must be tested for signs of

viral or bacterial infection at the time of delivery and 6 months later to cover window period of infection. Thus HAM must be preserved during this period. Cryopreservation is the most common method of storage, using the standard protocol proposed by Kim and Tseng (1995). Lyophilisation and storage in a dry form are other basic preservation methods (Dua et al. 2006; von Versen-Hoeynck et al. 2008; Thomassen et al. 2009).

The decontamination is highly important when HAM is intended to be stored cryopreserved in glycerol, mixture of glycerol with a culture medium or dimethyl sulfoxide solution (Maral et al. 1999; Tan et al. 2014; Duan-Arnold et al. 2015; Zidan et al. 2015; Paolin et al. 2016). During standard preservation, the morphology of HAM matrix does not seem to be altered dramatically, but the majority of resident cells seem to be devitalized (von Versen-Hoeynck et al. 2004; Hennerbichler et al. 2006; Aykut et al. 2014; Mrázová et al. 2015; Perepelkin et al. 2016).

To our best knowledge, the only commercially available decontamination solution with certification based on Directive 93/42/EEC (medical devices) is the BASE-128 from Alchimia (Italy), which contains AA (amphotericin B, cefotaxime, gentamicin, vancomycin) (Gatto et al. 2013). In most cases, laboratories prepare their own tissue sterilization solutions, composed of physiological saline or buffers and added AA and use various decontamination protocols (Lee and Tseng 1997; Ashraf et al. 2015; Duan-Arnold et al. 2015; Laurent et al. 2014). The impact of different AA present in decontamination solutions on HAM tissue is insufficiently examined (Aykut et al. 2014; Perepelkin et al. 2016).

The purpose of this study was to compare the overall effect of the commercial solution BASE-128 and laboratory decontamination solution (LDS), with analogous composition of AA, on HAM structure, focused on viability of EC. The BASE-128 is reported (by producer's *in vitro* time-kill studies) to effectively decontaminate the tissue, if one of the three protocols is followed: (1) 6 h, 37 °C, (2) 24 h, at room temperature (RT) or (3) 24 h, 4 °C. The HAM was incubated under these conditions in both BASE-128 and LDS and the viability of EC cells after decontamination was tested via trypan blue staining. Additionally, the fresh and cryopreserved samples of HAM (before/after decontamination) were tested for the presence of apoptotic (EC, MSC) cells.

Materials and methods

Tissue

The study followed the standards of the Ethics Committee of the General Teaching Hospital and First Medical Faculty of Charles University, and adhered to the tenets set out in the Declaration of Helsinki. Six term human placentas (P1–P6) from normal pregnancies were obtained with informed consent after delivery by elective caesarean section in the Motol University Hospital, Prague. Only healthy donors, screened for hepatitis B and C, syphilis, HIV and C-reactive protein (<10 mg/L), were involved. The placentas with evident pathologies or visible injuries, such as hematomas, were excluded. Immediately after delivery, each placenta was placed in a sterile container and overlaid with Hank's Balanced Salt Solution (HBSS, Sigma-Aldrich, Prague, Czech Republic). Special attention was paid to the gentle handling of each placenta during transport and subsequent manipulation.

Processing

The tissue was processed in aseptic conditions within 3 h after the delivery. Briefly, the placenta was cleansed of blood clots with sterile HBSS under a biosafety cabinet and two HAM sheets were peeled off by blunt dissection starting underneath the umbilical cord insertion and proceeding towards the placental disk edge (Fig. 1a). They were gently rinsed again with HBSS to obtain thin smooth HAM and then flattened onto two sheets (9.5 × 9.5 cm each) of sterile nitrocellulose membrane (NCM) carrier (Bio-Rad, Prague, Czech Republic), the epithelium surface facing up (Fig. 1b). Prior the use, 24 rectangles were marked on NCM sheets, 3 circular apertures (3 mm in diameter) punched in each rectangle and the sheets were autoclaved. Each of the two NCM sheets with HAM was cut into 2 × 24 rectangles (samples) (Fig. 1c), representing 48 subareas of placental amnion. Samples of HAM were either evaluated for the percentage of dead epithelial cells (%DEC) immediately after processing of the tissue (fresh HAM) or forwarded to decontamination procedures (incubated in respective solutions) and evaluated for %DEC afterwards (Fig. 1d).

Sample preparation, decontamination and cryopreservation

The HAM samples were placed into the BASE-128 solution (Alchimia, Ponte San Nicolò, Italy) or LDS with analogous AA composition. Dulbecco's Modified Eagle Medium (DMEM) with no AA (Gibco, Thermo Fisher Scientific, Prague, Czech Republic) was used as a control solution (Co). The BASE-128 is composed of a balanced saline solution, vitamins, minerals, glucose and AA: Amphotericin B sodium deoxycholate 13,500–16,500 IU/l (14.3–17.5 mg/L; potency: 944 IU/mg) (Rautmann et al. 2010), cefotaxime, gentamicin, vancomycin 115.2–140.8 mg/L (same for the three), according to the product specification sheet. The LDS was prepared by mixing the physiological saline (Fresenius Kabi, Bad Homburg, Germany) with the AA analogous to BASE-128. The AA concentrations in LDS were selected as mean values from AA concentration range published for BASE-128 by producer: Amphotericin B sodium deoxycholate 16 mg/L (Bristol-Myers Squibb, Farmar L'Aigle Usine, France), cefotaxime 130 mg/L, gentamicin 140 mg/L (Lek Pharmaceuticals, Ljubljana, Slovenia), vancomycin 130 mg/L (Mylan, S.A.S., France).

The two NCM sheets with HAM were cut into 48 rectangles (samples) (Fig. 1a–c). 12 samples per placenta, labelled as fresh HAM, were kept in DMEM for ≤1 h at RT, until assessment of %DEC. 24 samples per placenta were decontaminated with BASE-128 or LDS (12 samples each) and remaining 12 samples were stored in Co. Decontamination procedure followed three protocols: (1) 6 h at 37 °C in 5% CO₂ atmosphere (condition 1, C1); (2) 24 h at RT (condition 2, C2) and (3) 24 h at 4 °C (condition 3, C3). After incubation in individual conditions, the %DEC was assessed by trypan blue (TB) staining. Edge areas (3 × 10 mm) of all 48 specimens were cut (before/after decontamination) and either cryopreserved (−80 °C) embedded in Cryomount embedding medium (Histolab AB, Västra Frölunda, Sweden), or kept in Co (≤1 h at RT) for detection of apoptotic cells (EC, MSC). Cryomount medium contains water-soluble glycols and resins that help protect cell integrity during freezing.

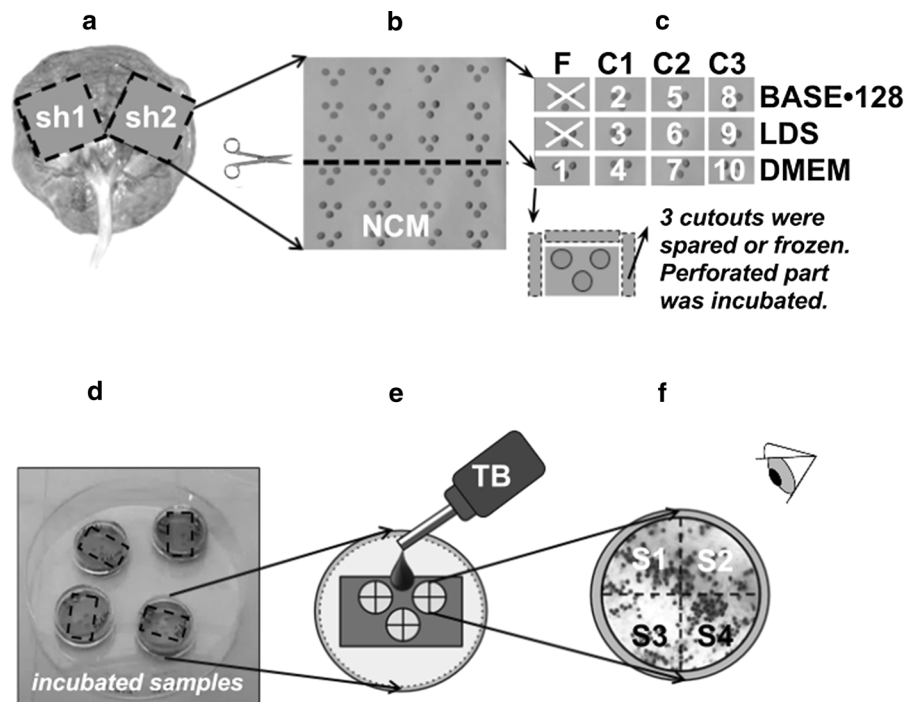


Fig. 1 Tissue sampling procedure—scheme. Two sheets (sh) of human amniotic membrane (HAM) were dissected from placenta (a), flattened onto nitrocellulose membrane (NCM), then divided into two halves (b), each of the 4 resulting parts cut into 12 rectangular pieces (c) and incubated under three conditions: 6 h, 37 °C, 5% CO₂ (C1), 24 h, room temperature (RT) (C2), 24 h, 4 °C (C3) and two decontamination solutions: commercial BASE•128 and laboratory decontamination solution (LDS). Alongside the decontaminated samples of HAM, control pieces of HAM were stored in a Dulbecco's modified Eagle's

medium (DMEM) under same conditions (C1–C3). Four pieces of fresh HAM (F) were stored in DMEM at RT for the assessment of dead epithelial cells before decontamination. We obtained 10 groups of samples; some pieces were used as spare ones (X). Three cutouts from each sample were cryopreserved or stored in DMEM, at RT, for assessment of apoptotic cells (c, d). Each piece of HAM on NCM with 3 circular perforations was stained using trypan blue (TB) (e). Each perforation was visually divided into four sectors (S1–S4) and photographs of each sector were taken at 200x magnification (f)

Assessment of cell survival in HAM

Each HAM sample on NCM, fresh and decontaminated, was rinsed with lukewarm phosphate buffered saline (PBS) and stained with 0.1% TB in PBS (Sigma-Aldrich, Prague, Czech Republic) for 70 s to stain dead cells (Fig. 1e) (Pegg 1989). The %DEC throughout the visible surface of HAM (spanning the NCM perforations) was examined under light microscope (Olympus BX51, Olympus Co., Tokyo, Japan) at 200× magnification. Each aperture was visually divided into four equal sectors (Fig. 1f) and one image of each sector recorded. The %DEC of sample was determined from collected images by computer assisted manual cell counting via Lucia computer analysis system (Laboratory Imaging, Prague, Czech Republic).

Additional staining of HAM epithelium with LIVE/DEAD® Viability/Cytotoxicity Kit for mammalian cells (Molecular Probes, Thermo Fisher, Prague, Czech Republic) was performed following the manufacturer's instructions and %DEC was determined from collected images (5–10 images per sample) by NIS Elements software (Laboratory Imaging for Nikon Co., Prague, Czech Republic). At least 1000 of EC in one micrograph were examined.

Assessment of apoptotic cells in HAM

The cryopreserved pieces of HAM samples (fresh and decontaminated, all conditions) were thawed at RT, washed in PBS, cut into 3 × 5 mm pieces and adhered to a microscope glass slide by drying at RT for a few minutes—one piece epithelial side up and the other

epithelial side down. Cells were then stained for fragmented DNA, i.e. free 3'-OH ends, via terminal deoxynucleotidyl transferase (TdT) dUTP nick-end labelling (TUNEL) method (Gavrieli et al. 1992), with in situ Cell Death Detection kit, Fluorescein (Roche Diagnostics, Mannheim, Germany) according to the manufacturer's instructions. The positive control, pre-treated with deoxyribonuclease I (Sigma-Aldrich, Prague, Czech Republic), and negative control (TdT omitted) were included and labelled on an extra glass slide. Samples of fresh HAM (before cryopreservation) were also TUNEL labelled. Following TUNEL, specimens were covered with Vectashield—DAPI mounting medium (Vector Laboratories, Inc. Burlingame, USA) to counterstain cell nuclei. Images of labelled EC and MSC were recorded with Vosskühler VDS CCD-1300 camera (VDS Vosskühler GmbH, Osnabrueck, Germany) using fluorescent microscope Olympus BX51 at 200× magnification. The EC/MSc exhibiting apoptotic changes were counted in collected images (5–10 sectors per image) by NIS Elements software. At least 1000 of EC and 100 MSC in one micrograph (cell nuclei in the same focus plane) were examined.

Statistical analysis

All data were processed in MS Excel and expressed as the mean \pm SD from values counted from the individual micrographs. The Student's *t* test (unpaired, two-tailed) was performed to compare the results of the individual decontamination conditions with the control and only the data with *p*-value <0.05 were considered statistically significant.

Results

The EC viability in fresh HAM

Epithelial cells with TB positive staining of cell nucleus were considered non-viable and included in total %DEC assessment, Fig. 2. Table 1 summarises the %DEC for six individual placentas before decontamination (fresh HAM). The important dispersion of average values and high standard deviations values reflects the significant variability of %DEC both in individual placentas and among them. The mean %DEC (\pm SD) in fresh HAM from all placentas (All, Table 1) was 12.9 ± 18.1 .

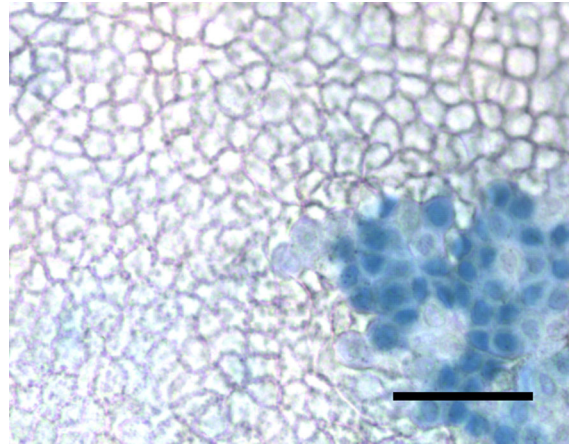


Fig. 2 The epithelial surface of the HAM sheet after preparation and after trypan blue (TB) staining, showing the island of dead epithelial cells (blue) surrounded by mosaic of polygonal viable epithelial cells. Pieces of HAM on nitrocellulose scaffold were stained with 0.1% TB in phosphate buffered saline for 70 s and observed under the light microscope at 200x magnification. The scale bar represents 50 μ m

The EC viability in decontaminated HAM

The mean %DEC (\pm SD) values in decontaminated HAMs (incubated in BASE-128 or LDS) and control HAMs (Co; incubated in DMEM) from all six placentas (P1–P6) were determined, Table 2. The visually confirmed increase in %DEC was observed when longer decontamination periods (C2, C3) were used. Compared to Co, decontamination by both BASE-12 and LDS at all conditions increased the average %DEC, however, only in LDS at C3 this increase was statistically significant ($p = 0.01$).

Due to the fact that relatively high variability in %DEC was present already in samples of fresh HAM, Table 1, we compared the mean %DEC of decontaminated HAM to the mean %DEC of the fresh HAM and expressed it as n-fold increase/decrease in %DEC for individual placentas and conditions (C1–C3; BASE-128, LDS, DMEM), Table 3. We also determined the statistical significance of these changes, relative to fresh HAM. As shown in Table 3, comparing the values of n-fold increase in %DEC (\uparrow %DEC) among LDS, BASE-128 and DMEM in each condition (C1–C3) individually, the increase was highest for LDS in 15 out of 18 cases, with the highest values in C3. The difference in n-fold increase in %DEC between BASE-128 and DMEM of each respective group was minimal. The slight decrease in %DEC

Table 1 The mean percentage of the dead epithelial cells (%DEC \pm SD) in fresh HAM (before decontamination) from six placentas (P1–P6)

Placenta	P1	P2	P3	P4	P5	P6	All
%DEC \pm SD	28.1 \pm 30.3	4.8 \pm 8.5	7.9 \pm 8.1	10.3 \pm 9.1	8.3 \pm 12.7	19.4 \pm 18.8	12.9 \pm 18.1

Samples were stored in DMEM at room temperature and processed within 1 h after dissection

SD standard deviation

Table 2 The mean percentage of the dead epithelial cells (%DEC \pm SD) in decontaminated HAM, from all six placentas

%DEC \pm SD	C1: 6 h 37 °C	C2: 24 h RT	C3: 24 h 4 °C
BASE·128	18.3 \pm 18.3	20.2 \pm 12.6	30.2 \pm 17.8
LDS	28.6 \pm 23.4	31.6 \pm 19.3	44.1 \pm 19.0
DMEM (Co)	13.2 \pm 13.0	12.2 \pm 12.5	25.2 \pm 20.5

The commercial decontamination solution BASE·128, laboratory-made decontamination solution (LDS) or Dulbecco's modified Eagle medium (DMEM) as a control solution (Co) were used. The HAM specimens were incubated for 6 h at 37 °C (C1), for 24 h at room temperature (RT) (C2), or for 24 h at 4 °C (C3). The statistically significant increase ($p < 0.05$) in %DEC was observed in C3 using LDS

SD standard deviation

(\downarrow %DEC), compared to the fresh HAM, was observed in some cases of cultivation of HAM in DMEM.

Treatment of HAM with BASE·128 at C1 resulted in significant %DEC worsening only for one placenta (P4) out of six, the same situation was observed for storage in DMEM (Table 3). Similarly, at C2, the %DEC change was statistically significant in two placentas (P1, P6) in case of HAM storage in BASE·128 (\uparrow %DEC) and in two placentas (P2: \uparrow %DEC, P6: \downarrow %DEC) in case of storage in DMEM. When using LDS, the %DEC increased almost for all placentas at all conditions with exception of P5 in C1 and P3 in C2. On the contrary, HAMS from most placentas were significantly affected (\uparrow %DEC) by storage at C3.

Assessment of apoptotic EC and MSC

The mean percentage of the apoptotic epithelial cells (%AEC) and the mean percentage of the apoptotic mesenchymal cells (%AMC) in HAM before/after decontamination with solutions (BASE·128, LDS) or incubation in Co are shown in Tables 4 and 5, respectively. In the fresh HAM samples (before/after

cryopreservation) from three placentas the mean %AEC was less than 1% and the mean %AMC was 42.0 \pm 18.5 (values from 16.1 to 59.7%). In all specimens after decontamination and in all conditions (before/after cryopreservation), the mean %AEC remained low, about 1–2% (Table 4) and mean %AMC increased significantly (except C3, BASE·128) up to 87.9% (C1, Co), compared to fresh HAM (Table 5). Changes in the mean %AEC among groups were not statistically significant.

Interestingly, during the microscopic evaluation of dead cells by TB staining, small intracellular and extracellular droplets of unknown origin, distributed throughout the HAM, were observed occasionally. Therefore we decided to stain HAM samples of all groups with histological dye Sudan III and Mayer's hematoxylin (performed at the Institute of Pathology, First Faculty of Medicine, Charles University; not included in "Materials and methods" section). It was determined that these droplets are of lipid origin and their presence is rather random (Fig. 3).

Discussion

Using perforated NCM as a carrier for HAM we have established a sampling scheme which can be used as a feasible model for the assessment of the quality of prepared HAM allowing the quick detection and visualisation of dead epithelial cells. The good adherence of the HAM tissue to the NCM during the whole procedure limited the HAM folding and thus minimized cell death as the consequence of mechanical stress.

We observed variations in the mean %DEC (4.8–28.1%) in the fresh HAM, despite the precautions we took. We suppose that this could be the result of the inherent tissue variability, the manipulation with placenta and stress applied on the cells exposed to

Table 3 The n-fold increase/decrease in %DEC in decontaminated HAM, expressed for six individual placentas (P1–P6)

	C1: 6 h 37 °C			C2: 24 h RT			C3: 24 h 4 °C		
	BASE-128	LDS	DMEM	BASE-128	LDS	DMEM	BASE-128	LDS	DMEM
P1	1.2 (0.637)	2.2 (5.26E-07)***	0.8 (0.344)	1.9 (2.77E-04)***	2.7 (6.78E-13)***	0.7 (0.207)	1.9 (6.93E-04)***	2.6 (2.46E-10)***	0.8 (0.430)
P2	2.2 (0.062)	4.5 (2.475E-04)***	0.9 (0.725)	1.4 (0.178)	3.6 (8.29E-04)***	2.1 (0.044)*	1.6 (0.120)	4.3 (2.15E-05)***	1.8 (0.076)
P3	1.3 (0.162)	2.1 (0.003)***	1.2 (0.213)	0.8 (0.357)	1.3 (0.306)	1.5 (0.053)	1.9 (0.004)***	1.6 (0.042)*	2.4 (3.78E-04)***
P4	2.1 (1.581E-04)***	2.4 (3.792E-04)***	1.6 (0.011)*	1.0 (0.897)	2.9 (5.56E-06)***	1.4 (0.096)	1.1 (0.336)	5.3 (2.76E-20)***	2.4 (1.34E-06)***
P5	1.0 (0.994)	1.8 (0.052)	1.0 (0.937)	1.3 (0.226)	2.9 (4.26E-09)***	0.7 (0.267)	4.8 (7.18E-14)***	7.0 (1.57E-31)***	4.2 (1.67E-15)***
P6	1.4 (0.069)	1.7 (0.003)***	0.9 (0.613)	1.7 (0.002)***	1.8 (0.003)***	0.5 (0.013)*	2.8 (8.50E-14)***	2.4 (1.10E-12)***	2.1 (2.22E-04)***

Mean %DEC value for decontaminated HAM was compared with the mean %DEC value for the fresh HAM of respective placenta. Samples of fresh HAM were stored in DMEM at room temperature (RT) and processed within 1 h after dissection. For decontamination, HAM samples were stored in BASE-128 or laboratory decontamination solution (LDS) and were incubated for 6 h at 37 °C (C1), for 24 h at RT (C2), or for 24 h at 4 °C (C3). Control HAM for each condition was stored in DMEM. Statistical significance (Student's *t*-test, unpaired, two-tailed): * *p* < 0.05; ** *p* < 0.01; *** *p* < 0.005 (*p*-value indicated in brackets)

Table 4 The mean percentage of the apoptotic epithelial cells (%AEC \pm SD) after HAM decontamination, related to fresh HAM

%AEC \pm SD	C1: 6 h 37 °C	C2: 24 h RT	C3: 24 h 4 °C
BASE-128	1.15 \pm 0.68	0.72 \pm 0.52	0.95 \pm 0.17
LDS	1.17 \pm 0.63	0.50 \pm 0.07	1.63 \pm 1.95
DMEM (Co)	1.73 \pm 0.42	0.86 \pm 0.26	1.28 \pm 1.23

HAM was treated with BASE-128 or laboratory-made decontamination solution (LDS) or stored in Dulbecco's modified Eagle medium (DMEM) as a control solution (Co). The HAM specimens were incubated for 6 h at 37 °C (C1), for 24 h at room temperature (RT) (C2), or for 24 h at 4 °C (C3). Samples from three placentas were analysed. Changes in the mean %AEC were not statistically significant (*p*-values are thus not indicated)

SD standard deviation

the environment during the experimental procedure. We could observe the worsened quality of HAM in cases of less careful tissue handling; these HAMs were excluded from our experiments. Rather high values of SD for individual placentas are a consequence of the heterogeneity of %DEC throughout the sampled subareas. Nevertheless, in general our results are in accordance with other studies showing a good viability of EC in fresh HAM after processing (>80%) (Hennerbichler et al. 2006; Laurent et al. 2014).

The viability of EC was higher after decontamination of HAM with BASE-128 compared to LDS. The lowest %DEC was found after the treatment with BASE-128 for 6 h at 37 °C. Storage for 24 h was less beneficial to the quality of the tissue than storage for 6 h, independent of the type of decontamination solution (BASE-128, LDS). The worst survival rate

of the EC was observed after storage of HAM in AA solutions (and DMEM) at low temperature, 4 °C. This observation is in accordance with some other studies (Jackson et al. 2015), where the best preservation of the cell/tissue morphology was observed at temperatures between 12 and 24 °C. Further research on the effect of storage in various conditions on HAM quality is necessary.

The LDS showed higher toxicity on cells, despite having the composition and concentration of AA (diluted in physiological saline) similar to BASE-128. Although there is no information about the exact composition of BASE-128, specifically about the concentrations of AA, its composition was indicated in the publication of Gatto et al. (2013), describing BASE-128 as a mixture of AA and nutrients diluted in RPMI 1640 medium. It was shown that cells exposed to the stress, such as nutrient deprivation, accumulate reactive oxygen species and eventually die after a relatively short time (Altman and Rathmell 2012; Cabodevilla et al. 2013). Thus, LDS higher cytotoxicity, compared to BASE-128, can be explained by the lack of nutrients, rather than by the presence of AA. Focused mainly on AA, we used LDS of simplified composition in the decontamination study. As we demonstrated, such solution has no dramatic impact on HAM epithelial cell viability and is simple to prepare at any time in the laboratory, when commercial solution is not available. Moreover, the basic formula of LDS can be optimised by enrichment with nutrient components to improve cell viability.

In our study we selected the TB staining as the fastest and simplest procedure for the detection of dead cells. Combined with the light microscopy we obtained information also about morphological

Table 5 The mean percentage of the apoptotic mesenchymal cells (%AMC \pm SD) after HAM decontamination, related to fresh HAM

%AMCs \pm SD (<i>p</i> -value)	C1: 6 h 37 °C	C2: 24 h RT	C3: 24 h 4 °C
BASE-128	84.9 \pm 14.0 (1.22E-04) ***	86.2 \pm 10.2 (3.38E-05) ***	63.2 \pm 31.5 (0.131)
LDS	82.2 \pm 19.2 (7.853E-04) ***	77.7 \pm 18.3 (0.002) ***	73.7 \pm 17.6 (0.004) ***
DMEM (Co)	87.9 \pm 12.3 (3.823E-05) ***	85.9 \pm 8.2 (2.359E-05) ***	75.3 \pm 16.5 (0.002) ***

HAM was decontaminated with BASE-128 or laboratory-made decontamination solution (LDS) or stored in Dulbecco's modified Eagle medium (DMEM) as a control solution (Co). The HAM specimens were incubated for 6 h at 37 °C (C1), for 24 h at room temperature (RT) (C2), or for 24 h at 4 °C (C3). Samples from three placentas were analysed. Statistical significance (Student's *t*-test, unpaired, two-tailed): * *p* < 0.05; ** *p* < 0.01; *** *p* < 0.005 (*p*-value indicated in brackets)

SD standard deviation

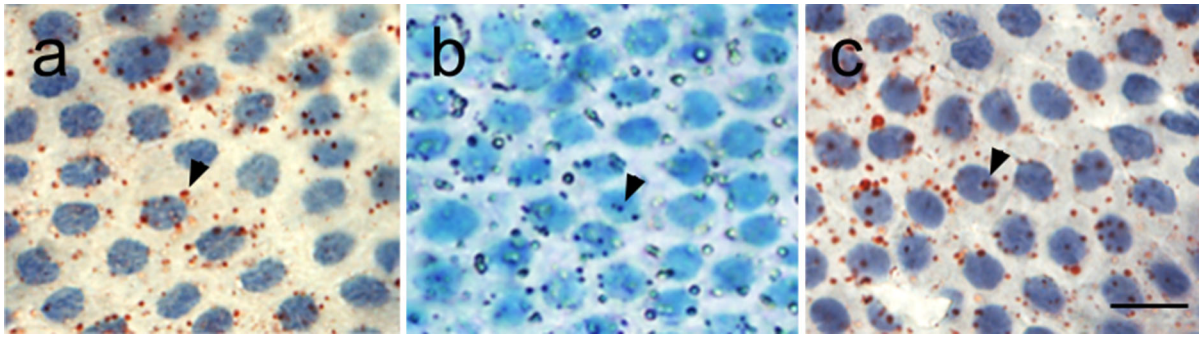


Fig. 3 The light micrograph of the HAM epithelium, with lipid droplets (*arrowheads*) occurring over and inside the cells in fresh HAM (**a**) and in HAM after incubation in BASE-128 solution for 6 h at 37 °C (**b**, **c**). HAM epithelial cells were

stained with trypan blue (**b**) or Sudan III and Mayer's hematoxylin (**a**, **c**). Magnification 400x. Scale bar represents 20 μ m

changes in evaluated tissue. Fluorometric cell viability assay has been shown to have higher efficiency than TB staining (Mascotti et al. 2000), however, this technique is time demanding and does not routinely allow to assess multiple specimens in a short time, as we needed for our experiment. Nevertheless, in order to verify the efficiency and reliability of TB staining, we assessed %DEC also via LIVE/DEAD[®] Viability/Cytotoxicity test of the selected samples. The results were very similar to those obtained by TB staining (data not shown). The final values of %DEC were slightly lower using LIVE/DEAD, however the tendency of increase in %DEC with prolonged incubation time and lower temperature was maintained. On the other hand the fluorescent staining showed to be rather impractical, when high number of samples has to be processed in limited time (not mentioning the cost aspect) and therefore we decided to continue processing the samples by TB staining.

Using TUNEL method we found that MSC (exhibiting about 42% apoptotic cells before and 63–88% after decontamination, respectively) are more susceptible to external stress stimuli than EC. The apoptosis of EC did not exceed 2% at both conditions. Partially, this result could be explained by the fact, that AEC are released from the basement membrane (Kumagai et al. 2001) during the procedure, whilst dead MSC remain confined in the stroma. The other plausible explanation is that the cells die by other, rather fast, mechanism than apoptosis (necrosis) and therefore cannot be identified using TUNEL assay. The potential effect of AA on induction of apoptotic cell death was thus not confirmed.

During the microscopic assessment of %DEC tiny droplets through HAM layers have been observed, independent of solution, time and temperature used. They were also present in fresh HAM. Using standard Sudan III staining, we identified them as lipid particles. Their presence can reflect the cellular damage or they can be naturally present in HAM. Further investigation will be necessary in order to explain this phenomenon.

In conclusion, we have shown that there are only small differences in cell survival between the application of commercial and laboratory decontamination solution (BASE-128 and LDS) and we examined various decontamination protocols. These findings may help to better understand the impact of conditions used for the processing and preservation of HAM on the final quality of the potential tissue graft.

Acknowledgements The research leading to these results has received funding from the Norwegian Financial Mechanism 2009–2014 and the Ministry of Education, Youth and Sports under Project Contract No. MSMT-28477/2014, Project 7F14156. Institutional support was provided by the PRVOUK-P24/LF1/3 and SVV Project No. 260256/2016 programs of Charles University. Authors thank Brigita Vesela, Dana Sadilkova, Zuzana Rejnysova from Institute of Pathology, First Faculty of Medicine, Charles University and General University Hospital in Prague, Czech Republic, for their excellent technical assistance with the Sudan III staining.

Compliance with ethical standards

Conflict of interest Ingrida Smeringaiova, Peter Trosan, Miluse Berka Mrstinova, Jan Matecha, Jan Burkert, Jan Bednar and Katerina Jirsova declares that they have no conflict of interest.

References


- Adds PJ, Hunt CJ, Dart JKG (2001) Amniotic membrane grafts, “fresh” or frozen? A clinical and in vitro comparison. *Br J Ophthalmol* 85(8):905–907
- Akle CA, Adinolfi M, Welsh KI, Leibowitz S, McColl I (1981) Immunogenicity of human amniotic epithelial cells after transplantation into volunteers. *Lancet* 2(8254):1003–1005
- Altman BJ, Rathmell JC (2012) Metabolic stress in autophagy and cell death pathways. *Cold Spring Harb Perspect Biol* 4(9):a008763
- Ashraf NN, Siyal NA, Sultan S, Adhi MI (2015) Comparison of efficacy of storage of amniotic membrane at -20 and -80 °C. *J Coll Physicians Surg Pak* 25(4):264–267
- Aykut V, Celik U, Celik B (2014) The destructive effects of antibiotics on the amniotic membrane ultrastructure. *Int Ophthalmol* 35(3):381–385
- Bourne GL (1960) The microscopic anatomy of the human amnion and chorion. *Am J Obstet Gynecol* 79:1070–1073
- Bourne GL (1962) The foetal membranes. A review of the anatomy of normal amnion and chorion and some aspects of their function. *Postgrad Med J* 38:193–201
- Cabodevilla AG, Sanchez-Caballero L, Nintou E et al (2013) Cell survival during complete nutrient deprivation depends on lipid droplet-fueled α -oxidation of fatty acids. *J Biol Chem* 288(39):27777–27788
- Dua HS, Gomes JAP, King AJ, Maharajan VS (2004) The amniotic membrane in ophthalmology. *Surv Ophthalmol* 49(1):51–77
- Dua HS, Maharajan VS, Hopkinson A (2006) Controversies and limitations of amniotic membrane in ophthalmic surgery. In: Reinhard T, Larkin DFP (eds) *Cornea and external eye disease*. Springer, Berlin, pp 21–33
- Duan-Arnold Y, Gyurdieva A, Johnson A et al (2015) Soluble factors released by endogenous viable cells enhance the antioxidant and chemoattractive activities of cryopreserved amniotic membrane. *Adv Wound Care* 4(6):329–338
- Ganatra MA, Durrani KM (1996) Method of obtaining and preparation of fresh human amniotic membrane for clinical use. *J Pak Med Assoc* 46(6):126–128
- Gatto C, Giurgola L, D’Amato-Tothova J (2013) A suitable and efficient procedure for the removal of decontaminating antibiotics from tissue allografts. *Cell Tissue Bank* 14(1):107–115
- Gavrieli Y, Sherman Y, Ben-Sasson SA (1992) Identification of programmed cell death in situ via specific labeling of nuclear DNA fragmentation. *J Cell Biol* 119(3):493–501
- Gholipourmalekabadi M, Sameni M, Radenkovic D et al (2016) Decellularized human amniotic membrane: How viable is it as a delivery system for human adipose tissue-derived stromal cells? *Cell Prolif* 49(1):115–121
- Gruss JS, Jirsch DW (1978) Human amniotic membrane: a versatile wound dressing. *Can Med Assoc J* 118(10):1237–1246
- Hennerbichler S, Reichl B, Pleiner D, Gabriel C, Eibl J, Redl H (2006) The influence of various storage conditions on cell viability in amniotic membrane. *Cell Tissue Bank* 8(1):1–8
- Ishino Y, Sano Y, Nakamura T, Connon CJ et al (2004) Amniotic membrane as a carrier for cultivated human corneal endothelial cell transplantation. *Invest Ophthalmol Vis Sci* 45(3):800–806
- Jackson C, Eidet JR, Reppe S, Aass HCD, Tønseth KA, Roald B, Lyberg T, Utheim TP (2015) Effect of storage temperature on the phenotype of cultured epidermal cells stored in xenobiotic-free medium. *Curr Eye Res* 41(6):757–768
- Khokhar S, Sharma N, Kumar H, Soni A (2001) Infection after use of nonpreserved human amniotic membrane for the reconstruction of the ocular surface. *Cornea* 20(7):773–774
- Kim JC, Tseng SC (1995) Transplantation of preserved human amniotic membrane for surface reconstruction in severely damaged rabbit corneas. *Cornea* 14(5):473–484
- King AE, Paltoo A, Kelly RW, Sallenne JM, Bocking AD, Challis JRG (2007) Expression of natural antimicrobials by human placenta and fetal membranes. *Placenta* 28(2–3):161–169
- Kumagai K, Otsuki Y, Ito Y et al (2001) Apoptosis in the normal human amnion at term, independent of Bcl-2 regulation and onset of labour. *Mol Hum Reprod* 7(7):681–689
- Laurent R, Nallet A, Obert L et al (2014) Storage and qualification of viable intact human amniotic graft and technology transfer to a tissue bank. *Cell Tissue Bank* 15(2):267–275
- Lee SH, Tseng SC (1997) Amniotic membrane transplantation for persistent epithelial defects with ulceration. *Am J Ophthalmol* 123(3):303–312
- Lindenmair A, Hatlapatka T, Kollwig G et al (2012) Mesenchymal stem or stromal cells from amnion and umbilical cord tissue and their potential for clinical applications. *Cells* 1(4):1061–1088
- Malhotra C, Jain AK (2014) Human amniotic membrane transplantation: different modalities of its use in ophthalmology. *World J Transplant* 4(2):111–121
- Mamede AC, Carvalho MJ, Abrantes AM et al (2012) Amniotic membrane: from structure and functions to clinical applications. *Cell Tissue Res* 349(2):447–458
- Maral T, Borman H, Arslan H et al (1999) Effectiveness of human amnion preserved long-term in glycerol as a temporary biological dressing. *Burns* 25(7):625–635
- Mascotti K, McCullough J, Burger SR (2000) HPC viability measurement: trypan blue versus acridine orange and propidium iodide. *Transfusion* 40(6):693–696
- Mejía LF, Acosta C, Santamaria JP (2000) Use of nonpreserved human amniotic membrane for the reconstruction of the ocular surface. *Cornea* 19(3):288–291
- Mrázová H, Koller J, Kubišová K et al (2015) Comparison of structural changes in skin and amnion tissue grafts for transplantation induced by gamma and electron beam irradiation for sterilization. *Cell Tissue Bank* 17(2):255–260
- Paolin A, Cogliati E, Trojan D et al (2016) Amniotic membranes in ophthalmology: long term data on transplantation outcomes. *Cell Tissue Bank* 17(1):51–58
- Pegg DE (1989) Viability assays for preserved cells, tissues, and organs. *Cryobiology* 26(3):212–231
- Perepelkin NMJ, Hayward K, Mokoena T et al (2016) Cryopreserved amniotic membrane as transplant allograft: viability and post-transplant outcome. *Cell Tissue Bank* 17(1):39–50
- Rautmann G, Daas A, Buchheit KH (2010) Collaborative study for the establishment of the second international standard for amphotericin B. *Pharmeur Bio Sci Notes* 2010(1):1–13

- Riau AK, Beurman RW, Lim LS, Mehta JS (2010) Preservation, sterilization and de-epithelialization of human amniotic membrane for use in ocular surface reconstruction. *Biomaterials* 31(2):216–225
- Singh R, Purohit S, Chacharkar MP et al (2007) Microbiological safety and clinical efficacy of radiation sterilized amniotic membranes for treatment of second-degree burns. *Burns* 33(4):505–510
- Tan EK, Cooke M, Mandrycky C et al (2014) Structural and biological comparison of cryopreserved and fresh amniotic membrane tissues. *J Biomater Tissue Eng* 4(5):379–388
- Thomasen H, Pauklin M, Steuhl KP, Meller D (2009) Comparison of cryopreserved and air-dried human amniotic membrane for ophthalmologic applications. *Graefe's Arch Clin Exp Ophthalmol* 247(12):1691–1700
- von Versen-Hoeynck F, Syring C, Bachmann S, Moller DE (2004) The influence of different preservation and sterilization steps on the histological properties of amnion allografts-light and scanning electron microscopic studies. *Cell Tissue Bank* 5(1):45–56
- von Versen-Hoeynck F, Steinfeld AP, Becker J et al (2008) Sterilization and preservation influence the biophysical properties of human amnion grafts. *Biologicals* 36(4):248–255
- Zidan SM, Eleowa SA, Nasef MA et al (2015) Maximizing the safety of glycerol preserved human amniotic membrane as a biological dressing. *Burns* 41(7):1498–1503

Appendix 5

Smeringaiova I, Nyc O, **Trosan P**, Spatenka J, Burkert J, Bednar J, Jirsova K: Antimicrobial efficiency and stability of two decontamination solutions. Cell Tissue Bank. 2018 Jul 30. Doi: 10.1007/s10561-018-9707-0. PMID: 30062597.

Antimicrobial efficiency and stability of two decontamination solutions

Ingrida Smeringaiova  · Otakar Nyc · Peter Trosan · Jaroslav Spatenka · Jan Burkert · Jan Bednar · Katerina Jirsova

Received: 23 May 2018 / Accepted: 22 June 2018
© Springer Nature B.V. 2018

Abstract Two decontamination solutions, commercially produced BASE•128 and laboratory decontamination solution (LDS), with analogous content of antibiotic and antimycotic agents, were compared in their antimicrobial efficiency and stability (pH and osmolarity). Both solutions were compared immediately after thawing aliquots frozen for 1, 3 or 6 months. Agar well diffusion method was used to test their antimicrobial efficiency against five human pathogens: *Staphylococcus aureus*, *Pseudomonas aeruginosa*, *Proteus mirabilis*, *Escherichia coli* and *Enterococcus faecalis*. The difference in the inhibition

of growth between the two decontamination solutions was mostly not statistically significant, with few exceptions. The most pronounced difference between the LDS and BASE•128 was observed in their decontamination efficacy against *E. coli* and *E. faecalis*, where the LDS showed to be more efficient than BASE•128. The osmolarity value of LDS decreased with cold-storage, the osmolarity values of the BASE•128 could not be measured as they were below the range of the osmometer. Slight changes were found in pH of the less stable LDS solution, whose pH increased from initial value 7.36 ± 0.07 to 7.72 ± 0.19 after 6 m-storage. We verified that BASE•128 and LDS are similarly efficient in elimination of possible placental bacterial contaminants and may be used for decontamination of various tissues.

I. Smeringaiova · P. Trosan · J. Bednar · K. Jirsova (✉)
Laboratory of the Biology and Pathology of the Eye,
Department of Paediatrics and Adolescent Medicine, First
Faculty of Medicine, Charles University and General
University Hospital, Prague, Czech Republic
e-mail: katerina.jirsova@lf1.cuni.cz

I. Smeringaiova · P. Trosan · J. Bednar · K. Jirsova
Laboratory of the Biology and Pathology of the Eye,
Institute of Biology and Medical Genetics, First Faculty of
Medicine, Charles University and General University
Hospital, Prague, Czech Republic

O. Nyc
Department of Clinical Microbiology, Second Faculty of
Medicine, Charles University, Prague, Czech Republic

I. Smeringaiova · P. Trosan · J. Spatenka ·
J. Burkert · K. Jirsova
Department of Transplantation and Tissue Bank, Motol
University Hospital, Prague, Czech Republic

Keywords Tissue decontamination · Amniotic membrane decontamination · Antimicrobial efficiency · Decontamination solution

Introduction

The therapeutic potential of human amniotic membrane (HAM) is increasingly appreciated in a variety of clinical indications, particularly in ophthalmology and chronic wounds treatment due to its positive effect on wound healing—accelerated regeneration with minimal inflammation and scarring (Ilic et al.

2016; Herndon and Branski 2017; Jirsova and Jones 2017). Despite HAM wide-spread use, the general standardized protocol for handling HAM before transplantation surgery has not been adopted yet (Hopkinson et al. 2006; Rahman et al. 2009).

Prior grafting, the sterility of the tissue must be assured. It was demonstrated that the type of the tissue processing and preservation has an impact on final concentrations of endogenous soluble proteins and overall survival of HAM cells (Solomon et al. 2002; Hopkinson et al. 2006; Hennerbichler et al. 2007; Wolbank et al. 2009). It was found that the process of decontamination may be affected by several variables such as temperature, contact period, pH and concentration of the disinfectant, bioburden, organic soil and hardness of water used for dilution (Singh et al. 2012).

When processing HAM several important steps have to be implemented, such as the evaluation of the donor's medical and social history, serological screening of the maternal blood or microbiological screening of HAM before and after its aseptic preparation and processing (Lee and Tseng 1997). Placentas retrieved by vaginal delivery are not considered suitable source of HAM for grafting due to the higher bioburden of pathogens from the vagina compared to placenta obtained during the elective caesarean section delivery (Dua and Azuara-Blanco 1999; Adds et al. 2001). The Gram-positive *Staphylococcus* species are the most prevalent pathogens found on HAM obtained from placentas after both vaginal deliveries and caesarean sections (Gannaway et al. 1984; Aghayan et al. 2013; Binte Atique et al. 2013). Gram-positive bacteria have been also determined as the most frequent cause of microbial infections of HAM transplants in ocular surgery (Marangon et al. 2004). Interestingly, no fungi nor yeast have been detected on HAM samples retrieved either way of the delivery (Gannaway et al. 1984; Adds et al. 2001). In any case, HAM with any positive microbiology result after decontaminating step are unsuitable for grafting (Keitel 2017). Despite sterile processing and grafting of HAM, together with the pre-operative microbiological screening, post-operative contamination by Gram-positive isolates in rates of 1.6–8.0% have been reported (Khokhar et al. 2001; Messmer 2001; Marangon et al. 2004).

The decontamination is a crucial step especially when final sterilisation step is not performed during HAM processing. The tissue can be stored by cryopreservation, lyophilisation or air-drying, the last two

procedures being often followed by gamma irradiation as a final tissue sterilisation step (Burgos and Sergeant 1983; Singh et al. 2003, 2006; Rodriguez-Ares et al. 2009; Mrázová et al. 2016). HAM is typically cryopreserved in glycerol (Maral et al. 1999; Riau et al. 2010; Zidan et al. 2015), in a cultivation medium, e.g. Dulbecco's modified Eagle's medium (DMEM) or Minimum Essential Medium with added glycerol (Kim and Tseng 1995; Lee and Tseng 1997; Thomasen et al. 2009) or in a buffer with added dimethyl sulphoxide (DMSO) (Hanada et al. 2001; Paolin et al. 2016; Perepelkin et al. 2016). The HAM can be cryopreserved also in medium without glycerol (Hennerbichler et al. 2007). Before cryopreservation, HAM is decontaminated typically by treatment with sterile aqueous solutions containing antibiotics and antifungal drugs (Kim et al. 2000; Niknejad et al. 2011; Malhotra and Jain 2014; Keitel 2017). Various decontamination protocols have been published (Lee and Tseng 1997; Laurent et al. 2014; Ashraf et al. 2015; Duan-Arnold et al. 2015; Paolin et al. 2016), but none is generally accepted as a "gold standard". Several certified ready-to-use decontamination solutions are now available, e.g. BASE•128 or X-VIVO 10 media, but there is a lack of optimized decontamination protocols (Rama et al. 2001; Gatto et al. 2013; Perepelkin et al. 2016).

As only a limited number of certified tissue decontamination solutions is commercially available, we have recently proposed an alternative decontamination product with cytotoxicity (as assessed by viability of HAM epithelial cells) comparable with commercial solution BASE•128 (Smringaiova et al. 2017). The decontamination solution prepared in our laboratory (LDS—Laboratory Decontamination Solution) contains only components (physiological saline, antibiotics) approved as medical drugs and therefore it can be readily accepted by national authorities. The purpose of this fellow study was to compare the antimicrobial efficiency and stability (assessed as change of pH and osmolarity) of BASE•128 and LDS, after 1-, 3- and 6-month lasting storage of their respective aliquots.

Materials and methods

Decontamination solutions

The main components of the commercial solution BASE•128 (Alchimia, Ponte San Nicolò, Italy) are

Amphotericin B sodium deoxycholate 13,500–16,500 IU/l (14.3–17.5 mg/l; potency: 944 IU/mg) (Rautmann et al. 2010), cefotaxime, gentamicin, vancomycin 115.2–140.8 mg/l (same for the three). Vitamins, glucose, and balanced RPMI 1640 solution are also present in BASE•128 (Gatto et al. 2013). The normal pH of BASE•128 ranges between 7.20 to 7.40 and its osmolality values are 280–320 mOsm/kg (product accompanying information).

The LDS was prepared by mixing a physiological saline (Fresenius Kabi, Bad Homburg, Germany) with the concentrations of the antibiotics and antimycotic selected as the average values of concentration ranges published for BASE•128: Amphotericin B sodium deoxycholate 16 mg/l (Bristol-Myers Squibb, Farmar L'Aigle Usine, France), cefotaxime 130 mg/l, gentamicin 140 mg/l (Lek Pharmaceuticals, Ljubljana, Slovenia), vancomycin 130 mg/l (Mylan, S.A.S., France), as described previously (Smeringaiova et al. 2017).

Three lots of both solutions were used for experiments. Because the BASE•128 is supplied in frozen form, LDS was also frozen after its preparation. Before the experiments, both solutions were thawed (T0) and then frozen in a form of appropriate aliquots. Solutions were then tested after 1 (T1), 3 (T2) and 6 months (T3) of storage at -20°C . Tested solutions were thawed at 4°C overnight, before the day of antimicrobial and stability testing.

Bacterial strains

To verify antibacterial activity of the two tested decontamination solutions the multi-resistant isolates from clinical material (Motol University Hospital) or bacteria deposited by a non-profit organization The Czech Collection of Microorganisms (CCM), with defined antibiogram, were used—Table 1. The determined sensitivity to selected antibiotics was interpreted according to the recommendations of Clinical breakpoints—Bacteria, v 8.0 of The European Committee on Antimicrobial Susceptibility Testing (EUCAST) (EUCAST v 8.0 2018) and the Performance Standards for Antimicrobial Susceptibility Testing, 28th Edition of the Clinical and Laboratory Standards Institute (CLSI) (CLSI 28th edn. 2018).

Antimicrobial activity

Antimicrobial activity test of the solutions was carried out by agar well diffusion method (AWDM). The AWDM is the second well-established method used for antimicrobial susceptibility testing, after the agar disk-diffusion method, used in many clinical microbiology laboratories. Both methods are equally valid for antimicrobial testing (Holder and Boyce 1994; Balouiri et al. 2016).

Three lots of both solutions were used for experiments. The Petri dishes with Mueller–Hinton agar (Oxoid Ltd., Hampshire, England) were inoculated with the bacterial pathogen, grown up to a density of an 0.5-McFarland Standard, then 1-cm wells were cut into the surface of the agar using a cork borer and 100 μl of the decontamination solution, either BASE•128 or LDS, was added into each well. The agar plates were incubated at 36°C for 18 h (in an appropriate atmosphere) to allow the antimicrobial agents to diffuse in the agar medium and inhibit the growth of the microbial strain tested. The experiment was performed twice in triplicates. The diameter (mm) of clear zone around the wells, called the zone of inhibition or inhibitory zone (IZ) was measured by a digital caliper.

Osmolarity and pH

The pH and osmolality values of both solutions were tested at T0–T3 directly after thawing of respective aliquot. The pH was determined by pH meter InoLAB pH 720 (WTW, Weilheim, Germany). The osmolality values were measured using TearLAB[®] Osmometer (TearLAB Corporation, San Diego, CA), following manufacturer's instructions. Both values, pH and osmolality, were measured at room temperature.

Statistical analysis

The statistical analysis of collected data was performed using The Excel[®] (Microsoft). The data were expressed as mean \pm standard deviation (SD). The differences in IZ were evaluated using the Mann–Whitney test (BASE•128 \times LDS at every time point T0–T3) and by Wilcoxon matched-pairs signed-ranks test (aliquot at T0 \times T1 \times T2 \times T3) using the GraphPad Prism software (version 7.04, GraphPad Software, CA, USA). A probability of 5% or less was

Table 1 Bacterial pathogens and their susceptibility to antibiotics (ATB), used in the present study

Bacterial strain (in-text abbreviation)	Source	Gram \pm	ATB susceptibility ^a	ATB resistance ^a
<i>Proteus mirabilis</i> (<i>P. mirabilis</i>)	Clinical isolate	–	Cefotaxime	Gentamicin, fluoroquinolones
<i>Pseudomonas aeruginosa</i> (<i>P. aeruginosa</i>)	ATCC ^b 27853	–	Gentamicin	Piperacilin, ceftazidime, carbapenems, fluoquinolones
<i>Staphylococcus aureus</i> —methicillin resistant (<i>S. aureus</i>) isolate	Clinical isolate	+	Vancomycin	Beta-laktam agents, gentamicin, clindamycin, fluoroquinolones
<i>Escherichia coli</i> (<i>E. coli</i>)	ATCC ^b 25922	–	Cefotaxime (cephalosporins), gentamicin (aminoglycosides)	Only natural resistance
<i>Enterococcus faecalis</i> (<i>E. faecalis</i>)	ATCC ^b 29212	+	Vancomycin (glycopeptides and lipoglycopeptides)	Only natural resistance

^aBased on the data from EUCAST and CLSI

^bSource of bacterial strain: American Type Culture Collection (ATCC)

considered significant. The change of pH and osmolarity was expressed as mean \pm SD, but the statistical analysis was not performed due to lack of data (two measurements in each sample group).

Results

Antimicrobial activity

The antimicrobial activity of tested decontamination solutions, BASE•128 and LDS, was assessed by AWDm and expressed as the IZ value (mean \pm standard deviation), Table 2.

Both solutions were the most effective at elimination of *P. mirabilis*, whereas the activity of both solutions against *P. mirabilis* remained stable throughout the experiment, Table 2. Both solutions had the second highest antimicrobial activity against *P. aeruginosa*. There was not any statistical difference between the antimicrobial efficacy of both solutions at any time, Table 2.

The BASE•128 and LDS had the lowest antimicrobial activity against *S. aureus*. The only statistically significant difference was observed between the IZ (mm) of BASE•128 and LDS at T0, Table 2.

The BASE•128 showed slightly lower antimicrobial efficiency against *E. coli* and *E. faecalis*, compared to LDS. Both solutions were less efficient against *E. faecalis*, compared to their efficacy against *E. coli*. The differences between the two solutions were statistically significant in all cases, Table 2.

We further compared the IZ between the aliquots of BASE•128 and LDS, after various periods of cold-storage (T0–T3). In a case of *P. mirabilis* and *E. coli*, comparing values of IZ assessed for different periods of storage of solutions, i.e. T0 \times T1 \times T2 \times T3, showed no statistically significant differences, Table 3.

The antimicrobial activity of both solutions against *S. aureus* slightly decreased with cold storage, being the lowest for both solutions at T2, Table 2. As shown in Table 3, when BASE•128 at T1/T2/T3 was compared to BASE•128 at T0, the decrease was statistically significant in all three cases. When LDS at T1/T2/T3 was compared to LDS at T0, the decrease was not statistically significant in any case, Table 3.

In case of *P. aeruginosa*, the antimicrobial efficacy of BASE•128 did not change significantly with prolonged storage (T1–T3), compared to solution at T0, Table 3. However, the antimicrobial efficacy of LDS against *P. aeruginosa* slightly decreased with prolonged storage, with lowest mean IZ (mm) value for LDS at T3, Table 2. This decrease was statistically significant, when compared to LDS at T1/T2/T3, Table 3.

Compared to BASE•128 at T0, the efficacy of BASE•128 against *E. faecalis* did not significantly change with prolonged storage. The highest efficacy against *E. faecalis* had the BASE•128 at T1 and this efficacy decreased with cold storage (T2, T3). This decrease was statistically significant only in two cases, Table 3. Antimicrobial efficacy of LDS against *E. faecalis* did not significantly change with prolonged storage, Table 3.

Table 2 The effect of cold storage of BASE•128 and LDS, on their antimicrobial activity against five bacterial strains

Organism	IZ (mm), mean ± SD							
	BASE•128				LDS			
	T0	T1	T2	T3	T0	T1	T2	T3
<i>P. mirabilis</i>	49.8 ± 0.4	49.0 ± 0	49.0 ± 0	49.2 ± 0.8	49.8 ± 0.4	49.3 ± 0.5	50.0 ± 0 (0.001)***	49.0 ± 1.1
<i>P. aeruginosa</i>	39.6 ± 2.9	39.4 ± 3.1	39.7 ± 2.5	39.1 ± 3.8	40.3 ± 2.9	40.0 ± 2.5	39.5 ± 2.0	38.3 ± 3.3
<i>S. aureus</i>	30.5 ± 0.5 (0.015)*	29.0 ± 0	27.3 ± 0.5	28.2 ± 0.1	29.2 ± 0.8	28.7 ± 0.5	27.2 ± 0.4	27.3 ± 0.5
<i>E. coli</i>	35.3 ± 0.5	36.7 ± 0.5	36.0 ± 0	35.3 ± 0.5	37.8 ± 0.4 (0.003)**	37.8 ± 0.4 (0.007)*	37.3 ± 0.8 (0.009)*	36.5 ± 0.5 (0.013)*
<i>E. faecalis</i>	32.3 ± 0.5	32.7 ± 0.5	31.5 ± 0.5	31.0 ± 0.6	37.0 ± 0 (0.002)**	36.0 ± 0.6 (0.004)**	36.7 ± 0.5 (0.004)**	36.5 ± 0.5 (0.004)**

The effect is expressed as a mean ± standard deviation (SD) of a diameter (mm) of the inhibitory zone (IZ), assessed by agar-well diffusion method. Statistically significant difference between the IZ of the two solutions, cold-stored for a period of 0 (T0), 1 (T1), 3 (T2) or 6 months (T3), was counted—the *P* values: **P* ≤ 0.05; ***P* ≤ 0.005; ****P* ≤ 0.001. The *P* values ≤ 0.05 are indicated in brackets, below the numerically higher mean IZ value out of a pair of means, relevant to compared solutions

Table 3 Statistical significance of difference in inhibitory zones (IZ) between 0 (T0), 1 (T1), 3 (T2) or 6 months (T3)-stored solution (BASE•128, LDS). The antimicrobial efficiency was tested against five bacterial strains

Organism	Wilcoxon test – IZ (<i>P</i> value)								
	BASE•128				LDS				
	T0	T1	T2	T3	T0	T1	T2	T3	
<i>P. mirabilis</i>	Difference not significant between any of the compared groups								
<i>P. aeruginosa</i>	ns				T0	–	ns	ns	0.001***
					T1	ns	–		0.001***
					T2	ns	ns	–	0.039*
					T3	0.001***	0.001***	0.039*	–
<i>S. aureus</i>	T0	T1	T2	T3	T0	T1	T2	T3	
	–	0.031*	0.031*	0.031*	T0	–	ns	ns	ns
	0.031*	–	0.031*	ns	T1	ns	–	0.031*	0.031*
	0.031*	0.031*	–	ns	T2	ns	0.031*	–	ns
	0.031*	ns	ns	–	T3	ns	0.031*	ns	–
<i>E. coli</i>	Difference not significant between any of the compared groups								
<i>E. faecalis</i>	T0	T1	T2	T3	T0	T1	T2	T3	
	–	ns	ns	ns	T0	ns			
	ns	–	0.031*	0.031*	T1				
	ns	0.031*	–	ns	T2				
	ns	0.031*	ns	–	T3				

Statistical significance (*P* value): **P* ≤ 0.05; ***P* ≤ 0.005; ****P* ≤ 0.001, *ns* not significant

Physical parameters

The LDS had higher pH values after storage, compared to BASE•128, Table 4. The most pronounced difference could be seen between the pH value of T3-LDS (pH 7.72 ± 0.19) and T3-BASE•128 (pH 7.58 ± 0.07), and between the T3-LDS and T0-LDS (pH 7.36 ± 0.07). The osmolarity values of the BASE•128 were mostly below range of the osmolarity measurement instrument, used in the study. However, the osmolarity values of LDS could be measured and they dropped from 392.00 units (T0) to 277.50 units (T3), Table 4.

Discussion

We evaluated and compared the antimicrobial efficacy and stability in time of two solutions, BASE•128 and LDS, which can be used for the decontamination of HAM prior to its surgical application. This study is a follow-up to our previous research (Smeringaiova et al. 2017), in which we compared the effect of the same solutions on viability of cells present in HAM.

We used both standard and clinical bacterial strains to investigate antibacterial property of the decontamination solutions by simple and quick method, the AWDM, which allows a comparison of inhibitory activity levels of the tested substances.

Both solutions were the most effective at elimination of *P. mirabilis*, the Gram-negative bacterium, which is susceptible to most antibiotics, except tetracyclines (EUCAST v 8.0 2018; CLSI 28th edn. 2018). *Proteus* species are part of normal human intestinal flora, but can also colonize both the skin and oral mucosa of patients and hospital personnel. *P.*

mirabilis causes 90% of *Proteus* infections (Gonzales 2017). According to the data from EUCAST and CLSI, the *P. mirabilis* is sensitive to cefotaxime, with the following susceptibility breakpoints: IZ ≥ 20 mm (EUCAST); IZ ≥ 26 or 23 mm (CLSI), assessed by the disk diffusion method. Our data shows that both solutions had sufficient antimicrobial efficacy against the *P. mirabilis*, with the IZ about 49 mm, and that they both retained antimicrobial efficacy against *P. mirabilis* after prolonged storage.

The decontamination efficacy of the two solutions against the remaining three common bacterial species was as follows: *P. aeruginosa* > *E. coli* > *E. faecalis*. The Gram-negative bacteria *P. aeruginosa* is a multi-drug resistant pathogen, susceptible to gentamicin. *P. aeruginosa* is one of the most frequent bacteria linked with ventilator-associated pneumonia (Friedrich 2017; Ramirez-Estrada et al. 2016). The *P. aeruginosa* was also detected in patients following HAM transplantation (Marangon et al. 2004). The susceptibility breakpoints of gentamicin for *P. aeruginosa* are: IZ ≥ 15 mm (EUCAST, CLSI). Despite small numerical differences, the efficacy of both solutions against *P. aeruginosa* was similar and the IZ reached values greater than the susceptibility breakpoints. The BASE•128 retained its antimicrobial efficacy after prolonged storage, thus being more stable than LDS.

The *E. coli*, present in normal human gastrointestinal tract, is responsible for common (extra-) intestinal bacterial infections, such as urinary tract infection, wound infections, neonatal sepsis, etc. It is a Gram-negative bacterium, most frequently found in the genital tract of women (Guiral et al. 2011), thus the *E. coli* is present on HAM after normal vaginal delivery (Gannaway et al. 1984; Adds et al. 2001). Standardly, these bacteria are sensitive to

Table 4 Stability of the tested solutions (BASE•128, LDS), stored for different time-periods, i.e. 0 (T0), 1 (T1), 3 (T2) or 6 months (T3), expressed as changes in pH and osmolarity

Parameter	Mean \pm SD							
	BASE•128				LDS			
	T0	T1	T2	T3	T0	T1	T2	T3
pH	7.46	7.61 ± 0.03	7.52 ± 0.09	7.58 ± 0.07	7.36 ± 0.07	7.61 ± 0.07	7.60 ± 0.03	7.72 ± 0.19
Osmol (mOsm/l)	BR	288.50 ± 19.90	BR	BR	392.00	285.00 ± 4.24	285.00 ± 8.49	277.50 ± 2.12

BR below range of TearLAB® Osmometer

cephalosporins (cefotaxime) or aminoglycosides (gentamicin) (Madappa 2017). The EUCAST and CLSI susceptibility breakpoints of cefotaxime for *E. coli* are the same as for the *P. mirabilis*, the susceptibility breakpoints of gentamicin for *E. coli* are as follows: the $IZ \geq 17$ mm (EUCAST) and $IZ \geq 15$ mm (CLSI).

Enterococci are part of the normal human intestinal flora. These Gram-positive bacteria can cause life-threatening infections in humans. The *E. faecalis* can be found on HAM after both vaginal and caesarean section delivery (Addis et al. 2001). These bacteria are resistant to many commonly used antimicrobial agents; resistance to vancomycin is becoming more common (Faron et al. 2016). The susceptibility breakpoints of vancomycin for *E. faecalis* are as follows: the $IZ \geq 12$ mm (EUCAST) and $IZ \geq 17$ mm (CLSI). Both tested solutions were efficient against the *E. coli* and *E. faecalis*. However, the LDS was more efficient against the *E. coli* and *E. faecalis* than BASE•128, and this difference was statistically significant. The efficacy of BASE•128 against *E. coli* was better than that against *E. faecalis*.

The *S. aureus* is Gram-positive bacteria causing serious infections with growing incidence, accompanied by a rise in antibiotic-resistant strains, such as methicillin-resistant *S. aureus* and vancomycin-resistant strains (WHO 2018; Baorto 2017; de Kraker et al. 2011). The *S. aureus* is present on HAM after both vaginal and caesarean section delivery (Addis et al. 2001; Marangon et al. 2004; Aghayan et al. 2013). The susceptibility breakpoints of vancomycin are reported only in a form of minimum-inhibitory concentrations by EUCAST and CLSI. In our study, both tested solutions showed the lowest efficacy against *S. aureus*. At T0, the BASE•128 was slightly more efficient in elimination of *S. aureus* than LDS, and the efficacy of BASE•128 decreased after cold storage. Of note, the vancomycin is a glycopeptide with a large molecule (molar mass $1449.3 \text{ g mol}^{-1}$) thus its diffusion rate in the Mueller–Hinton agar is slower than that of cefotaxime (molar mass 455.5 g mol^{-1}) and gentamicin (molar mass 477.6 g mol^{-1}). This may partially explain the lowest diameters of the IZ detected in case of *E. faecalis* and *S. aureus*, both susceptible to vancomycin. On the other hand, the bactericidal in vitro effect of vancomycin is enhanced, when used in combination with cefotaxime and gentamicin (Lam and Bayer 1984).

We observed the changes in pH and osmolarity of the two decontamination solutions, which are standardly cold-stored as batches before use. The reason of such storage is primarily the preservation of the substances, such as antibiotics or vitamins, in their active state. The starting pH of BASE•128 (T0) was 7.46, and slightly increased after cold storage (pH 7.58 after 6 months). The normal pH of fresh BASE•128 is pH 7.20–7.40. The BASE•128 was used as a reference solution to LDS, thus was frozen and thawed more than one time, as recommended by manufacturer. The pH change of LDS was more prominent, with an increase from pH 7.36 (T0) to pH 7.72 after 6 months (T3). Thus, the use of both solutions in fresh state is preferred, especially if the preservation of vital cells in HAM is important. Due to lack of data for BASE•128 it is difficult to compare the differences in osmolarity values between the two tested solutions. From a collected data, specifically the pH values, it seems that the BASE•128 is, with its current formula, a slightly more physiochemically stable solution than LDS, however, the improvement of formula of LDS is possible in the future.

There is a lack of solutions for decontamination of HAM before its use, which is essential to avoid transmission of pathogens from donors to patients. In our previous study (Smeringaiova et al. 2017) we offered the LDS, as an alternative solution to commercial BASE•128, with a sufficient preservation of viable epithelial cells in HAM. In this study we showed that the antimicrobial efficacy of LDS against common clinical pathogens is comparable to the one of BASE•128, and that the stability of LDS is good, but can be improved by proper changing of the current formula. In general, the differences between the two solutions are very weak and both solutions are suitable for successful HAM decontamination.

Acknowledgements This work was supported by European Regional Development Fund, Project BBMRI-CZ III: EF16_013/0001674. Institutional support was provided by Progres-Q26/LF1 and by SVV, Project 260367/2017.

Compliance with ethical standards

Conflict of interest The authors declare that they have no conflicts of interest. The funding organizations had no role in the design or conduct of this research.

References

- Adds PJ, Hunt C, Hartley S (2001) Bacterial contamination of amniotic membrane. *Br J Ophthalmol* 85(2):228–230
- Aghayan HR, Goodarzi P, Baradaran-Rafii A, Larijani B, Moradabadi L, Rahim F, Arjmand B (2013) Bacterial contamination of amniotic membrane in a tissue bank from Iran. *Cell Tissue Bank* 14(3):401–406
- Ashraf NN, Siyal NA, Sultan S, Adhi MI (2015) Comparison of efficacy of storage of amniotic membrane at-20 and-80 degrees centigrade. *J Coll Phys Surg Pak* 25(4):264–267
- Balouiri M, Sadiki M, Ibnsouda SK (2016) Methods for in vitro evaluating antimicrobial activity: a review. *J Pharm Anal* 6(2):71–79
- Baorto EP (2017) *Staphylococcus aureus* infection. Medscape. <https://emedicine.medscape.com/article/971358-overview>. Accessed 11 May 2018
- Binte Atique F, Ahmed KT, Asaduzzaman SM, Hasan KN (2013) Effects of gamma irradiation on bacterial microflora associated with human amniotic membrane. *Biomed Res Int* 2013:586561
- Burgos H, Sergeant RJ (1983) Lyophilized human amniotic membranes used in reconstruction of the ear. *J R Soc Med* 76(5):433
- Clinical and Laboratory Standards Institute (2018) M100—performance standards for antimicrobial susceptibility testing, 28th edn. Clinical and Laboratory Standards Institute, Wayne
- de Kraker ME, Wolkewitz M, Davey PG, Koller W, Berger J, Nagler J et al (2011) Clinical impact of antimicrobial resistance in European hospitals: excess mortality and length of hospital stay related to methicillin-resistant *Staphylococcus aureus* bloodstream infections. *Antimicrob Agents Chemother* 55(4):1598–1605
- Dua HS, Azuara-Blanco A (1999) Amniotic membrane transplantation. *Br J Ophthalmol* 83(6):748–752
- Duan-Arnold Y, Gyurdieva A, Johnson A, Jacobstein DA, Danilkovitch A (2015) Soluble factors released by endogenous viable cells enhance the antioxidant and chemoattractive activities of cryopreserved amniotic membrane. *Adv Wound Care* 4(6):329–338
- Faron ML, Ledeboer NA, Buchan BW (2016) resistance mechanisms, epidemiology, and approaches to screening for vancomycin-resistant enterococcus in the health care setting. *J Clin Microbiol* 54(10):2436–2447
- Friedrich M (2017) *Pseudomonas aeruginosa* infections. Medscape. <https://emedicine.medscape.com/article/226748-overview>. Accessed 10 May 2018
- Gannaway WL, Barry AL, Trelford JD (1984) Preparation of amniotic membranes for surgical use with antibiotic solutions. *Surgery* 95(5):580–585
- Gatto C, Giurgola L, D'Amato Tothova J (2013) A suitable and efficient procedure for the removal of decontaminating antibiotics from tissue allografts. *Cell Tissue Bank* 14(1):107–115
- Gonzales G (2017) *Proteus* infections. Medscape. <https://emedicine.medscape.com/article/226434-overview>. Accessed 10 May 2018
- Guiral E, Bosch J, Vila J, Soto SM (2011) Prevalence of *Escherichia coli* among samples collected from the genital tract in pregnant and nonpregnant women: relationship with virulence. *FEMS Microbiol Lett* 314(2):170–173
- Hanada K, Shimazaki J, Shimmura S, Tsubota K (2001) Multilayered amniotic membrane transplantation for severe ulceration of the cornea and sclera. *Am J Ophthalmol* 131(3):324–331
- Hennerbichler S, Reichl B, Pleiner D, Gabriel CH, Eibl J, Redl H (2007) The influence of various storage conditions on cell viability in amniotic membrane. *Cell Tissue Bank* 8(1):1–8
- Herndon DN, Branski LK (2017) Contemporary methods allowing for safe and convenient use of amniotic membrane as a biologic wound dressing for burns. *Ann Plast Surg* 78(2 Suppl 1):S9–S10
- Holder IA, Boyce ST (1994) Agar well diffusion assay testing of bacterial susceptibility to various antimicrobials in concentrations non-toxic for human cells in culture. *Burns* 20(5):426–429
- Hopkinson A, McIntosh RS, Tighe PJ, James DK, Dua HS (2006) Amniotic membrane for ocular surface reconstruction: donor variations and the effect of handling on TGF-beta content. *Investig Ophthalmol Vis Sci* 47(10):4316–4322
- Ilic D, Vicovac L, Nikolic M, Lazic Ilic E (2016) Human amniotic membrane grafts in therapy of chronic non-healing wounds. *Br Med Bull* 117(1):59–67
- Jirsova K, Jones GLA (2017) Amniotic membrane in ophthalmology: properties, preparation, storage and indications for grafting—a review. *Cell Tissue Bank* 18(2):193–204
- Keitel S (2017) Guide to the quality and safety of tissues and cells for human application, European Committee (Partial Agreement) on organ transplantation, European Directorate for the Quality of Medicines and HealthCare (EDQM), 3rd edn, Council of Europe, pp 197–201
- Khokhar S, Sharma N, Kumar H, Soni A (2001) Infection after use of nonpreserved human amniotic membrane for the reconstruction of the ocular surface. *Cornea* 20(7):773–774
- Kim JC, Tseng SC (1995) Transplantation of preserved human amniotic membrane for surface reconstruction in severely damaged rabbit corneas. *Cornea* 14(5):473–484
- Kim JS, Kim JC, Na BK, Jeong JM, Song CY (2000) Amniotic membrane patching promotes healing and inhibits proteinase activity on wound healing following acute corneal alkali burn. *Exp Eye Res* 70(3):329–337
- Lam K, Bayer AS (1984) In vitro bactericidal synergy of gentamicin combined with penicillin G, vancomycin, or cefotaxime against group G streptococci. *Antimicrob Agents Chemother* 26(2):260–262
- Laurent R, Nallet A, Obert L, Nicod L, Gindraux F (2014) Storage and qualification of viable intact human amniotic graft and technology transfer to a tissue bank. *Cell Tissue Bank* 15(2):267–275
- Lee SH, Tseng SC (1997) Amniotic membrane transplantation for persistent epithelial defects with ulceration. *Am J Ophthalmol* 123(3):303–312
- Madappa T (2017) *Escherichia coli* (*E. coli*) infections medication. medscape. <https://emedicine.medscape.com/article/217485-medication>. Accessed 10 Feb 2018
- Malhotra C, Jain AK (2014) Human amniotic membrane transplantation: different modalities of its use in ophthalmology. *World J Transplant* 4(2):111–121

- Maral T, Borman H, Arslan H, Demirhan B, Akinbingol G, Haberal M (1999) Effectiveness of human amnion preserved long-term in glycerol as a temporary biological dressing. *Burns* 25(7):625–635
- Marangon FB, Alfonso EC, Miller D, Remonda NM, Muallem MS, Tseng SC (2004) Incidence of microbial infection after amniotic membrane transplantation. *Cornea* 23(3):264–269
- Messmer EM (2001) Hypopyon after amniotic membrane transplantation. *Ophthalmology* 108(10):1714–1715
- Mrázová H, Koller J, Kubišová K, Fujeříková G, Klincová E, Babal P (2016) Comparison of structural changes in skin and amnion tissue grafts for transplantation induced by gamma and electron beam irradiation for sterilization. *Cell Tissue Bank* 17(2):255–260
- Niknejad H, Deihim T, Solati-Hashjin M, Peirovi H (2011) The effects of preservation procedures on amniotic membrane's ability to serve as a substrate for cultivation of endothelial cells. *Cryobiology* 63(3):145–151
- Paolin A, Cogliati E, Trojan D, Griffoni C, Grassetto A, Elbadawy HM, Ponzin D (2016) Amniotic membranes in ophthalmology: long term data on transplantation outcomes. *Cell Tissue Bank* 17(1):51–58
- Perepelkin NMJ, Hayward K, Mokoena T, Bentley MJ, Ross-Rodriguez LU, Marquez-Curtis L, McGann LE, Holovati JL, Elliott JA (2016) Cryopreserved amniotic membrane as transplant allograft: viability and post-transplant outcome. *Cell Tissue Bank* 17(1):39–50
- Rahman I, Said DG, Maharajan VS, Dua HS (2009) Amniotic membrane in ophthalmology: indications and limitations. *Eye (Lond)* 23(10):1954–1961
- Rama P, Giannini R, Bruni A, Gatto C, Tiso R, Ponzin D (2001) Further evaluation of amniotic membrane banking for transplantation in ocular surface diseases. *Cell Tissue Bank* 2(3):155–163
- Ramirez Estrada S, Borgatta B, Rello J (2016) *Pseudomonas aeruginosa* ventilator-associated pneumonia management. *Infect Drug Resist* 20(9):7–18
- Rautmann G, Daas A, Buchheit KH (2010) Collaborative study for the establishment of the second international standard for amphotericin B. *Pharmeuropa Bio Sci Notes* 1:1–13
- Riau AK, Beuerman RW, Lim LS, Mehta JS (2010) Preservation, sterilization and de-epithelialization of human amniotic membrane for use in ocular surface reconstruction. *Biomaterials* 31(2):216–225
- Rodriguez-Ares MT, López-Valladares MJ, Touriño R, Vieites B, Gude F, Silva MT, Couceiro J (2009) Effects of lyophilization on human amniotic membrane. *Acta Ophthalmol* 87(4):396–403
- Singh R, Gupta P, Kumar P, Kumar A, Chacharkar MP (2003) Properties of air dried radiation processed amniotic membranes under different storage conditions. *Cell Tissue Bank* 4(2–4):95–100
- Singh R, Gupta P, Purohit S, Kumar P, Vajjapurkar SG, Chacharkar MP (2006) Radiation resistance of the microflora associated with amniotic membranes. *World J Microbiol Biotechnol* 22(1):23–27
- Singh M, Sharma R, Gupta PK, Rana JK, Sharma M, Taneja N (2012) Comparative efficacy evaluation of disinfectants routinely used in hospital practice: India. *Indian J Crit Care Med* 16(3):123
- Smeringaiova I, Trosan P, Mrstinova MB, Matecha J, Burkert J, Bednar J, Jirsova K (2017) Comparison of impact of two decontamination solutions on the viability of the cells in human amnion. *Cell Tissue Bank* 18(3):413–423
- Solomon A, Meller D, Prabhasawat P, John T, Espana EM, Steuhl KP, Tseng SC (2002) Amniotic membrane grafts for nontraumatic corneal perforations, descemetocoeles, and deep ulcers. *Ophthalmology* 109(4):694–703
- The European Committee on Antimicrobial Susceptibility Testing (EUCAST) (2018) Breakpoint tables for interpretation of MICs and zone diameters. Version 8.0. <http://www.eucast.org>. Accessed 5 Feb 2018
- Thomassen H, Pauklin M, Steuhl KP, Meller D (2009) Comparison of cryopreserved and air-dried human amniotic membrane for ophthalmologic applications. *Graefes Arch Clin Exp Ophthalmol* 247(12):1691–1700
- Wolbank S, Hildner F, Redl H, van Griensven M, Gabriel C, Hennerbichler S (2009) Impact of human amniotic membrane preparation on release of angiogenic factors. *J Tissue Eng Regen Med* 3(8):651–654
- World Health Organization (2018) WHO publishes list of bacteria for which new antibiotics are urgently needed. <http://www.who.int/en/news-room/detail/27-02-2017-who-publishes-list-of-bacteria-for-which-new-antibiotics-are-urgently-needed>. Accessed 11 May 2018
- Zidan SM, Eleowa SA, Nasef MA, Abd-Almuktader MA, Elbatawy AM, Borhamy AG, Aboliela MA, Ali AM, Algarni MR (2015) Maximizing the safety of glycerol preserved human amniotic membrane as a biological dressing. *Burns* 41(7):1498–1503

Appendix 6

Trosan P, Smeringaiova I, Brejchova K, Bednar J, Benada O, Kofronova O, Jirsova K: The enzymatic de-epithelialization technique determines denuded amniotic membrane integrity and viability of harvested epithelial cells. PLoS One. 2018 Mar 27;13(3):e0194820. Doi: 10.1371/journal.pone.0194820. PMID: 29584778.

RESEARCH ARTICLE

The enzymatic de-epithelialization technique determines denuded amniotic membrane integrity and viability of harvested epithelial cells

Peter Trosan^{1,2*}, Ingrida Smeringaiova^{1,2}, Kristyna Brejchova¹, Jan Bednar^{1,2}, Oldrich Benada³, Olga Kofronova³, Katerina Jirsova^{1,2}

1 Laboratory of the Biology and Pathology of the Eye, Department of Paediatrics and Adolescent Medicine, First Faculty of Medicine, Charles University and General University Hospital, Prague, Czech Republic, **2** Laboratory of the Biology and Pathology of the Eye, Institute of Biology and Medical Genetics, First Faculty of Medicine, Charles University and General University Hospital, Prague, Czech Republic, **3** Institute of Microbiology of the Czech Academy of Sciences, Prague, Czech Republic

* peter.trosan@lf1.cuni.cz



OPEN ACCESS

Citation: Trosan P, Smeringaiova I, Brejchova K, Bednar J, Benada O, Kofronova O, et al. (2018) The enzymatic de-epithelialization technique determines denuded amniotic membrane integrity and viability of harvested epithelial cells. PLoS ONE 13(3): e0194820. <https://doi.org/10.1371/journal.pone.0194820>

Editor: Alexander V. Ljubimov, Cedars-Sinai Medical Center, UNITED STATES

Received: October 6, 2017

Accepted: March 9, 2018

Published: March 27, 2018

Copyright: © 2018 Trosan et al. This is an open access article distributed under the terms of the [Creative Commons Attribution License](https://creativecommons.org/licenses/by/4.0/), which permits unrestricted use, distribution, and reproduction in any medium, provided the original author and source are credited.

Data Availability Statement: The authors confirm that all data underlying the findings are fully available without restriction. All relevant data are within the paper.

Funding: This work was supported by the Norwegian Financial Mechanism 2009-2014 and the Ministry of Education, Youth and Sports under Project Contract no. MSMT-28477/2014, project 7F14156 (<http://www.msmt.cz/vyzkum-a-vyvoj-2/financial-andreporting-issues-in-the-czech->

Abstract

The human amniotic membrane (HAM) is widely used for its wound healing effect in clinical practice, as a feeder for the cell cultivation, or a source of cells to be used in cell therapy. The aim of this study was to find effective and safe enzymatic HAM de-epithelialization method leading to harvesting of both denuded undamaged HAM and viable human amniotic epithelial cells (hAECs). The efficiency of de-epithelialization using TrypLE Express, trypsin/ethylenediaminetetraacetic (EDTA), and thermolysin was monitored by hematoxylin and eosin staining and by the measurement of DNA concentration. The cell viability was determined by trypan blue staining. Scanning electron microscopy and immunodetection of collagen type IV and laminin $\alpha 5$ chain were used to check the basement membrane integrity. De-epithelialized hAECs were cultured and their stemness properties and proliferation potential was assessed after each passage. The HAM was successfully de-epithelialized using all three types of reagents, but morphological changes in basement membrane and stroma were observed after the thermolysin application. About 60% of cells remained viable using trypsin/EDTA, approximately 6% using TrypLE Express, and all cells were lethally damaged after thermolysin application. The hAECs isolated using trypsin/EDTA were successfully cultured up to the 5th passage with increasing proliferation potential and decreased stem cell markers expression (*NANOG*, *SOX2*) in prolonged cell culture. Trypsin/EDTA technique was the most efficient for obtaining both undamaged denuded HAM and viable hAECs for consequent culture.

norwegian). This study was further supported by the Progres Q25/LF1 (<http://www.cuni.cz/UK-7368.html>), European Regional Development Fund, project EF16_013/0001674 (http://ec.europa.eu/regional_policy/en/funding/erdf/) and by BBMRI_CZ LM2015089 (<http://biobanka.lf1.cuni.cz/cz/>) projects. PT was supported by SVV, project 260367/2017 (<http://www.cuni.cz/UK-3362.html>). The electron microscopy facility of IMIC was supported by the project LO1509 of the Ministry of Education, Youth and Sports of the Czech Republic (<http://www.msmt.cz/?lang=2>).

Competing interests: The authors have declared that no competing interests exist.

Introduction

The human amniotic membrane (HAM) is the inner layer of the fetal membranes. It consists of a single layer of epithelial cells, basement membrane (BM), and an avascular stroma [1]. The two cell types of different embryological origin are located in the HAM: human amniotic epithelial cells (hAECs) derived from the embryonic ectoderm, and mesenchymal stromal cells (hAMSCs) derived from the embryonic mesoderm [1].

The wound healing effect of HAM mediated by numerous growth factors and cytokines and the presence of stem cells continuously increase interest in its potential in the medical treatment and tissue engineering [2–7]. The application of HAM is best established in ophthalmology, where it is used clinically for its wound-healing effect and as a substrate for limbal stem cells (LSCs) cultivation and consequent treatment in limbal stem cells deficiency (LSCD) [8].

Many published reports discussed whether intact or denuded HAM is more suitable for culture of LSCs. It has been shown that intact HAM mostly supports the growth of limbal explants [9–11], while denuded HAM is more suitable as a substrate for enzymatically dispersed LSCs [12–17]. Koizumi et al. found that denuded HAM supported the growth of well-stratified and differentiated LSCs, while on intact HAM a monolayer of less differentiated limbal cells was formed [18]. LSCs cultured on denuded HAM were better attached to the stroma [18].

The expression of stemness genes, e.g. octamer-4 (OCT-4), sex determining region Y-box 2 (SOX2), fibroblast growth factor 4, zinc finger protein 42 (REX-1), nanog homeobox (NANOG), ATP-binding cassette sub-family G member 2 (ABCG2) and bone marrow stromal cell antigen-1 (BST-1), was reported in hAECs [19]. The hAECs have highly multipotent differentiation ability and could be differentiated into all three germ layers [20]. Furthermore, these cells have immunoprivileged characteristics, expressing only very low levels of class IA and II human leukocyte antigens [21]. The ability to differentiate, low immunogenicity and anti-inflammatory effect indicate their potential to be used in the treatment of a various diseases and disorders, such as the treatment of Type I diabetes [22] or cardiovascular regeneration [23]. The hAECs can also be utilized for tissue engineering of skin [24] or as a feeder for expanding of various stem cells types, including human LSCs [22], or human and murine embryonic stem cells [25, 26]. Li et al. found that supernatant from hAECs inhibited the chemotactic activity of neutrophils and macrophages as well as reduced the proliferation of T and B cells after mitogenic stimulation [27].

Denuded HAM and hAECs can therefore be used separately for various purposes. Several approaches and methods exist to denude HAM. The most frequently used method is treatment with the trypsin/ethylenediaminetetraacetic acid (EDTA) [28, 29]. Besides that, sodium dodecyl sulphate (SDS) [30], Tris/EDTA followed by incubation with SDS [31], Tris/EDTA/aprotinin [32], EDTA [18], thermolysin [33], dispase [14] NaOH [34], or ammonium hydroxide [35], were successfully used.

The best established method for the isolation of viable hAECs is the trypsin/EDTA treatment [36–40], and its modified forms like several trypsin/EDTA incubation steps [41] or treatment with dispase [42, 43].

Each of the mentioned techniques has different effects on biological and physical properties of both HAM and hAECs. Many of these treatments take hours and may damage denuded HAM integrity, or viability of hAECs and hAMSCs or decrease the activity of growth factors. EDTA itself does not remove epithelium completely [14, 17], treatment with dispase can damage BM structure [13]. However, these studies were focused on either de-epithelialization or on obtaining of viable hAECs only.

In this study, TrypLE Express, trypsin/EDTA and thermolysin were applied to obtain both viable hAECs and undamaged denuded HAM at the same time. TrypLE Express is a recombinant fungal trypsin-like protease with similar dissociation kinetics to porcine trypsin, which has been successfully used for dissociation of human pluripotent stem cells [44]. Trypsin/EDTA application is generally used to detach seeding cells from the culture flask and for de-epithelialization of HAM [13, 36, 39]. Thermolysin is a zinc neutral, heat-stable metalloproteinase isolated from the *Bacillus stearothermophilus*, and it has been demonstrated that its use generated fully denuded HAM without any mechanical scrapping [33].

The aim of our study was to identify an enzymatic method which would result in two simultaneous advantages: 1) a complete HAM de-epithelialization safe for BM and stroma, and 2) harvesting viable hAECs usable for subsequent culture.

Materials and methods

Tissue

The study followed the standards of the Ethics Committee of Motol University Hospital, Prague and the General Teaching Hospital and 1st Medical Faculty of Charles University in Prague, and adhered to the tenets set out in the Declaration of Helsinki. Twelve term human placentas were obtained after the delivery by elective caesarean section (with donor informed consent) from the Motol University Hospital, Prague (study EK-503/16 approved on 04/14/2016). The donors were tested negative for hepatitis B, C, syphilis, HIV, and with CRP less than 10 mg/l. Each placenta was immediately placed in a sterile container filled with Hank's Balanced Salt Solution without calcium and magnesium (HBSS, Sigma-Aldrich, St. Louis, MO, USA). Special attention was paid to the gentle handling of each placenta during procurement, transport and subsequent manipulation. The preparation of HAM started at most within 2 h after the delivery. HAM was mechanically peeled off of the chorion and washed several times with HBSS to remove blood clots and debris. HAM was flattened onto a sterile nitrocellulose membrane (Bio-Rad, Hercules, CA, USA) with the epithelium surface facing up, cut into 2 x 2 cm (for consequent de-epithelialization) or 9 x 9 cm pieces (for the cell culture after de-epithelialization).

HAM de-epithelialization and hAECs isolation

Three different protocols were used for HAM de-epithelialization: 1) incubation with TrypLE Express (Gibco, Grand Island, NY, USA) at 37°C for 10 min; 2) incubation with 0.1% w/v trypsin (Sigma-Aldrich)/0.25% w/v EDTA (Sigma-Aldrich) at 37°C for 30 min; 3) incubation with 125 µg/ml thermolysin (Sigma-Aldrich) at 37°C for 9 min. The incubations were stopped with the Dulbecco's modified Eagle medium (DMEM; Gibco) containing 10% fetal calf serum (FCS; Gibco), and antibiotics mixture (10 µl/ml of Antibiotic-Antimycotic (100X); Gibco), hereafter referred as the complete DMEM medium. After each de-epithelialization process, HAM pieces were gently scrapped with the cell scraper (Biologix, Shandong, P.R. China) to remove hAECs in sterile petri dish. The medium with cells was collected, centrifuged at 140g for 8 min and resuspended in complete DMEM medium. All experiments were done in duplicates from 8 placentas.

The viability of the hAECs was determined by exclusion of 0.1% w/v trypan blue dye (Gibco) and hAECs were counted with a hemocytometer. De-epithelialized and intact (used as a control) HAMs were frozen in Cryomount (Histolab AB, Askim, Sweden) and stored at -80°C. Tissues were cryosectioned at a thickness of 7 µm, and four slices were mounted per slide.

Hematoxylin and eosin staining (H&E)

HAMs and HAM cryosections of the control and de-epithelialized HAMs were stained using H&E for the morphological assessment. The samples were examined by light microscopy with the use of Olympus BX51 (Olympus Co., Tokyo, Japan) at a magnification of 100 and 200x.

DNA analysis

After each de-epithelialization processes, the tissues of size 1 x 1 cm were placed into Eppendorf tube and cut out with scissors. Intact HAM of the same size was used as a control. Tri Reagent (Molecular Research Center, Cincinnati, OH, USA) was added to the tissues, and total DNA was extracted according to the manufacturer's instructions. The concentration of the DNA was measured with NanoDrop (Thermo Scientific, Waltham, MA, USA).

Immunostaining

Cryosections of the control and de-epithelialized HAMs from five independent experiments were fixed with iced acetone for 10 min. The samples were incubated with mouse anti-collagen type IV $\alpha 2$ chain (MAB1910; 1:300, Chemicon International, Billerica, MA, USA) or mouse anti-laminin $\alpha 5$ chain antibody (M0638; 1:25, DakoCytomation, Glostrup, Denmark) for one h at room temperature, washed three times with phosphate-buffered saline (PBS) and then incubated with a secondary donkey anti-mouse IgG antibody conjugated with fluorescein (FITC) (715-095-151; 1:200, Jackson ImmunoResearch Laboratories, West Grove, PA, USA). The samples were rinsed with PBS and mounted on slides and DNA counterstained using Vectashield—propidium iodide (Vector Laboratories, Inc. Burlingame, USA). Visualization was performed using Olympus BX51 fluorescence microscope (Olympus Co., Tokyo, Japan) at a magnification of 200x. Images were recorded using a Vosskühler VDS CCD-1300 camera, (VDS Vosskühler GmbH, Germany), and NIS Elements software (Laboratory Imaging, Czech Republic) was used for image analysis.

Scanning electron microscopy (SEM)

Samples of intact and denuded HAM scaffolds (from two placentas) mounted in a CellCrown™ inserts (Scaffdex Oy, Tampere, Finland) were fixed in PBS buffered 3% glutaraldehyde, washed in PBS, postfixed with 1% OsO₄, dehydrated in a graded ethanol series (25, 50, 75, 90, 96, and 100%) and critical point dried in a K850 Critical Point Dryer (Quorum Technologies Ltd, Ringmer, UK). The dried samples were sputter-coated with 3 nm of platinum in a Q150T Turbo-Pumped Sputter Coater (Quorum Technologies Ltd, Ringmer, UK). The final samples were examined in a FEI Nova NanoSEM scanning electron microscope (FEI, Brno, Czech Republic) at 5 kV using ETD, CBS and TLD detectors. Stereo-pair images were taken at tilts of -6°, 0° and +6° of compucentric goniometer stage. Final R-GB anaglyphs were constructed in a “Stereo module” of AnalySis3.2 software suite (EMSIS GmbH, Germany).

Cell culture

The hAECs harvested from three placentas after trypsin/EDTA de-epithelialization from 9 x 9 cm HAM pieces were cultured in complete DMEM medium in 25-cm² tissue culture flasks (Techno Plastic Products, Trasadingen, Switzerland). Medium was changed every 3–4 days. When the cell culture confluence reached about 80–90%, the cells were passaged with 1 ml of TrypLE Express for 5 min in 37°C. The hAECs were collected, centrifuged at 140g for 8 min and counted with hemocytometer. After every passage, the cells (10×10^3 cells) were used for the WST-1 assay, approximately 100×10^3 cells were transferred to the Eppendorf tubes with

Tri Reagent (Molecular Research Center, Cincinnati, OH) and one third of the cells were put back to the culture flask and cultured to the next confluence and passage. The cell images were taken before each passage, and similarly the metabolic activity and gene expression of the cells was determined.

Determination of metabolic cell activity

The metabolic activity of living cells was determined by the WST-1 assay as we described before [45]. In brief, the hAECs (10×10^3 cells) were cultured in complete DMEM medium with or without epidermal growth factor (EGF) (Gibco) in 96-well tissue culture plate (VWR, Radnor, PA, USA) for 24 h at 37°C in an atmosphere of 5% CO₂. WST-1 reagent (Roche, Mannheim, Germany) (10 μ l/100 μ l of the medium) was added to each well, and the plates were incubated for another 4 h to form formazan [46]. Formazan-containing medium (100 μ l) was transferred from each well into the new 96-well tissue culture plate and the absorbance was measured using a Tecan Infinite M200 (Tecan, Männedorf, Switzerland) at a wave-length of 450 nm.

Isolation of RNA and reverse transcription PCR (RT-PCR)

The cells were transferred into Eppendorf tubes containing 500 μ l of TRI Reagent and total RNA was extracted according to the manufacturer's protocol as was described previously [47]. RNA quality was analyzed by λ 260/ λ 280 spectrophotometer analysis (Nanodrop). One μ g of RNA was treated with deoxyribonuclease I (Promega, Madison, WI) and used for subsequent reverse transcription. The first-strand cDNA was synthesized using random hexamers (Promega) in a total reaction volume of 25 μ l using M-MLV Reverse Transcriptase (Promega).

The first strand cDNA product (2 μ l) was amplified in a total volume of 20 μ l PCR assay, containing 10 μ l PPP Master Mix (Top Bio, Vestec, Czech republic), 1 μ l of each primer and was filled up to a total volume with PCR water (Top Bio). The primers for β -ACTIN, SOX2, OCT-4, OCT-4A and NANOG were selected from previous works and specificity was examined with Primer-BLAST software (NCBI) [20, 39, 48]. Two pairs of primers for OCT-4 were used, because there are two possible spliced variants (OCT-4A and OCT-4B). Product sizes, annealing temperatures and primer sequences are listed in Table 1. The PCR cycles included denaturation at 94°C for 2 min followed by 35 to 40 cycles as follows: denaturation at 94°C for 30 s, annealing 57°C to 64°C for 30 s, elongation at 72°C for 1 min and 72°C extension for 10 min at the end of the program. RT-PCR products were visualized with Gel Red (Biotium, CA, USA) on a 1% agarose gel. Amplification of the housekeeping gene β -ACTIN transcripts was performed simultaneously in order to confirm RNA integrity. Induced pluripotent stem cells (iPS) were used as positive control and corneal fibroblasts as negative control for expression of stem cell markers. Both cell types were prepared as was described previously [49, 50]. Non template control (NTC) reactions were used without cDNA.

Statistical analysis

The statistical significance of differences between individual groups was calculated using the Student's t-test.

Results

De-epithelialization of HAM and BM integrity

The integrity of HAM, the quality of de-epithelialization, and potential presence of hAECs were verified by H&E staining and SEM analysis. The surface of intact HAM consists of cuboidal epithelial cells, mesenchymal cells were observed scattered in the stroma (Fig 1).

Table 1. Primer sequences used for real-time PCR.

Primer	Sequence (5'-3')	Product size (bp)	Annealing temperature (°C)	Cycles	References
β-ACTIN	F: cgcaccactggcattgtcat R: ttctccttgatgtcacgcac	208	57	35	[20]
SOX2	F: gccgagtggaaacttttgtc R: gttcatgtgcgtaactgt	264	57	40	[20]
NANOG	F: ctgtgatttggggcctgaa R: tgtttgcctttgggactggt	153	57	35	[39]
OCT-4	F: gaggagtcccaggacatgaa R: gtggctctggctgaacacctt	151	57	40	[20]
OCT-4A	F: cttctcgcctccaggt R: aaatagaacccccagggtgagc	496	64	35	[48]

<https://doi.org/10.1371/journal.pone.0194820.t001>

All three enzymatic methods (TrypLE Express, trypsin/EDTA, and thermolysin) were comparable in term of efficiency of HAM de-epithelialization. Only few epithelial cells occasionally rested on denuded HAM with no difference of the used treatment. The hAMSCs from non-treated HAM exhibited spindle-shaped morphology, similarly as hAMSCs after TrypLE Express and trypsin/EDTA treatments. The thermolysin application led to loss of mesenchymal spindle-shaped cell morphology, showing rather round cell shape (Fig 1).

The DNA concentration in denuded HAM was significantly lower after the treatment with all de-epithelialization agents compared to control untreated samples (Fig 2). The small residual amount of DNA in treated specimens represents DNA of hAMSCs.

The mosaic layer of hAECs covered with dense microvilli was determined at the surface of intact HAM by SEM analysis (Fig 3A, 3B and 3C). BM is well preserved after trypsin/EDTA treatment, some residues of extracellular matrix (ECM) from epithelial cell layer are clearly detectable (Fig 3G, 3H and 3I). Partial damage of BM was observed after applying TrypLE Express treatment, but BM stayed still mostly intact (Fig 3D, 3E and 3F). When thermolysin was used for decellularization, the BM was damaged and numerous lesions were observed revealing the collagen network of compact layer under BM (Fig 3J, 3K and 3L), suggesting aggressive proteolysis.

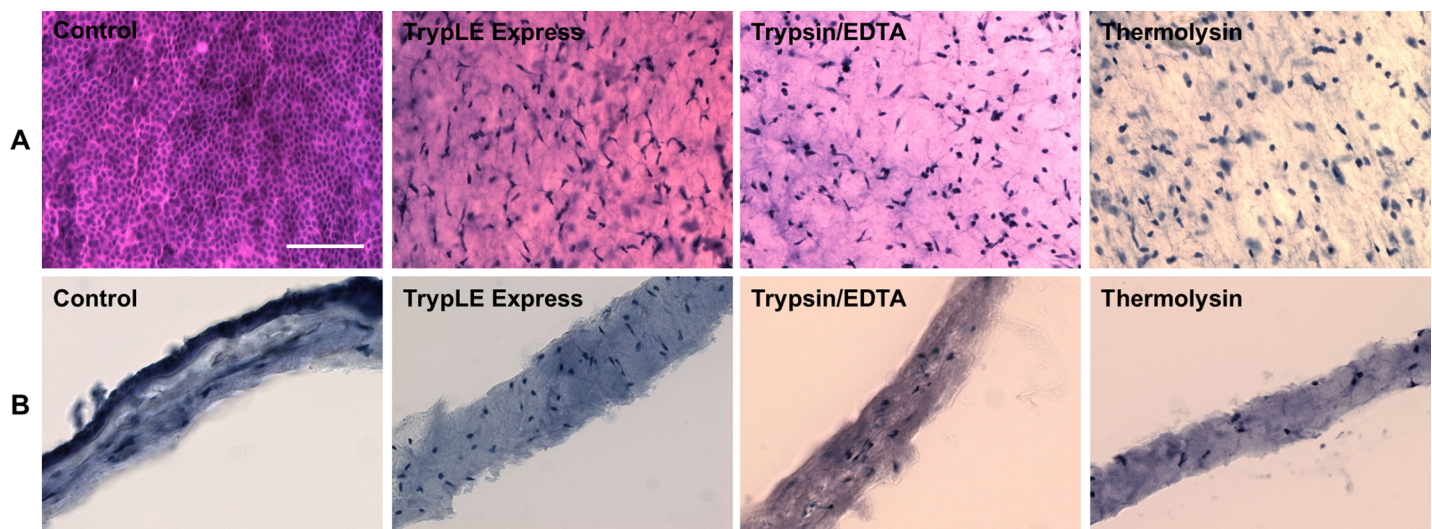


Fig 1. Comparison of the intact and denuded HAMs and HAM cryosections. Comparison of the intact (Control) and denuded HAMs (A) and HAM cryosections (B) after TrypLE Express, trypsin/EDTA and thermolysin treatment stained with H/E for light microscopy. Scale bar represents 100 μm.

<https://doi.org/10.1371/journal.pone.0194820.g001>

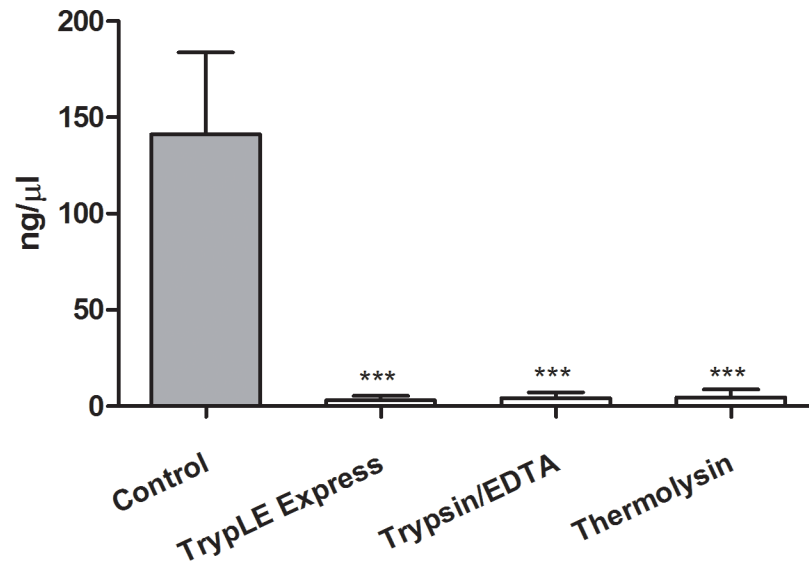


Fig 2. Comparison of the DNA concentrations. Comparison of the DNA concentration in the tissues from the intact (Control) and denuded HAMs with TrypLE Express (TrypLE), trypsin/EDTA and thermolysin treatment directly after de-epithelialization. Each bar represents mean \pm SD from 3 determinations ($***P < 0.001$).

<https://doi.org/10.1371/journal.pone.0194820.g002>

Collagen type IV and laminin $\alpha 5$ chain showed clear positivity in BM of all control specimens and specimens after TrypLE Express and trypsin/EDTA treatment (Fig 4). After thermolysin application, two staining patterns were observed: in HAM specimens from three placentas, the staining for both proteins was properly localized just in BM without any visible integrity deterioration, on the other hand, the positive signal of collagen type IV and laminin $\alpha 5$ was spread throughout the whole amniotic stroma in specimens from other two placentas. In these samples the positive line representing BM was not apparent (Fig 4A and 4B). Intact HAM was used as a negative control without using primary antibody.

Viability, morphology, growth and expression pattern of hAECs

The viability of obtained hAECs immediately after de-epithelialization reached approximately 6% after TrypLE Express, and about 60% after trypsin/EDTA treatment (Fig 5). Only dead cells and cellular fragments were observed after de-epithelialization using thermolysin.

The hAECs harvested after trypsin/EDTA treatment were successfully cultured from all three HAMs. The morphology of hAECs changed from cuboidal shape at the beginning of the culture to more mesenchymal shape cells in the 4th and 5th passage (Fig 6). The higher proliferation activity was observed in later passages. When hAECs were co-cultured with EGF for 24 hours, the metabolic activity was slightly, but not significantly increased (Fig 7).

The expression of three stem cell markers in cultured hAECs was detected. SOX2 was present up to 2nd passage, NANOG up to 4th passage, and OCT-4 was present in all passages (Fig 8). No band was observed when primers for transcription variant specific for stem cells (OCT-4A) were used.

Discussion

The three tested de-epithelialization approaches were efficient to remove epithelial cells from HAM surface. However, only the treatment with trypsin/EDTA was effective for simultaneous harvesting of viable hAECs. We have shown, that gentle mechanical scrapping necessary to

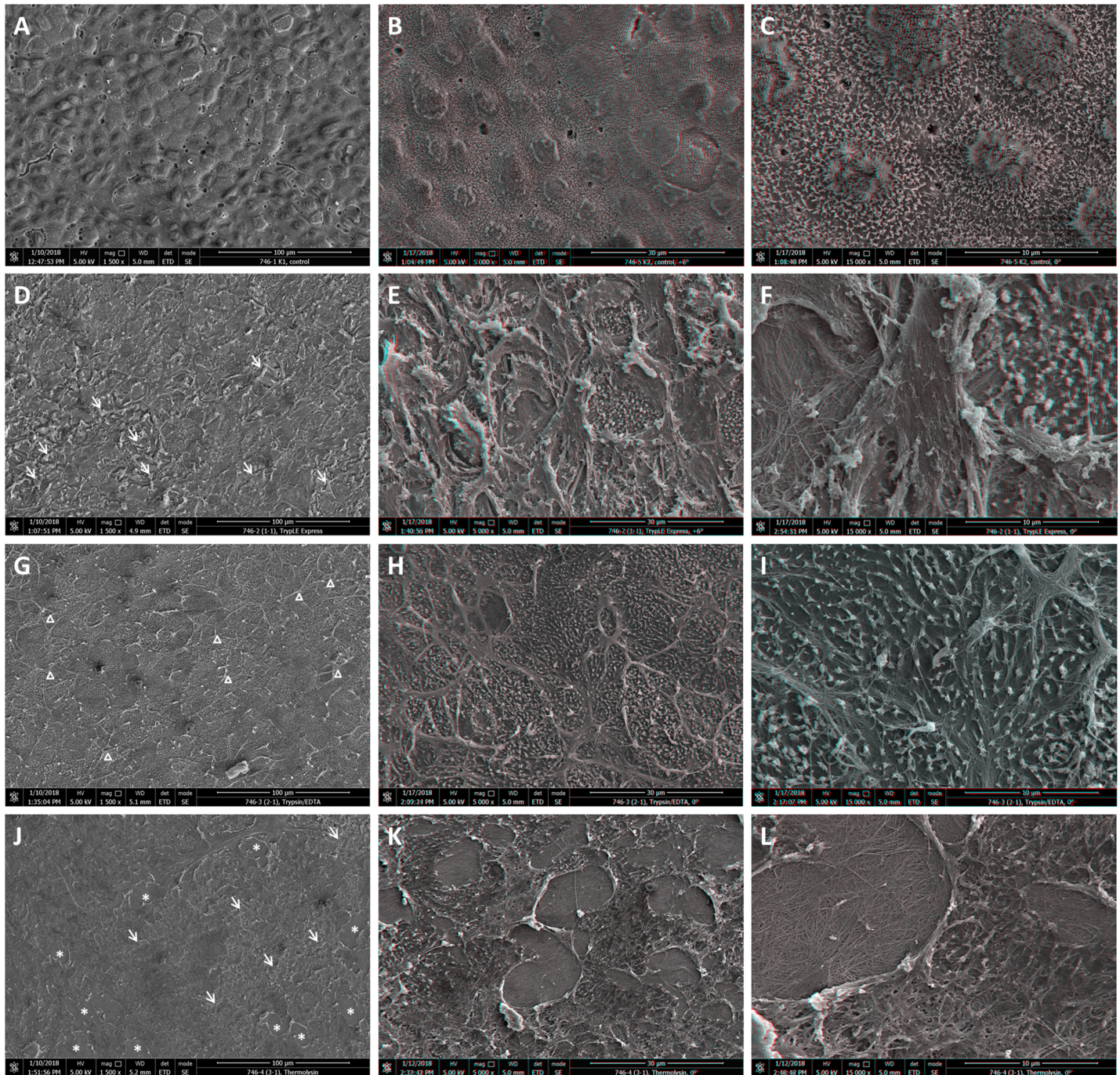


Fig 3. Topography of intact and denuded HAM. Scanning electron micrographs (A, D, G, J) and stereo anaglyphs (B, C, E, F, H, I, K, L) of the intact (A, B, C) and denuded HAM by TrypLE Express (D, E, F), trypsin/EDTA (G, H, I) and thermolysin (J, K, L). Areas of damaged BM are marked by arrows, ruptured gaps by *, the residues of ECM by Δ . Red-green or red-cyan glasses required for proper view of stereo anaglyphs.

<https://doi.org/10.1371/journal.pone.0194820.g003>

remove up to 100% of hAECs after each treatment does not affect the integrity of BM. The staining of HAM and DNA concentration measurement demonstrated the efficiency of all three de-epithelialization processes, with no significant difference between the methods.

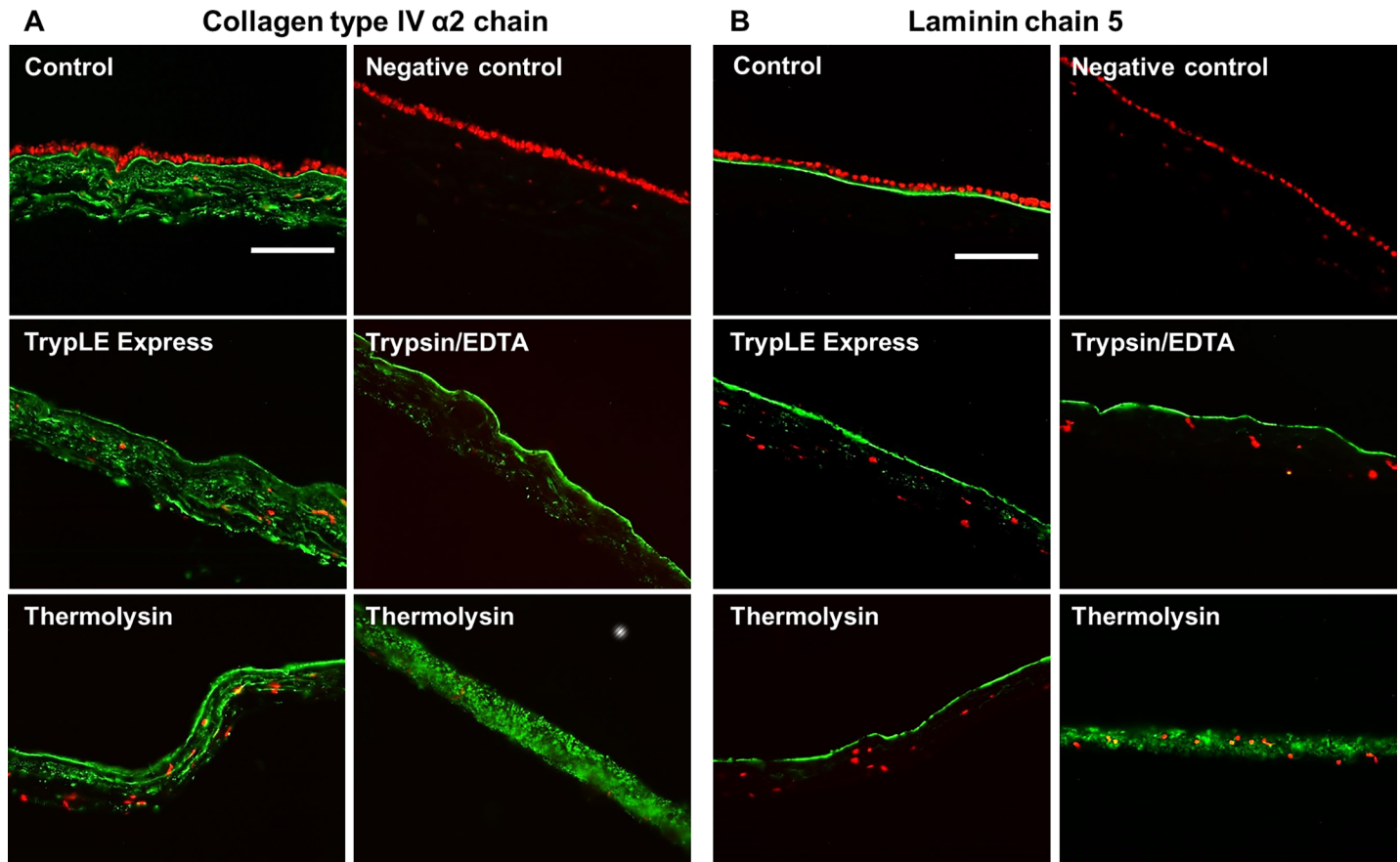


Fig 4. Immunostaining of BM. Distribution of BM collagen type IV $\alpha 2$ chain (green; A) or laminin $\alpha 5$ (green; B) in intact (Control) and denuded HAM: TrypLE Express, trypsin/EDTA, thermolysin treatment. Intact HAM (primary antibody omitted), was used as negative control. Cell nuclei were stained with the propidium iodide (red). Scale bar represents 100 μm .

<https://doi.org/10.1371/journal.pone.0194820.g004>

On the other hand, the detections of collagen type IV and laminin $\alpha 5$ as ubiquitous components of BM [51, 52] revealed some differences between used protocols. The regular staining of BM after TrypLE Express and trypsin/EDTA treatment indicates its integrity and is in agreement with previously published data [13]. We have shown that relatively low trypsin concentration (0.1% w/v) in trypsin/EDTA mixture does not affect BM integrity and cell vitality. BM degradation has been documented after treatment with higher (0.25% w/v) trypsin concentration [13]. The results from SEM analysis thoroughly confirm our original conclusions based on histology and immunohistochemistry data. Smooth surface and the presence of BM after trypsin/EDTA treatment were also already detected [13]. In our experiments only partial damage of BM has been noticed when TrypLE Express was used.

Different situation was observed after de-epithelialization using thermolysin, where almost 50% of specimens showed, beside integral BM staining, signal of collagen type IV and laminin $\alpha 5$ dispersed in HAM stroma. Also loss of hAMSCs spindle shape morphology is consistent with damages induced by thermolysin. SEM analysis showed that BM was damaged and ruptured. The collagen fibres of the underlying compact layer were seen at locations where BM was missing. The similar image of collagen fibres was observed after de-epithelialization by disperse when entire BM was absent [13]. Thermolysin is a heat-stable metalloproteinase which acts specifically at hemidesmosome complex at the level of BM [53], most likely targeting

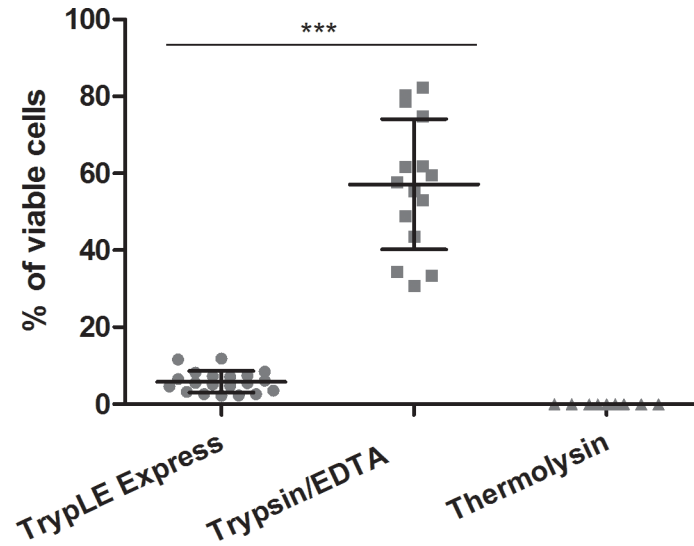


Fig 5. The viability of hAECs. Comparison of the hAECs viability after TrypLE Express, trypsin/EDTA and thermolysin treatment. Cells were stained with trypan blue and counted via hemocytometer. Each bar represents mean \pm SD from 15 determinations (** $P < 0.001$).

<https://doi.org/10.1371/journal.pone.0194820.g005>

collagen IV but not laminin [53, 54]. Hopkinson et al. also noted certain damage of BM when thermolysin in combination with mechanical scrapping was used [33]. The improvement of BM integrity was achieved, when mechanical removal was replaced by simple washing [33].

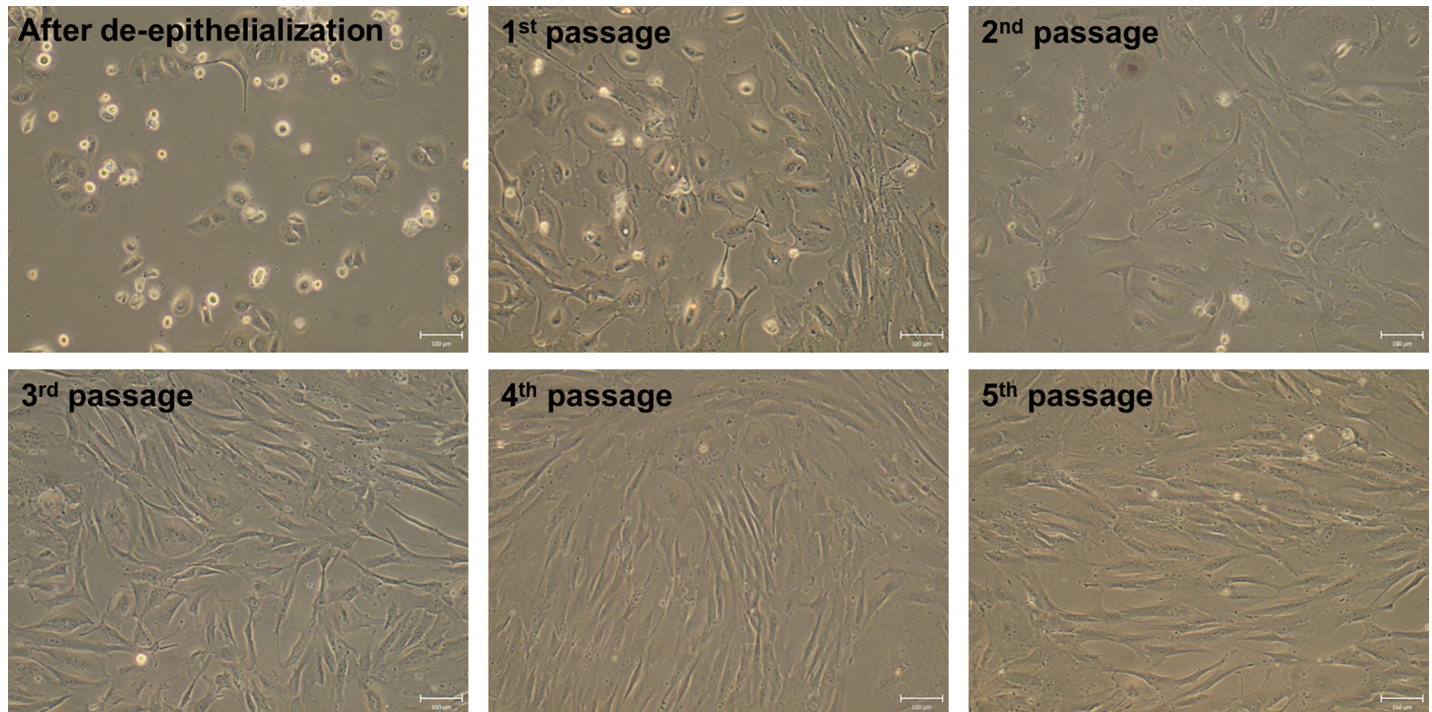


Fig 6. The morphology of hAECs. The comparison of morphology of cultured hAECs after trypsin/EDTA treatment in complete DMEM medium. The cells for the light microscopy were photographed before each passage (after de-epithelialization, before 1st, 2nd, 3rd, 4th and 5th passage). Results of one out of 3 identical experiment is shown. Scale bars represent 100 μ m.

<https://doi.org/10.1371/journal.pone.0194820.g006>

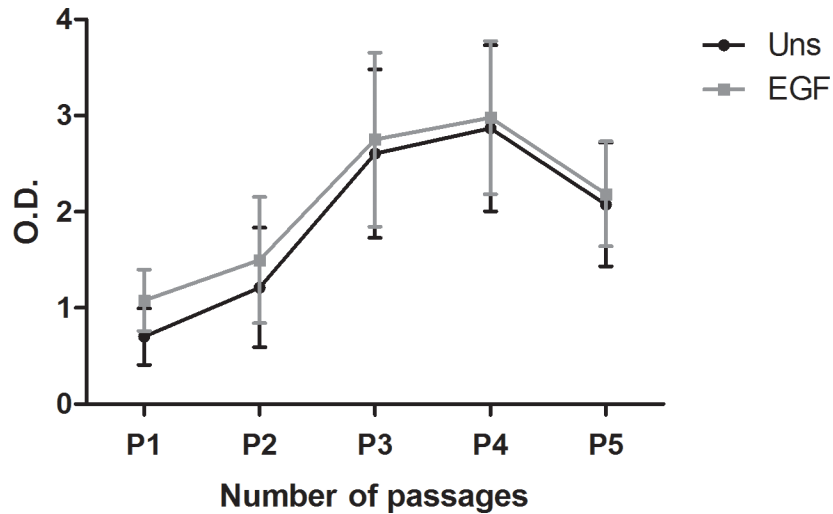


Fig 7. The metabolic activity of hAECs. Comparison of metabolic activity of the epithelial cells unstimulated (Uns) and stimulated with EGF (EGF) after each passage. WST-1 reagent was added to the cell cultures for 4 h to form formazan. The absorbance was measured at a wave-length of 450 nm. Each bar represents mean \pm SD from 3 determinations.

<https://doi.org/10.1371/journal.pone.0194820.g007>

Unfortunately, we were unable to denude the HAM completely with thermolysin only. The fragility and difficult handling of HAM after thermolysin treatment has been also reported in another study [34]. We consider that the damage of the BM is caused by the natural activity of this enzyme due to cleavage of collagen IV. Moreover the lesions are often of round or oval shape (see Fig 3K and 3L), but not cracks, as it would correspond to scraping damage.

De-epithelialization using thermolysin resulted in complete loss of hAECs viability. On the other hand thermolysin was successfully used for the isolation of epidermal or intestinal epithelial cells [53, 55], which are probably less sensitive to enzymatic treatment than the hAECs.

The highest viability of hAECs (about 60%) after trypsin/EDTA indicates that this method is gentle and safe. We have also tried to culture hAECs harvested after TrypLE Express method

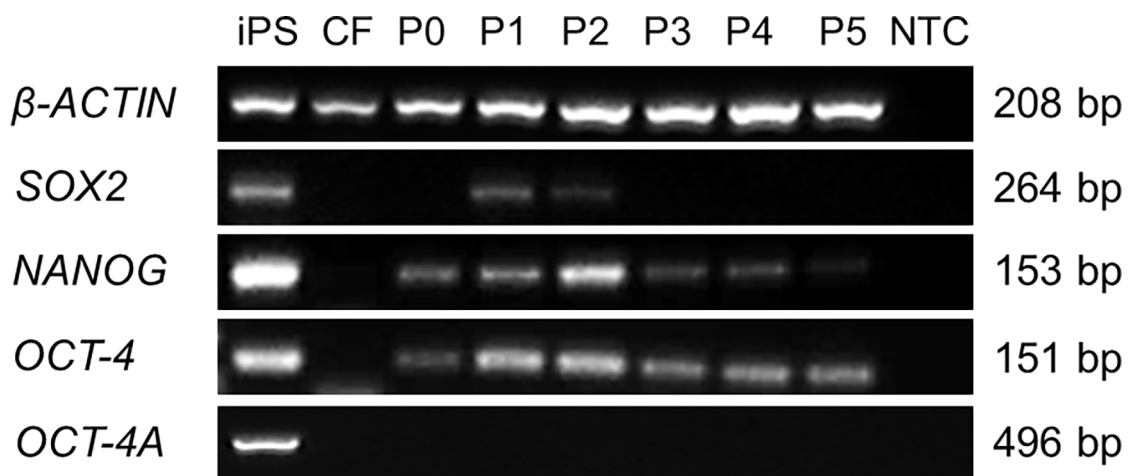


Fig 8. The RT-PCR analysis of hAECs. The RT-PCR analysis of hAECs after de-epithelialization and each passage (P0-P5). The iPS cells were used as a positive (iPS) and corneal fibroblasts as negative control (CF). Sample without cDNA (NTC) was used as non-template control. One representative experiment of 3 (with identical results) is shown.

<https://doi.org/10.1371/journal.pone.0194820.g008>

(6% viability), but these cells (probably due to low initial amount of cells) were growing very slowly and reached full confluence only after extended time periods. The viability of hAECs after TrypLE Express treatment did not change even if we used a prolonged time period (30 min). The hAECs obtained by trypsin/EDTA treatment were successfully cultured up to 5th passage and their proliferation activity increased after each passage up to the 4th one. It was reported that addition of EGF as mitogenesis promoter [56] significantly increases proliferative capacity of hAECs [41]. The addition of EGF for to 24-h culture period did not change proliferation activity significantly. The longer cultivation periods in our study was omitted as it has been found that 7-day cultivation of hAECs with EGF led to significantly increased proliferation, but lower expression of pluripotent genes *OCT-4*, *SOX2* and *NANOG* [57]. Our hAECs, isolated with trypsin/EDTA method, changed their morphology during culture and passaging from more cuboidal morphology at the beginning of culture to more mesenchymal shape from the 3rd passage. Similar observation was also described repeatedly [36]. Morphology and proliferation changes could be caused by epithelial to mesenchymal transition by autocrine production of transforming growth factor- β during the culture of hAECs [58].

It has been shown that hAECs express molecular markers of pluripotent stem cells: *NANOG*, *SOX2* and *OCT-4* [20, 39]. We detected the expression of *NANOG* in cells after de-epithelialization and throughout cultivation; *SOX2* was present in two first passages only. The detection of *OCT-4* was more complex due to its nature. *OCT-4* plays a crucial role in regulating the self-renewal and maintaining pluripotency [59, 60] and encodes two main variants known as *OCT-4A* and *OCT-4B* [61]. While the expression of *OCT-4A* is restricted to embryonic stem cells and embryonal carcinoma cells, *OCT-4B* can be detected in various nonpluripotent cell types [48, 62, 63]. In recent studies some authors still used the primers fitted on both variants for PCR analysis [39, 57, 64]. Using primers suitable for both variants, we detected expression of *OCT-4* in each passage, but *OCT-4A* spliced variant (primers selected based on the work of Atlasi et al. [48]), was not detected in any passage of the cells. On the contrary, Izumi et al. confirmed *OCT-4A* expression in naive (but not cultured) hAECs by using a commercially available primer and probe set that matches *OCT-4A* specific exons by quantitative RT-PCR [65]. In summary, our data on detection of expression of pluripotent stem cell markers suggest that stemness of cultured hAECs decreases with each passage.

Out of three tested de-epithelialization protocols (TrypLE Express, trypsin/EDTA, thermolysin) trypsin/EDTA application showed to be the most efficient when both viable hAECs and intact BM are requested. We would like to stress here, that the term “intact” is used for visibly least damaged BM (judged by the SEM analysis) where no observable lesions were detected contrary to BM obtained by other two methods (see Fig 3). This does not necessarily mean, that some eventual minor structural modification do not occur during trypsin/EDTA treatment (e.g. collagen fiber structure modification), however, these have not an impact on the integrity of BM. The major goal of this study was to establish the conditions under which both undamaged BM and viable hAECs can be obtained and our results demonstrate, that the trypsin/EDTA treatment is the most efficient approach. It leads to successful de-epithelialization of HAM with undamaged BM with well-preserved integrity and at the same time to harvesting of viable epithelial cells which can be cultured up to 5th passage with gradually increasing proliferation capacity. The stemness properties of these cells, however, decrease with higher passages. The cell viability, on the other hand also correlates well with level of BM damage. The method which yields no viable cell (thermolysin) also provides BM with most profound lesions, while intact BM (Trypsin/EDTA, Fig 3G, 3H and 3I) correlates with the best viability of harvested cells (Fig 4). Therefore, we suggest that the trypsin/EDTA method is the method of choice when both intact HAM and viable hAECs are needed for subsequent use.

Acknowledgments

We thank to Department of Obstetrics and Gynecology, Motol University Hospital and Department of Obstetrics and Gynecology, First Faculty of Medicine, Charles University and General University Hospital in Prague for providing of placentas. We thank to Robert Dobrovolny, Ph.D. for providing us with iPS cells.

Author Contributions

Conceptualization: Peter Trosan, Katerina Jirsova.

Data curation: Peter Trosan.

Funding acquisition: Katerina Jirsova.

Investigation: Peter Trosan, Ingrida Smeringaiova, Kristyna Brejchova, Oldrich Benada, Olga Kofronova.

Methodology: Peter Trosan, Katerina Jirsova.

Supervision: Katerina Jirsova.

Validation: Peter Trosan, Jan Bednar, Katerina Jirsova.

Writing – original draft: Peter Trosan.

Writing – review & editing: Jan Bednar, Katerina Jirsova.

References

1. van Herendael BJ, Oberti C, Brosens I. Microanatomy of the human amniotic membranes. A light microscopic, transmission, and scanning electron microscopic study. *American journal of obstetrics and gynecology*. 1978; 131(8):872–80. Epub 1978/08/15. PMID: [686087](#).
2. Koizumi N, Inatomi T, Quantock AJ, Fullwood NJ, Dota A, Kinoshita S. Amniotic membrane as a substrate for cultivating limbal corneal epithelial cells for autologous transplantation in rabbits. *Cornea*. 2000; 19(1):65–71. PMID: [10632011](#).
3. Shimazaki J, Yang HY, Tsubota K. Amniotic membrane transplantation for ocular surface reconstruction in patients with chemical and thermal burns. *Ophthalmology*. 1997; 104(12):2068–76. PMID: [9400767](#).
4. Tseng SC, Prabhasawat P, Lee SH. Amniotic membrane transplantation for conjunctival surface reconstruction. *American journal of ophthalmology*. 1997; 124(6):765–74. PMID: [9402822](#).
5. Mohan R, Bajaj A, Gundappa M. Human Amnion Membrane: Potential Applications in Oral and Periodontal Field. *J Int Soc Prev Commu*. 2017; 7(1):15–21. https://doi.org/10.4103/jispcd.JISPCD_359_16 PubMed PMID: WOS:000395980100003. PMID: [28316944](#)
6. Tenenhaus M. The Use of Dehydrated Human Amnion/Chorion Membranes in the Treatment of Burns and Complex Wounds Current and Future Applications. *Ann Plas Surg*. 2017; 78:S11–S3. <https://doi.org/10.1097/Sap.0000000000000983> PubMed PMID: WOS:000392860000004. PMID: [28079550](#)
7. Jirsova K, Jones GLA. Amniotic membrane in ophthalmology: properties, preparation, storage and indications for grafting—a review. *Cell Tissue Bank*. 2017; 18(2):193–204. <https://doi.org/10.1007/s10561-017-9618-5> PubMed PMID: WOS:000401422700006. PMID: [28255771](#)
8. Tsai RJ, Li LM, Chen JK. Reconstruction of damaged corneas by transplantation of autologous limbal epithelial cells. *N Engl J Med*. 2000; 343(2):86–93. <https://doi.org/10.1056/NEJM200007133430202> PMID: [10891515](#).
9. Kolli S, Lako M, Figueiredo F, Mudhar H, Ahmad S. Loss of corneal epithelial stem cell properties in outgrowths from human limbal explants cultured on intact amniotic membrane. *Regenerative medicine*. 2008; 3(3):329–42. <https://doi.org/10.2217/17460751.3.3.329> PMID: [18462056](#).
10. Li W, Hayashida Y, He H, Kuo CL, Tseng SC. The fate of limbal epithelial progenitor cells during explant culture on intact amniotic membrane. *Investigative ophthalmology & visual science*. 2007; 48(2):605–13. <https://doi.org/10.1167/iov.06-0514> PMID: [17251456](#); PubMed Central PMCID: PMC3197022.

11. Sudha B, Sitalakshmi G, Iyer GK, Krishnakumar S. Putative stem cell markers in limbal epithelial cells cultured on intact & denuded human amniotic membrane. *The Indian journal of medical research*. 2008; 128(2):149–56. PMID: [19001678](#).
12. Riau AK, Beuerman RW, Lim LS, Mehta JS. Preservation, sterilization and de-epithelialization of human amniotic membrane for use in ocular surface reconstruction. *Biomaterials*. 2010; 31(2):216–25. <https://doi.org/10.1016/j.biomaterials.2009.09.034> PMID: [19781769](#).
13. Zhang T, Yam GH, Riau AK, Poh R, Allen JC, Peh GS, et al. The effect of amniotic membrane de-epithelialization method on its biological properties and ability to promote limbal epithelial cell culture. *Investigative ophthalmology & visual science*. 2013; 54(4):3072–81. <https://doi.org/10.1167/iov.12-10805> PMID: [23580491](#).
14. de Melo GB, Gomes JA, da Gloria MA, Martins MC, Haapalainen EF. [Morphological assessment of different amniotic membrane epithelial denuding techniques]. *Arquivos brasileiros de oftalmologia*. 2007; 70(3):407–11. PMID: [17768545](#).
15. Higa K, Shimmura S, Kato N, Kawakita T, Miyashita H, Itabashi Y, et al. Proliferation and differentiation of transplantable rabbit epithelial sheets engineered with or without an amniotic membrane carrier. *Investigative ophthalmology & visual science*. 2007; 48(2):597–604. <https://doi.org/10.1167/iov.06-0664> PMID: [17251455](#).
16. Shortt AJ, Secker GA, Lomas RJ, Wilshaw SP, Kearney JN, Tuft SJ, et al. The effect of amniotic membrane preparation method on its ability to serve as a substrate for the ex-vivo expansion of limbal epithelial cells. *Biomaterials*. 2009; 30(6):1056–65. <https://doi.org/10.1016/j.biomaterials.2008.10.048> PMID: [19019426](#).
17. Shortt AJ, Secker GA, Rajan MS, Meligonis G, Dart JK, Tuft SJ, et al. Ex vivo expansion and transplantation of limbal epithelial stem cells. *Ophthalmology*. 2008; 115(11):1989–97. <https://doi.org/10.1016/j.ophtha.2008.04.039> PMID: [18554721](#).
18. Koizumi N, Rigby H, Fullwood NJ, Kawasaki S, Tanioka H, Koizumi K, et al. Comparison of intact and denuded amniotic membrane as a substrate for cell-suspension culture of human limbal epithelial cells. *Graefes's archive for clinical and experimental ophthalmology = Albrecht von Graefes Archiv fur klinische und experimentelle Ophthalmologie*. 2007; 245(1):123–34. <https://doi.org/10.1007/s00417-005-0095-3> PMID: [16612639](#).
19. Simat SF, Chua KH, Abdul Rahman H, Tan AE, Tan GC. The stemness gene expression of cultured human amniotic epithelial cells in serial passages. *The Medical journal of Malaysia*. 2008; 63 Suppl A:53–4. PMID: [19024980](#).
20. Miki T, Lehmann T, Cai H, Stolz DB, Strom SC. Stem cell characteristics of amniotic epithelial cells. *Stem cells*. 2005; 23(10):1549–59. <https://doi.org/10.1634/stemcells.2004-0357> PMID: [16081662](#).
21. Ilancheran S, Michalska A, Peh G, Wallace EM, Pera M, Manuelpillai U. Stem cells derived from human fetal membranes display multilineage differentiation potential. *Biol Reprod*. 2007; 77(3):577–88. <https://doi.org/10.1095/biolreprod.106.055244> PMID: [17494917](#).
22. Chen YT, Li W, Hayashida Y, He H, Chen SY, Tseng DY, et al. Human amniotic epithelial cells as novel feeder layers for promoting ex vivo expansion of limbal epithelial progenitor cells. *Stem cells*. 2007; 25(8):1995–2005. <https://doi.org/10.1634/stemcells.2006-0677> PubMed PMID: WOS:000248411000015. PMID: [17495107](#)
23. Fang CH, Jin J, Joe JH, Song YS, So BI, Lim SM, et al. In vivo differentiation of human amniotic epithelial cells into cardiomyocyte-like cells and cell transplantation effect on myocardial infarction in rats: comparison with cord blood and adipose tissue-derived mesenchymal stem cells. *Cell transplantation*. 2012; 21(8):1687–96. <https://doi.org/10.3727/096368912X653039> PMID: [22776022](#).
24. Ito A, Takizawa Y, Shinkai M, Honda H, Hata K, Ueda M, et al. Proliferation and stratification of keratinocyte on cultured amniotic epithelial cells for tissue engineering. *J Biosci Bioeng*. 2003; 95(6):589–93. <https://doi.org/10.1263/Jbb.95.589> PubMed PMID: WOS:000184813200007. PMID: [16233462](#)
25. Avila-Gonzalez D, Vega-Hernandez E, Regalado-Hernandez JC, De la Jara-Diaz JF, Garcia-Castro IL, Molina-Hernandez A, et al. Human amniotic epithelial cells as feeder layer to derive and maintain human embryonic stem cells from poor-quality embryos. *Stem Cell Res*. 2015; 15(2):322–4. <https://doi.org/10.1016/j.scr.2015.07.006> PMID: [26246271](#).
26. Lai DM, Cheng WW, Liu TJ, Jiang LZ, Huang Q, Liu T. Use of Human Amnion Epithelial Cells as a Feeder Layer to Support Undifferentiated Growth of Mouse Embryonic Stem Cells. *Cloning Stem Cells*. 2009; 11(2):331–40. <https://doi.org/10.1089/clo.2008.0047> PubMed PMID: WOS:000267016400014. PMID: [19508128](#)
27. Li HC, Niederkorn JY, Neelam S, Mayhew E, Word RA, McCulley JP, et al. Immunosuppressive factors secreted by human amniotic epithelial cells. *Investigative ophthalmology & visual science*. 2005; 46(3):900–7. <https://doi.org/10.1167/iov.04-0495> PubMed PMID: WOS:000227216900018. PMID: [15728546](#)

28. Madhira SL, Vemuganti G, Bhaduri A, Gaddipati S, Sangwan VS, Ghanekar Y. Culture and characterization of oral mucosal epithelial cells on human amniotic membrane for ocular surface reconstruction. *Mol Vis*. 2008; 14(24–25):189–96. PubMed PMID: WOS:000256595500001.
29. Sangwan VS, Vemuganti GK, Singh S, Balasubramanian D. Successful reconstruction of damaged ocular outer surface in humans using limbal and conjunctival stem cell culture methods. *Biosci Rep*. 2003; 23(4):169–74. PMID: [14748537](https://pubmed.ncbi.nlm.nih.gov/14748537/).
30. Wilshaw SP, Kearney JN, Fisher J, Ingham E. Production of an acellular amniotic membrane matrix for use in tissue engineering. *Tissue engineering*. 2006; 12(8):2117–29. <https://doi.org/10.1089/ten.2006.12.2117> PMID: [16968153](https://pubmed.ncbi.nlm.nih.gov/16968153/).
31. Roy R, Haase T, Ma N, Bader A, Becker M, Seifert M, et al. Decellularized amniotic membrane attenuates postinfarct left ventricular remodeling. *The Journal of surgical research*. 2016; 200(2):409–19. <https://doi.org/10.1016/j.jss.2015.08.022> PMID: [26421709](https://pubmed.ncbi.nlm.nih.gov/26421709/).
32. Wilshaw SP, Kearney J, Fisher J, Ingham E. Biocompatibility and potential of acellular human amniotic membrane to support the attachment and proliferation of allogeneic cells. *Tissue engineering Part A*. 2008; 14(4):463–72. <https://doi.org/10.1089/tea.2007.0145> PMID: [18370928](https://pubmed.ncbi.nlm.nih.gov/18370928/).
33. Hopkinson A, Shanmuganathan VA, Gray T, Yeung AM, Lowe J, James DK, et al. Optimization of amniotic membrane (AM) denuding for tissue engineering. *Tissue engineering Part C, Methods*. 2008; 14(4):371–81. <https://doi.org/10.1089/ten.tec.2008.0315> PMID: [18821842](https://pubmed.ncbi.nlm.nih.gov/18821842/).
34. Saghizadeh M, Winkler MA, Kramerov AA, Hemmati DM, Ghiam CA, Dimitrijevic SD, et al. A simple alkaline method for decellularizing human amniotic membrane for cell culture. *PloS one*. 2013; 8(11): e79632. <https://doi.org/10.1371/journal.pone.0079632> PMID: [24236148](https://pubmed.ncbi.nlm.nih.gov/24236148/); PubMed Central PMCID: [PMC3827346](https://pubmed.ncbi.nlm.nih.gov/PMC3827346/).
35. Noguchi Y, Uchida Y, Endo T, Ninomiya H, Nomura A, Sakamoto T, et al. The induction of cell differentiation and polarity of tracheal epithelium cultured on the amniotic membrane. *Biochemical and biophysical research communications*. 1995; 210(2):302–9. PMID: [7755604](https://pubmed.ncbi.nlm.nih.gov/7755604/).
36. Fatimah SS, Ng SL, Chua KH, Hayati AR, Tan AE, Tan GC. Value of human amniotic epithelial cells in tissue engineering for cornea. *Human cell*. 2010; 23(4):141–51. <https://doi.org/10.1111/j.1749-0774.2010.00096.x> PMID: [21166885](https://pubmed.ncbi.nlm.nih.gov/21166885/).
37. Miki T, Marongiu F, Ellis E, S CS. Isolation of amniotic epithelial stem cells. *Current protocols in stem cell biology*. 2007; Chapter 1: Unit 1E 3. <https://doi.org/10.1002/9780470151808.sc01e03s3> PMID: [18785168](https://pubmed.ncbi.nlm.nih.gov/18785168/).
38. Pratama G, Vaghjiani V, Tee JY, Liu YH, Chan J, Tan C, et al. Changes in culture expanded human amniotic epithelial cells: implications for potential therapeutic applications. *PloS one*. 2011; 6(11): e26136. <https://doi.org/10.1371/journal.pone.0026136> PMID: [22073147](https://pubmed.ncbi.nlm.nih.gov/22073147/); PubMed Central PMCID: [PMC3206797](https://pubmed.ncbi.nlm.nih.gov/PMC3206797/).
39. Evron A, Goldman S, Shalev E. Human amniotic epithelial cells cultured in substitute serum medium maintain their stem cell characteristics for up to four passages. *International journal of stem cells*. 2011; 4(2):123–32. PMID: [24298345](https://pubmed.ncbi.nlm.nih.gov/24298345/); PubMed Central PMCID: [PMC3840962](https://pubmed.ncbi.nlm.nih.gov/PMC3840962/).
40. Mahmood R, Choudhery MS, Mehmood A, Khan SN, Riazuddin S. In Vitro Differentiation Potential of Human Placenta Derived Cells into Skin Cells. *Stem Cells Int*. 2015. doi: Artn 841062 <https://doi.org/10.1155/2015/841062> PubMed PMID: WOS:000357813100001. PMID: [26229539](https://pubmed.ncbi.nlm.nih.gov/26229539/)
41. Tabatabaei M, Mosaffa N, Nikoo S, Bozorgmehr M, Ghods R, Kazemnejad S, et al. Isolation and partial characterization of human amniotic epithelial cells: the effect of trypsin. *Avicenna journal of medical biotechnology*. 2014; 6(1):10–20. PMID: [24523953](https://pubmed.ncbi.nlm.nih.gov/24523953/); PubMed Central PMCID: [PMC3895574](https://pubmed.ncbi.nlm.nih.gov/PMC3895574/).
42. Diaz-Prado S, Muinos-Lopez E, Hermida-Gomez T, Rendal-Vazquez ME, Fuentes-Boquete I, de Toro FJ, et al. Multilineage differentiation potential of cells isolated from the human amniotic membrane. *J Cell Biochem*. 2010; 111(4):846–57. <https://doi.org/10.1002/jcb.22769> PMID: [20665539](https://pubmed.ncbi.nlm.nih.gov/20665539/).
43. Rutigliano L, Corradetti B, Valentini L, Bizzaro D, Meucci A, Cremonesi F, et al. Molecular characterization and in vitro differentiation of feline progenitor-like amniotic epithelial cells. *Stem Cell Res Ther*. 2013; 4(5):133. <https://doi.org/10.1186/scrt344> PMID: [24405576](https://pubmed.ncbi.nlm.nih.gov/24405576/); PubMed Central PMCID: [PMCPMC3854755](https://pubmed.ncbi.nlm.nih.gov/PMCPMC3854755/).
44. Nishishita N, Muramatsu M, Kawamata S. An effective freezing/thawing method for human pluripotent stem cells cultured in chemically-defined and feeder-free conditions. *American journal of stem cells*. 2015; 4(1):38–49. PMID: [25973330](https://pubmed.ncbi.nlm.nih.gov/25973330/); PubMed Central PMCID: [PMC4396159](https://pubmed.ncbi.nlm.nih.gov/PMC4396159/).
45. Trosan P, Javorkova E, Zajicova A, Hajkova M, Hermankova B, Kossl J, et al. The Supportive Role of Insulin-Like Growth Factor-I in the Differentiation of Murine Mesenchymal Stem Cells into Corneal-Like Cells. *Stem Cells Dev*. 2016; 25(11):874–81. <https://doi.org/10.1089/scd.2016.0030> PMID: [27050039](https://pubmed.ncbi.nlm.nih.gov/27050039/).
46. Zajicova A, Pokorna K, Lencova A, Krulova M, Svobodova E, Kubinova S, et al. Treatment of ocular surface injuries by limbal and mesenchymal stem cells growing on nanofiber scaffolds. *Cell transplantation*. 2010; 19(10):1281–90. <https://doi.org/10.3727/096368910X509040> PMID: [20573307](https://pubmed.ncbi.nlm.nih.gov/20573307/).

47. Trosan P, Svobodova E, Chudickova M, Krulova M, Zajicova A, Holan V. The key role of insulin-like growth factor I in limbal stem cell differentiation and the corneal wound-healing process. *Stem Cells Dev.* 2012; 21(18):3341–50. <https://doi.org/10.1089/scd.2012.0180> PMID: 22873171; PubMed Central PMCID: PMC3516427.
48. Atlasi Y, Mowla SJ, Ziaee SA, Gokhale PJ, Andrews PW. OCT4 spliced variants are differentially expressed in human pluripotent and nonpluripotent cells. *Stem cells.* 2008; 26(12):3068–74. <https://doi.org/10.1634/stemcells.2008-0530> PMID: 18787205.
49. Dudakova L, Liskova P, Trojek T, Palos M, Kalasova S, Jirsova K. Changes in lysyl oxidase (LOX) distribution and its decreased activity in keratoconus corneas. *Exp Eye Res.* 2012; 104:74–81. <https://doi.org/10.1016/j.exer.2012.09.005> PMID: 23041260.
50. Reboun M, Rybova J, Dobrovolny R, Vcelak J, Veselkova T, Storkanova G, et al. X-Chromosome Inactivation Analysis in Different Cell Types and Induced Pluripotent Stem Cells Elucidates the Disease Mechanism in a Rare Case of Mucopolysaccharidosis Type II in a Female. *Folia Biol-Prague.* 2016; 62(2):82–9. PubMed PMID: WOS:000377711700004.
51. Aplin JD, Campbell S, Allen TD. The extracellular matrix of human amniotic epithelium: ultrastructure, composition and deposition. *Journal of cell science.* 1985; 79:119–36. PMID: 3914477.
52. Modesti A, Scarpa S, D'Orazi G, Simonelli L, Caramia FG. Localization of type IV and V collagens in the stroma of human amnion. *Progress in clinical and biological research.* 1989; 296:459–63. PMID: 2740400.
53. Germain L, Guignard R, Rouabhia M, Auger FA. Early basement membrane formation following the grafting of cultured epidermal sheets detached with thermolysin or Dispase. *Burns: journal of the International Society for Burn Injuries.* 1995; 21(3):175–80. PMID: 7794497.
54. Miyoshi S, Nakazawa H, Kawata K, Tomochika K, Tobe K, Shinoda S. Characterization of the hemorrhagic reaction caused by *Vibrio vulnificus* metalloprotease, a member of the thermolysin family. *Infection and immunity.* 1998; 66(10):4851–5. PMID: 9746589; PubMed Central PMCID: PMC108600.
55. Perreault N, Beaulieu JF. Use of the dissociating enzyme thermolysin to generate viable human normal intestinal epithelial cell cultures. *Exp Cell Res.* 1996; 224(2):354–64. <https://doi.org/10.1006/excr.1996.0145> PubMed PMID: WOS:A1996UJ21000015. PMID: 8612712
56. Carpenter G, Cohen S. Epidermal growth factor. *Annual review of biochemistry.* 1979; 48:193–216. <https://doi.org/10.1146/annurev.bi.48.070179.001205> PMID: 382984.
57. Fatimah SS, Tan GC, Chua KH, Tan AE, Hayati AR. Effects of epidermal growth factor on the proliferation and cell cycle regulation of cultured human amnion epithelial cells. *J Biosci Bioeng.* 2012; 114(2):220–7. <https://doi.org/10.1016/j.jbiosc.2012.03.021> PMID: 22578596.
58. Alcaraz A, Mrowiec A, Insausti CL, Garcia-Vizcaino EM, Ruiz-Canada C, Lopez-Martinez MC, et al. Autocrine TGF-beta induces epithelial to mesenchymal transition in human amniotic epithelial cells. *Cell transplantation.* 2013; 22(8):1351–67. <https://doi.org/10.3727/096368912X657387> PMID: 23031712.
59. Scholer HR, Ruppert S, Suzuki N, Chowdhury K, Gruss P. New type of POU domain in germ line-specific protein Oct-4. *Nature.* 1990; 344(6265):435–9. <https://doi.org/10.1038/344435a0> PMID: 1690859.
60. Niwa H, Miyazaki J, Smith AG. Quantitative expression of Oct-3/4 defines differentiation, dedifferentiation or self-renewal of ES cells. *Nat Genet.* 2000; 24(4):372–6. <https://doi.org/10.1038/74199> PMID: 10742100.
61. Takeda J, Seino S, Bell GI. Human Oct3 gene family: cDNA sequences, alternative splicing, gene organization, chromosomal location, and expression at low levels in adult tissues. *Nucleic Acids Res.* 1992; 20(17):4613–20. PMID: 1408763; PubMed Central PMCID: PMC334192.
62. Cauffman G, Liebaers I, Van Steirteghem A, Van de Velde H. POU5F1 isoforms show different expression patterns in human embryonic stem cells and preimplantation embryos. *Stem cells.* 2006; 24(12):2685–91. <https://doi.org/10.1634/stemcells.2005-0611> PMID: 16916925.
63. Lee J, Kim HK, Rho JY, Han YM, Kim J. The human OCT-4 isoforms differ in their ability to confer self-renewal. *J Biol Chem.* 2006; 281(44):33554–65. <https://doi.org/10.1074/jbc.M603937200> PMID: 16951404.
64. Garcia-Castro IL, Garcia-Lopez G, Avila-Gonzalez D, Flores-Herrera H, Molina-Hernandez A, Portillo W, et al. Markers of Pluripotency in Human Amniotic Epithelial Cells and Their Differentiation to Progenitor of Cortical Neurons. *PloS one.* 2015; 10(12):e0146082. <https://doi.org/10.1371/journal.pone.0146082> PMID: 26720151; PubMed Central PMCID: PMC4697857.
65. Izumi M, Pazin BJ, Minervini CF, Gerlach J, Ross MA, Stolz DB, et al. Quantitative comparison of stem cell marker-positive cells in fetal and term human amnion. *J Reprod Immunol.* 2009; 81(1):39–43. <https://doi.org/10.1016/j.jri.2009.02.007> PMID: 19501410.